Project ID: MR1 - 1601

Equine Lung Function Testing Device

A Major Qualifying Project Report submitted to the faculty of

WORCESTER POLYTECHNIC INSTITUTE

In partial fulfillment of the requirements for the degree of Bachelor of Science

Submitted by:

Lucy Garvey

Lubna Hassan

Kyla Nichols

Allison Paquin

April 27, 2017

Professor Marsha Rolle, Advisor
Department of Biomedical Engineering

Professor Robert Daniello, Advisor
Department of Mechanical Engineering

Abstract

Up to 80 percent of horses experience respiratory disorders in their lifetime due to their living environment (Kusano, Ishikawa, Kazuhiro, & Kusunose, 2008). Current diagnostic methods are invasive and expensive. Cummings School of Veterinary Medicine at Tufts University is the only facility in New England with a non-invasive equine respiratory testing device. However, this device poses a risk to operators because it is not well attached, weighs 3 pounds, and protrudes 12 inches from the horse's muzzle, causing it to disconnect and harm the operator if the horse moves suddenly. Seeking improvements, our team designed a safer, less expensive, non-invasive device to measure equine lung function to improve testing availability and market potential. This small, lightweight device uses a thermistor-based sensor to measure airflow at low flow speeds. A unique LabVIEW program displays the airflow in a way that is easy for the veterinarian to use for diagnoses.

Acknowledgments

We would like to thank our project advisors, Professor Marsha Rolle and Professor Robert Daniello, and our project sponsor, Dr. Melissa Mazan, for their help and support throughout the project. We also would like to thank Lisa Wall, Elyse Favreau, Professor Brian Savilonis, Professor David Olinger, Peter Hefti, and Randy Robinson for providing testing equipment, knowledge, and assistance throughout the project.

Executive Summary

Introduction

Equine lung function disorders caused by poor air quality in stables are common (Robinson, 2003). Horses cannot be tested using the same methods as humans because of physiological differences, including their noncompliant nature. Horses cannot respond to verbal requests resulting in most current diagnostic methods, such as endoscopy, being invasive and expensive. Thus, veterinarians only test lung function as a last resort, which is detrimental because if not diagnosed early, permanent damage of pulmonary tissue can occur. Cummings School of Veterinary Medicine at Tufts University performs equine lung function testing with non-invasive devices that measure pressure drop using a Fleisch pneumotachograph (Figure i.1). The pneumotachograph data is converted to flow rate and displayed with data measured by Respiratory Inductance Plethysmography (RIP) bands placed around the horse's abdomen and thorax. Variations between the pneumotachograph and RIP band signals indicate pulmonary disorders. Although functional, the current device has several drawbacks, including danger due to its size (12 inches), weight (3 lbs.), and unpredictability of horses' movement, cost ($18,000), resistance to breathing, and limited accuracy. We were tasked with developing a device to measure equine lung function that improves the overall device. It must also be compatible with typical equine breathing patterns. Based on our sponsor's needs, we created functional blocks for our design including: calibration, measuring airflow, signal processing, and device exterior development (Figure i.1).

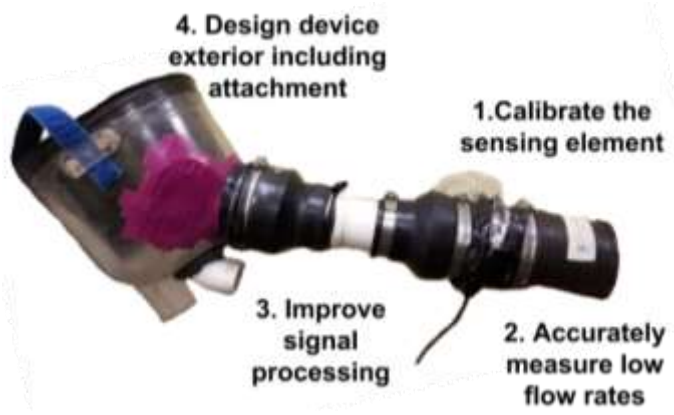

Figure i.1: Current device labeled with functional blocks

Materials and methods

Concept selection

Four alternative design concepts were developed. To select the best design for our application, we reviewed research papers, consulted our advisors, and developed a design matrix to rank each design. To assess feasibility, SolidWorks' Flow Simulation was used to produce velocity and pressure cut plots, identifying significant eddying or resistance. Calculations were completed to determine the inertial impact on overspeeding, the deflection caused by a breath, and the pressure drop through the capillaries.

Wind sensor calibration

Zero-point testing was conducted with Modern Device's Rev C Wind Sensor to find the adjustment factor for the sensor's reading at 0 MPH that is incorporated into the sensor's calibration equation. The sensor was placed under a glass bowl to restrict airflow, and was connected to LabVIEW via a USB-6000 data acquisition (DAQ) box (National Instruments). The LabVIEW program acquired voltage signals and converted them to wind speeds.

Wind sensor verification

The sensor was tested in WPI's Aerospace department's wind tunnel to verify functionality at high speeds. The sensor was tested at 20, 35, and 50 MPH and data was collected using LabVIEW. To verify the sensor's function at lower speeds, it was tested in a low flow wind tunnel constructed from PVC pipe, PVC reducers, a ¼-in. NPT ball valve, a regulator, a compressed airline, a flow straightener, and a rotameter and Testo hot wire probe for comparison. To verify the sensor's response to cyclic flow, it was compared to the pneumotachograph using a combination of syringe and human breathing tests. We created a 4.07 L syringe using a 4-in. diameter 2 ft. PVC pipe, a machined aluminum piston, a wooden dowel handle, and 2-240 O-rings for sealing. This syringe was used to calibrate the pneumotachograph with a cyclic flow of a known volume. After calibration, a team member breathed through the pneumotachograph and the new sensor, simultaneously. Data was collected for the sensor in LabVIEW and the pneumotachograph in Open Pleth (a proprietary software). The raw data for each was then overlaid on a graph in EXCEL.

Results

Final concept selection

SolidWorks models of our four alternative designs and flow simulations were created (Figure i.2 and Figure i.3).

a. b. c. d.

Figure i.2: a. Improved Fleisch Pneumotachograph; b. Three-cup anemometer; c. Strain gauge on hair like structures; d. Hot-wire anemometer concept (arrow indicates sensor).

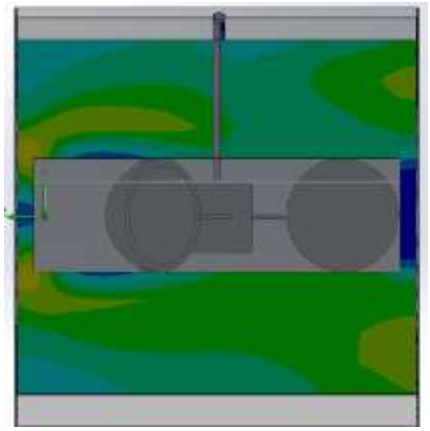

Figure i.3: Velocity cut plot for three-cup anemometer

Constructing a smaller, safer, less expensive Fleisch pneumotachograph proved infeasible because of the manufacturing requirements and associated cost. The size is also difficult to reduce without drastically increasing resistance, as determined by our flow simulations. Experimental results from the three-cup anemometer model showed that the device's inertia causes overspeeding, resulting in a 2 second response time (Chen, 2016). The breathing rate of a horse (5 seconds per breath) is too fast for this response time to be accurate. Significant eddying was also seen in the velocity plot which adds resistance to breathing (Figure i.3). The strain

gauges on hair-like structures could work at faster wind speeds, but for a horse's breath (0.2 MPH) the structures would only deflect approximately 0.308 nm which is too small for a strain gauge to measure accurately. Based on simulations and research, the team determined that the hot-wire concept was the most feasible. To remove concerns of fragility and response to moisture, thermistor-based sensors that work similarly to hot-wire anemometry were acquired. Our prototype incorporated a Rev C Wind Sensor that is accurate at low wind speeds.

Wind sensor calibration

An adjustment factor of approximately 0.35 was determined for a 5 V excitation voltage. A LabVIEW calibration program was developed to automatically find the adjustment factor before performing a test.

Wind sensor verification

In order to verify functionality a calibrated wind tunnel was used. The sensor read values similar to the wind tunnel with an R^2 value of 0.9963 (Figure i.4).

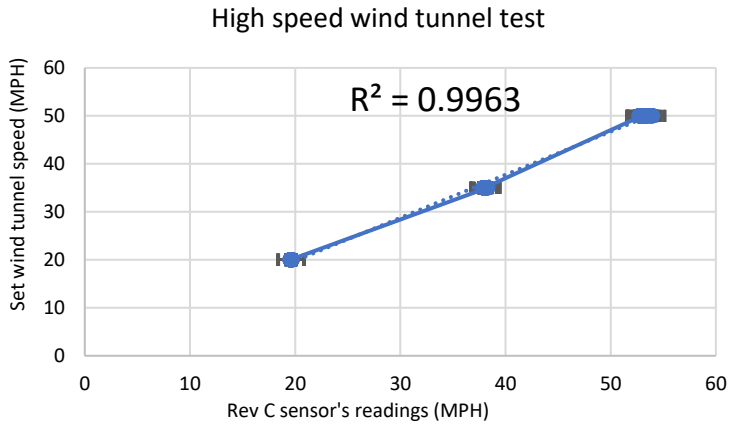

Figure i.4: High speed wind tunnel test results

To confirm the sensor's function at low flows, a low flow wind tunnel constructed by the team was used and the sensor's readings were compared to the readings of a Testo 405i hot wire probe. The readings of both were not significantly different proven by the low P-value found with a T-test (Figure i.5).

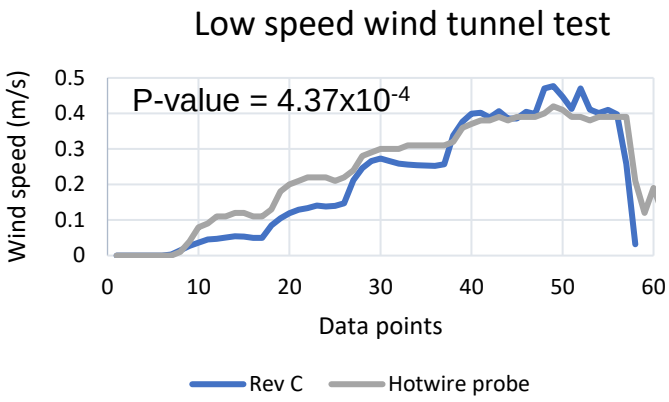

Figure i.5: Rev C compared to Testo 405i hot wire probe in low flow wind tunnel

To confirm the sensor responded to cyclic flow, like that produced by a horse's breath, breathing tests from human subjects were also completed. Figure i.6 shows the comparison of the pneumotachograph and Rev C. The results closely overlapped.

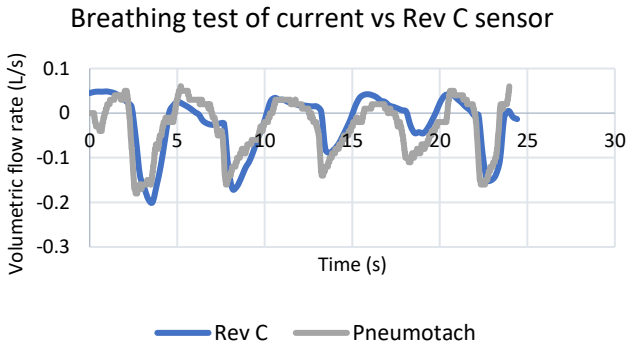

Figure i.6: Pneumotachograph and Rev C sensor data overlaid after human breathing test

Wind sensor validation

After verifying the sensors functionality at low, cyclic flows it was determined ready for clinical tests. These clinical tests were performed to validate that the sensor accurately measured equine lung function and met the objectives of the project. The device was tested on three different horses. Two of these horses were unsedated and the last was mildly sedated because of another procedure. The results produced similar maximum flow rates to past tests conducted with the Fleisch pneumotachograph in Open Pleth. Figure i.7 shows a representative data sample of these clinical tests.

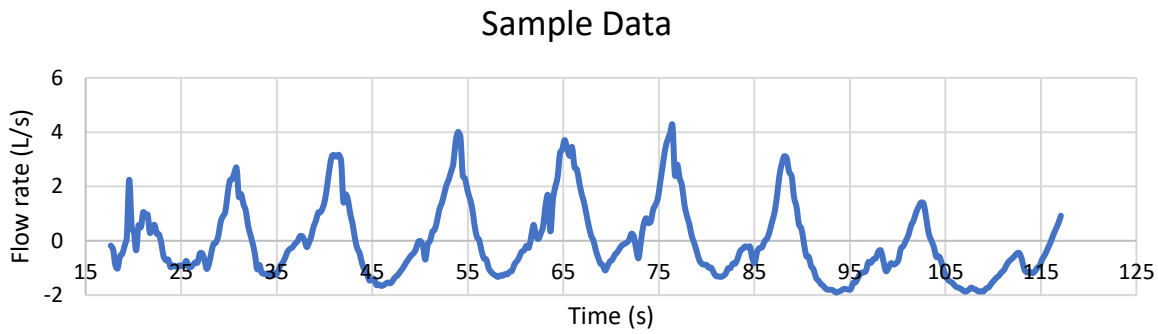

Figure i.7: Sample data from clinical tests conducted at Cummings School

Discussion and conclusion

We successfully evaluated the feasibility of a new design to test equine lung function. The design met our objectives of being non-invasive and compatible with non-compliant breathing. It also minimizes resistance to the horse's breathing, is less expensive, and is reduced significantly in size (2.5 in.) and weight (0.32 lbs.) to minimize the risk of injury for the user. We also improved our data acquisition program. Most anemometry devices that measure flow in both directions require multiple sensing elements. Therefore, we developed a LabVIEW program that acquires and displays the flow and volume data and we developed a MATLAB program that accounts for the flow in both directions, using a single sensor. Once these programs were completed and a housing was created for the sensing element, our design met all of our functional blocks and was tested clinically on horses. The results of these clinical tests closely matched results from past tests with the pneumotachograph. These clinical tests also proved our device was improved from the pneumotachograph because it was used on unsedated horses with only one veterinarian whereas, the pneumotachograph requires horses to be slightly sedated and have multiple veterinarians present to perform the test.

Authorship

Lucy Garvey
Chapter 1
Chapter 2: 2.1, 2.4
Chapter 3: 3.2, 3.5
Chapter 4: 4.2, 4.3, 4.4
Chapter 5: 5.2
Chapter 6: 6.2
Chapter 7
Chapter 8

Lubna Hassan
Chapter 1
Chapter 2: 2.7, 2.8
Chapter 3: 3.1, 3.5
Chapter 4: 4.2, 4.3, 4.4
Chapter 5: 5.2
Chapter 6: 6.2
Chapter 7
Chapter 8

Kyla Nichols
Chapter 1
Chapter 2: 2.3, 2.6, 2.9
Chapter 3: 3.2, 3.3, 3.5
Chapter 4
Chapter 5: 5.2
Chapter 6
Chapter 7
Chapter 8

Allison Paquin
Chapter 1
Chapter 2: 2.0, 2.2, 2.5,
Chapter 3: 3.1, 3.2, 3.4, 3.5
Chapter 4: 4.2, 4.3, 4.4
Chapter 5:
Chapter 6: 6.2
Chapter 7
Chapter 8

Each team member contributed equally to the editing of the report.

Table of Contents

List of Figures

List of Tables

1.0 Introduction

Equine lung function disorders are a more common occurrence than one might expect. As many as 80% of stabled horses can suffer from inflammatory airway disease due to the environment in which they live (Cummings Veterinary Medical Center, 2016). A majority of horses are housed in stables with poor air quality due to hay, dirt, and dust. Even sport horses kept in athletic facilities experience pulmonary disorders, with at least 70% affected (Robinson, 2003). Horses are part of a well-established industry; the horse racing industry generates an average of $1.2 million dollars from bets for each race in the United States (McManus, Albrecht, & Graham 2013). Activities like horse racing, pulling, or driving rely heavily on a functional respiratory system. This makes identifying and treating pulmonary disorders exceptionally critical.

Veterinarians traditionally use two invasive methods to test an equine's lung function. The first is considered the conventional method, which uses an esophageal balloon to collect pressure data in order to analyze muscle work, resistance, and lung volume. Once the analysis is complete a disorder can be diagnosed. The second common method is a sampling method called Bronchoalveolar Lavage (BAL). In this method, a sample of fluid is retrieved from the distal airways and alveoli using an endoscope and is then prepared and analyzed to determine the infection type. These procedures are highly invasive, time consuming, and cause stress for the horse. Complex, invasive testing procedures are also expensive and often delayed until symptoms are severe. Late diagnosis of respiratory disorders can lead to permanent damage of the horse's pulmonary tissue, making early diagnosis critical.

Dr. Melissa Mazan, a veterinarian at Cummings School of Veterinary Medicine at Tufts University, specializes in equine lung function analysis. She currently performs lung function testing with either a passive airflow device or a forced oscillatory mechanics (FOM) device that both use a Fleisch pneumotachograph to measure lung pressure, flow, and volume. These procedures are non-invasive and allow for the early detection of subclinical respiratory disorders. The data collected is processed by a virtual interface, so signals can be analyzed for abnormalities in the horse's pulmonary function. Both devices were developed by her colleague, Dr. Andrew Hoffman, another equine lung function expert at Cummings School of Veterinary Medicine.

The passive device is used more frequently than the FOM device because it is simpler to operate and can be used with horses of all ages. Whereas, the FOM device can only be used on young racehorses and sport horses because older horses or severely affected horse's breathing rate too closely matches the frequency of the sine waves to be distinguishable. Although the passive device has proven to be an effective testing mechanism, it poses some concerns that need to be addressed. The Fleisch pneumotachograph used for the current device is no longer in production, making it difficult to replace. The current device is also extremely expensive and has limited accuracy. The Fleisch pneumotachograph itself cost $8,000 and can only be calibrated to an accuracy of ± 3.33%. The remaining system components cost approximately $10,000 resulting in a total system cost of approximately $18,000 (Mazan, Personal Communication, September 9, 2016). The current device is also heavy, approximately 3 lbs., and protrudes from the horse's muzzle, approximately 12 in., posing risk of injury to human operators. Head injuries to the human operator occurred when horses swung their head while wearing the device. The costs, risks, and inconveniences of using the device in the field makes the Fleisch pneumotachograph inaccessible to other veterinarians. Thus, Cummings School of Veterinary Medicine at Tufts is the only location in the Northeast that uses the Fleisch pneumotachograph (Mazan, Personal Communication, September 9, 2016).

Our team was tasked with developing an improved, non-invasive, device to measure equine lung function. Based on our sponsor's needs, the device must be able to accurately measure equine lung function (ideally calibrated to ± 0.33%), the device cannot require compliant breathing or add resistance to the horse's normal breathing, and lastly, the device must minimize the risk for the human user. Some additional goals of our project are a lighter, compatible with LabVIEW, and portable device that meets veterinary standards. Our sponsor would also like our device to have a final cost of $1,000 or less. By having the device cost $1,000, rather than the current $18,000, the market for the device increases because more veterinarians would be able to afford the device. The device needs to be lighter and shorter to remove the need to hold it during testing. This will also reduce the risk to the human user because they will not need to stand near the horse's swinging head while performing the test, thus reducing the likelihood of direct physical injuries. Dr. Mazan would like the data collected by the device to be processed with LabVIEW because Open Pleth, the current software program,

is difficult to use and LabVIEW allows output customization. A schematic that displays the overall devices is shown in Figure 1.1A and Figure 1.1B. It summarizes the current devices limitations that we hope to address with our new device.

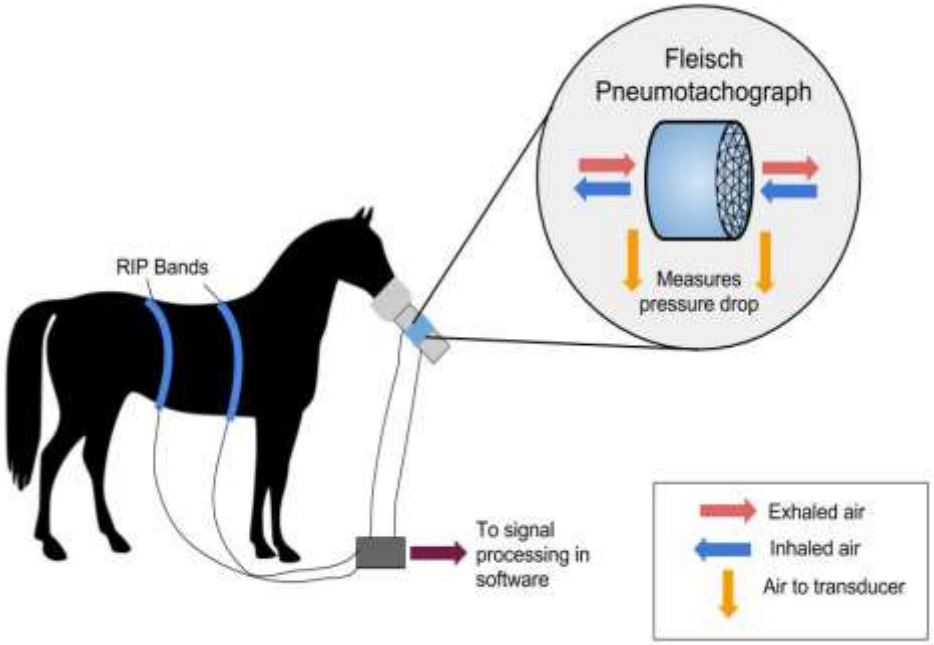

A.

B.

Figure 1.1: A) Schematic of the two components of the current device on a horse, B) Fleisch pneumotachograph current component with parts and limitations labeled

Our designed device allows for an affordable, simplified approach to detect and diagnose abnormalities in equine pulmonary systems as early as possible. The device attaches to the horse's muzzle with a facemask in order to measure the lung function and produce a signal to analyze any abnormalities. It could work in conjunction with respiratory impedance plethysmography (RIP) bands that measure the horse's lung volume based on changes in voltage in the bands. The signals from the airflow sensor and the RIP bands are processed in LabVIEW to produce a volumetric flow rate versus time graph. Once the RIP bands are incorporated, the signals can be overlaid in the display in order to analyze the visual differences between them. The device also protrudes 2.5 in. from the current mask and weighs less than 0.32 lbs., making the device safer for the human user.

Our new device was tested and validated using different methods to determine if the device meets all of the objectives. The weight and safety to the human user were validated by comparing the weight and length of protrusion of the new device to the original device. Next, the accuracy of the flow measurement was determined by comparing the calibrated output signals of the new device to the outputs of the current device. To validate the new design, both devices were compared in a controlled airflow environment and clinically on a horse. A successful new device should be smaller, lighter, and provide the same function as the current device with increased accuracy and more efficient operation.

This report illustrates our knowledge of the current device and its associated limitations, the design process that we followed to arrive at our final new design that addresses the current devices limitations, and the testing we conducted to validate that design. The report is arranged into eight chapters progressing from the literature review to the project strategy to the design process and then the final design verification, the design validation, the discussion, and the conclusions and recommendations.

The literature review discusses the significance of equine lung function testing by illustrating the differences between horse's and human's respiratory systems and the complications these differences can lead to in pulmonary testing. The current test methods are also described to illustrate the design space for a newly designed non-invasive equine lung function testing device. The project strategy explains the development of the client statement and the objectives for the project, while also defining the stakeholders. The design process chapter

discusses four alternative design ideas and the steps that were taken to choose our final design. A final design was chosen based on a concept similar to hot-wire anemometry. The final design verification chapter includes our raw data and results from calibrating and testing the final design. The final design validation chapter explains attributes of our final design and the objectives that it meets. The discussion chapter includes the significance of the project and compares our final design to current methods. The conclusions and recommendations chapter summarizes our successes and future work that still needs to be completed to improve upon the design.

2.0 Literature Review

This literature review was written to give the reader an overview of the equine respiratory system, the prevalence of equine respiratory disease, and the current testing methods available for these diseases. There are many differences present between the respiratory system of horses compared to humans, so the testing methods applied need to be different than those used for humans. These differences and the methods for detecting disorders are explained in detail in this chapter.

2.1 Equine respiratory system

The respiratory system's, or pulmonary system's, main purpose is to provide the pathway into the body for air to transfer oxygen and carbon dioxide into and out of the blood respectively (Davis, 2013; Marieb & Hoehn, 2012). The entire process of inhaling oxygen and exhaling carbon dioxide is called respiration (Marieb & Hoehn, 2012). Airflow travels through the horse's pulmonary system first though the upper respiratory tract (URT) and then the lower respiratory tract (LRT) (Davis, 2013; Crabbe, 2007). The URT consists of nostrils, nasal passages, the pharynx, the larynx, and the trachea. The LRT consists of the structures in the lung including the bronchi, bronchioles, and alveoli (Davis, 2013).

The inhaling of air begins at the start of the URT, the nostrils (Davis, 2013; The British Horse Society, 2011; Crabbe, 2007). There are cartilage rings inside the opening of the nostrils that can expand and allow for increased airflow, which is necessary during exercise (Crabbe, 2007). Air continues through the nostrils and nasal passages to the pharynx. The pharynx in a horse has two purposes; to facilitate airflow to the larynx and to transport food to the esophagus from the oral cavity (Davis, 2013; Crabbe, 2007). The soft palate separates the oral cavity from the pharynx and only allows airflow through the oral cavity when the horse is swallowing (Davis, 2013). The epiglottis also assists in keeping food from entering the larynx by separating the trachea and esophagus. When air is flowing into the trachea the epiglottis blocks the esophagus by lying flat over the esophagus. When the horse is swallowing food, the epiglottis blocks the trachea using the same mechanism (Crabbe, 2007). Together the soft palate and epiglottis cause horses to be obligatory nose breathers (Davis, 2013; Crabbe, 2007). Figure 2.1 shows airflow into the horse as it inhales. It clearly displays that the horse is an obligatory nose breather because the soft palate's location does not allow airflow from the mouth to the trachea.

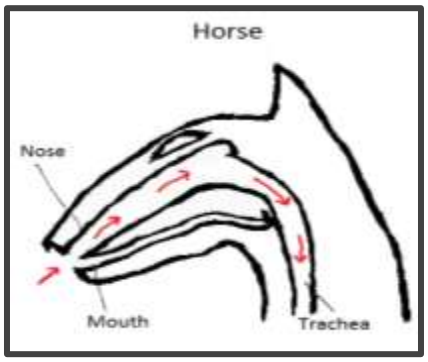

Figure 2.1: Airflow into the horse during inspiration

As air flows through the trachea, it will leave the URT at body temperature and enter the LRT through two bronchi (Davis, 2013; The British Horse Society, 2011; Crabbe, 2007). One bronchi branch goes into the left lung and the other bronchi branch goes into the right lung. However, the internal structures of the lungs are not completely divided, which results in a risk of respiratory disease in both lungs (Crabbe, 2007). The two bronchi branches proceed to branch further forming into bronchioles. At the end of the bronchioles are alveoli, also known as alveolar sacs. In the alveoli, oxygen in the air diffuses into the pulmonary capillary circulation to be absorbed by the blood and carbon dioxide diffuses into the alveoli (Davis, 2013; The British Horse Society, 2011). This process of diffusing oxygen from the air into the blood is called oxygen exchange (Raven & Rashmir-Raven, 1996). The carbon dioxide in the alveoli is then exhaled out of the horse, which concludes one breath of airflow through the respiratory system (Davis, 2013).

2.1.1 Respiratory system: horse versus human

The capacity of the respiratory system of a horse is drastically different than that of a human. An average adult horse's total lung capacity is around 50 L, with most of the capacity due to the LRT (Raven & Rashmir-Raven, 1996). In comparison, the average adult human's total lung capacity is around 6 L (American Lung Association, 2016). A horse at rest can have a respiratory rate, amount of air inspired during breathing, as high as 75 L/min with each breath averaging approximately 7.5 L (Raven & Rashmir-Raven, 1996). A human at rest maintains a respiratory rate of 7.5 L/min; the equivalent volume of one horse breath (Molecular Products Ltd, n.d.; Raven & Rashmir-Raven, 1996). Horses running or galloping do not voluntarily

breathe, instead horses sync their stride to their respiratory rate. This means the horse's respiratory cycle is timed so it exhales as its hooves land because the forward force of landing assists by forcibly pushing air out of the lungs. Therefore, adult horses drastically increase their respiratory rates from rest at 75 L/min up to 1500 L/min while galloping (Raven & Rashmir-Raven, 1996). A human under max exertion can only reach respiratory rates of 65 L/min and the stride and respiratory rate of a human are not synched (Molecular Products Ltd, n.d.). The differences between the horse's and human's respiratory system are summarized in Table 2.1. The differences are important to understand when analyzing testing methods for lung function.

Table 2.1: Horses' vs. Humans' Respiratory System

	Horses	Humans
Breathing Method	Obligatory nose breathers	Nose and mouth breathers
Lung Capacity	50 L	6 L
Maximum Respiratory Rate	1500 L/min	65 L/min
Patient Type	Non-compliant	Compliant

To better illustrate the difference in airflow through the horse's and human's respiratory system Figure 2.2 was created.

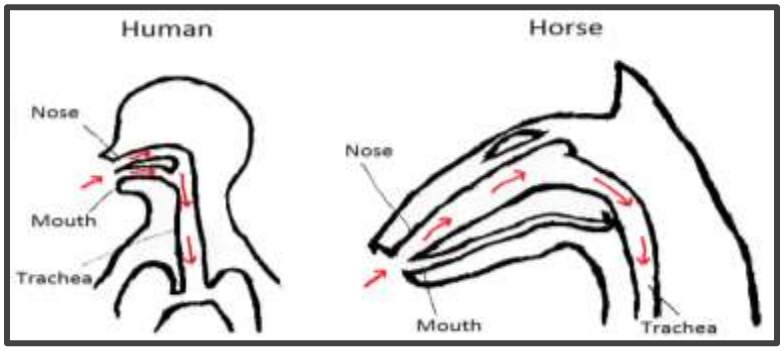

Figure 2.2: Comparison of airflow through a horse and a human

As seen in Figure 2.2 the human can breathe through both their nasal passages and their mouth. This flow of air meets in the trachea and then flows into the lungs, but for the horse it can only breathe through its nose because it's mouth does not connect to the trachea.

The horse's and human's respiratory systems may be different in terms of size and physiology, but they have a variety of similar defense mechanisms to protect from disease. The process of heating inspired air to body temperature filters large particles from entering the LRT (Davis, 2013; The British Horse Society, 2011; Crabbe, 2007). Smaller particles, such as viruses, bacteria, and dust, are able to bypass the heat filter and continue down the respiratory tract as far as the alveoli (The British Horse Society, 2011). Most of the respiratory system has a protective lining formed from secreted mucus that creates a liquid barrier (The British Horse Society, 2011). The protective mucus lining also supports millions of cilia, microscopic projections, directed upward and away from the LRT. The cilia have two functions, one is to catch dust and move the dust away from the LRT and toward the back of the throat (The British Horse Society, 2011; Crabbe, 2007). The other is to prepare the air before it enters the lungs (Crabbe, 2007). Horses' grazing posture of directing the head downwards naturally clears their airways. However, even with the horse's natural defense mechanisms, they are still susceptible to diseases caused by bacteria, viruses, and inflammation from dust.

2.2 Respiratory disorders of horses

Equine respiratory disorders are more common than one may think. Horses can have a number of disorders including recurrent airway obstruction, inflammatory airway disease, and other less common disorders. It is often difficult to diagnose a specific disorder because it is challenging to differentiate between them. Unlike with other animals, the symptoms and results of specific tests do not lead to one specific diagnosis. Veterinarians have to stay up to date with frequently changing disorder definitions. A correct diagnosis is also difficult because the disorders are often subclinical, so the horse may suffer for extended periods of time before a test is performed or a clinical level disorder is detected. Wrong diagnoses can be extremely serious because different treatment methods are used for each disorder. Incorrect treatment can cause the actual disorder to drastically worsen.

2.2.1 Recurrent airway obstruction (RAO)

Recurrent airway obstruction (RAO) is commonly seen in older horses that are experiencing airway obstruction, inflammation, mucus accumulation, or tissue remodeling. RAO is the most commonly diagnosed lower airway disease in horses and is very similar to noneosinophilic asthma in humans. RAO is believed to be caused primarily by an allergic

reaction to inhaled molds. Many horses live in closed barns where hay is stored. It is very common for this hay to produce a dusty and moldy living environment, which aggravates the respiratory system of horses causing diseases such as RAO. The most common sign of RAO is frequent labored breathing. Fortunately, RAO is completely reversible if diagnosed early and correctly. The most common steps that can be taken to reverse the effects of RAO are to reduce the dust in the horses living environment and administer a bronchodilator (Kutasi, Balogh, Lajos, Nagy, & Szenci, 2011).

2.2.2 Inflammatory airway disease (IAD)

RAO and inflammatory airway disease (IAD) are very similar, but they can be differentiated at the clinical level. IAD is a nonseptic inflammation of the lower airways that is common in young sport horses and can be caused by many different factors. These factors can include dust and mold spores in their living environment, immunological factors, and infectious agents. If IAD is left undiagnosed and untreated it can progress into RAO. IAD is commonly left untreated because most cases have subclinical symptoms that go unrecognized by the owner. IAD is the most commonly diagnosed disorder in the racehorse and sport horse community and is the second most diagnosed disorder for all horses behind RAO (Kutasi, et al., 2011).

2.2.3 Other disorders

It is much less common than RAO and IAD, but horses can get pulmonary disorders caused by infections. These disorders can be caused by bacterial, viral, fungal, or parasitic agents. Infections are typically seen in older horses that have been subjected to increased stresses including long distance travel or strenuous exercise (Kutasi, et al., 2011).

Exercise-induced pulmonary hemorrhage is common in racehorses and sport horses, but most commonly in racehorses who have to over exert themselves for short periods of time. This most commonly occurs because of inflammation in the upper and lower airways that applies excessive stress to the pulmonary circulatory system. These hemorrhages can be very serious and should be treated immediately, but they do not have significant symptoms, so they often go undetected for a long period of time. This is the second most common disorder diagnosed in young racehorses after IAD. Lastly, it is very rare, but horses can be diagnosed with granulomatous, neoplastic disease, or pneumonia (Kutasi, et al., 2011).

2.3 Diagnosing disorders

Veterinarians commonly encounter horses with lung function disorders. One of the first tasks a veterinarian will complete is checking the contagious nature of the disorder. Horses often live closely with other animals and the risk of any contagious infections spreading should be minimized. A detailed history of the patient is often established. This helps the veterinarian learn about potential causes of the disorder and the severity. The horse's age, breed, sex, origin, environment, herd or group history, vaccination, deworming, and medical history are all required information the veterinarian will ask the client (Kutasi et al., 2011). These questions provide insight into the potential causes behind any disorders. For example, a horse living in a barn storing damp hay will be more susceptible to respiratory infections (Robinson, 2003). The veterinarian will also inquire about any symptoms the horse might be displaying. These include:

- Cough
- Nasal and or ocular discharge
- Exercise intolerance
- Respiratory distress
- Sneezing
- Abnormal respiratory noise
- Elevated breathing rate
- Abnormal respiration pattern
- Depression
- Fever
- Anorexia

The veterinarian could also ask about previous medications used or other horses the patient has been exposed to. Before any further testing, the condition of the horse will be examined. This includes noting the manner of movement, demeanor, body condition, abdominal movement, presence of nostril flare, and respiratory rate. Adult horses breathe 12-20 times per minute, foals can be up to 40 times a minute (Katusi et al., 2011). The horse will be further examined, looking at mucus membranes, any swelling, abnormal nasal discharge, signs of pain, or swollen glands. A stethoscope is then used to see if any abnormal breathing sounds can be heard. If a brown bag is placed over the horse's nose, the horse has to breathe deeper and the veterinarian can hear better. During the bag rebreathing exam, wheezes and crackles could be a sign of an obstruction and tracheal rattling could be mucus accumulation in the lower airways.

Coughing while the bag is on or prolonged recovery time after the bag is removed are signs of a respiratory disorder (Katusi et al, 2011). For IAD, oftentimes the blood chemistry is completely normal, but accumulation of bacteria in the trachea could be a sign of the disease (Robinson, 2003). After understanding the horse's past, further testing can be completed to determine if a lung function disorder is present.

2.4 Pulmonary function tests

Pulmonary function tests (PFTs), or lung function tests, are tests employed to determine the quality of the respiratory system's performance (U.S. National Library of Medicine, 2015). Most tests focus on measuring lung function through defining lung capacity, respiratory rate, and proficiency of oxygen exchange to the blood (U.S. National Library of Medicine, 2015).

A diagnosis process for humans includes different PFTs to help determine the presence of a pulmonary disorder. Often the first step is a physical examination with a stethoscope (Myers & Bass, 2010). Doctors listen with a stethoscope for any abnormal respiratory sounds (Myers & Bass, 2010; Yu, Tsai, Huang, & Lin, 2013). Wheezing, a sound commonly associated with asthma, through a stethoscope produces a high-pitched whistling sound (Myers & Bass, 2010; Yu, et al., 2013). When wheezing becomes severe enough, it is heard without a stethoscope (Myers & Bass, 2010). However, wheezing can be mild to the point of only being recognized when a person is instructed to forcibly exhale while a doctor listens with a stethoscope to hear the whistling sound (Myers & Bass, 2010). Hearing wheezing through a stethoscope is not enough to provide a diagnosis of asthma, instead other PFTs must be conducted to fully determine the presence of asthma or other pulmonary disorders.

Spirometry is a common PFT to determine the presence of different lung diseases. It measures the amount of air a person exhales and the speed of exhalation (U.S. National Library of Medicine, 2015). This test is dependent on compliant breathing, a person's ability to follow directions to breath at a specific time with a certain amount of effort (U.S. National Library of Medicine, 2015). Often spirometry is conducted with a person postured in a sitting position with a mouthpiece to breathe in (U.S. National Library of Medicine, 2015).

Methacholine challenge tests use spirometry to determine lung function while breathing in specific agents such as methacholine or histamine (American Thoracic Society, 2009). When people with asthma breathe in methacholine, their airways begin to tighten and restrict breathing

in a measurable way (American Thoracic Society, 2009). The methacholine challenge test is more useful in disproving a diagnosis of asthma because if a person's airways do not tighten with methacholine they cannot have asthma (Scope, Contraindications, & Training, 1999).

Spirometry and spirometry with methacholine challenge tests require compliant breathing. Human infants and animals are unable to follow directions to provide maximum exhalation (Rozanski & Hoffman, 1999). Tidal breathing flow-volume loops, a pulmonary function test that does not require complaint breathing, was initially designed for human infants, but was determined useful for pulmonary disorders in animals such as dogs and cats (Rozanski & Hoffman, 1999). As the infant or animal breathes into this device, it measures respiratory rates through a pneumotachograph with a pressure transducer (Rozanski & Hoffman, 1999). This process takes several minutes because the flow-volume loops require time to appear consistent in shape and there needs to be breathing patterns without crying, purring, or panting (Rozanski & Hoffman, 1999).

As described in section 2.3, many other tests and questionnaires are completed before a non-compliant animal is tested for a lung function disorder. Lung function testing is only performed as a last resort if no other testing methods such as x-rays, heartworm, fecal, blood, and urine tests did not provide a clear diagnosis (PetWave, 2015). Once all of these methods are exhausted and a diagnosis is not identified, lung function testing is considered. Typically, lung function testing is invasive, expensive, and has many limitations as described in section 2.5.

2.5 Equine pulmonary function tests

There are many different techniques for testing lung function in horses including imaging, taking samples, laboratory diagnostic techniques, and newer methods that focus on the actual breathing patterns of the horse. Each one of these techniques has different advantages and disadvantages, so they are used in different situations.

2.5.1 Imaging

Imaging is typically used for horses that have clear symptoms of a pulmonary disorder. Most of these techniques are invasive, but they can provide a proper diagnosis. The key imaging techniques that are used currently include endoscopy, radiography, and thoracic ultrasonography.

Respiratory tract endoscopy is commonly used for diagnosing horses who are experiencing abnormal nasal discharge, coughs, or poor performance during exercise. Endoscopy

allows for imaging of the upper respiratory tract and the proximal lower respiratory tract. This procedure is performed by inserting an endoscope through the nares (nostrils) of the horse into the upper respiratory system (Pusterla, Watson, & Wilson, 2006). RT Endoscopy is advantageous because it provides an accurate diagnosis and it does not always require sedation, but is disadvantageous because it is an invasive procedure (Kutasi, et al., 2011).

Radiography is another common imaging method used for diagnosing lung function disorders in horses. Radiography is key to locating the cause of a disease because it identifies fluid-air lines in the lung. This equipment is advantageous because it can image the small areas of the lung including the paranasal sinuses, the guttural pouches, and the retropharyngeal area that the other imaging technologies cannot access. A major disadvantage with radiography is that it has very limited usage due to the fact that it is not readily available (Pusterla, et al., 2006).

When analyzing a horse using radiography veterinarians are looking for one of four common patterns, which include the alveolar pattern, the interstitial pattern, the reticular pattern, and the bronchial pattern. These are typical patterns to look for in any species when using radiography, but unlike in other species, horses do not have one diagnosis that matches with each distinct pattern. For horses, each pattern represents a range of possible diagnoses that often overlap with each other. The major limitation of diagnosing by fluid-air line patterns is that the most common pattern, the interstitial pattern, does not clearly define any specific disorders. Table 2.2 illustrates the overlapping and ever changing definitions that veterinarians need to be aware of when caring for a horse with a pulmonary disease.

Table 2.2: Air-fluid patterns common in horses and what disorders they represent

Pattern	Disorders
Alveolar	Pulmonary edema, hemorrhage, lung consolidation, or neoplastic infiltration
Interstitial	Variety of diseases, has no clear definition of diagnosed disorders
Reticular	Most common with viral, bacterial, and fungal infections Also, present in horses with pulmonary edema, interstitial pneumonia, and pulmonary fibrosis
Bronchial	Bronchitis or bronchiolitis

Thoracic ultrasonography is more readily available than radiography, so it is used more often especially if pleural effusion, pulmonary consolidation, pulmonary or mediastinal abscesses, tumors or granulomata are being detected. The main limitations of ultrasonography are the lengthy process to prepare the horse and the ease of doing something improperly. These limitations combined can lead to an inefficient and frustrating test. Ultrasonography also has a very limited number of disorders that it can diagnosis (Pusterla, et al., 2006).

2.5.2 Sampling

There are many sampling methods that can be used to diagnose equine respiratory disorders. These diagnostic techniques include tracheal wash, bronchoalveolar lavage (BAL) fluid cytology and culture, thoracentesis, and percutaneous lung biopsy. Similar to imaging, each one of these techniques is invasive.

Tracheal washes can detect many different disorders by collecting a sample from the distal trachea. This can be done using an endoscope or a percutaneous tracheal wash. The percutaneous tracheal wash requires surgical skin preparation and has a risk of infection at the insertion site, but if the sample needs to be cultivated for diagnosis, this method is required. Endoscopy can acquire the sample, but it will be contaminated by the nasopharyngeal bacteria, so it can only be used for cytological examination. Acute inflammation, bacterial pneumonia, credence, fungal infections, viral infection, and nonsepetic inflammation can be detected with this method of sampling. Table 2.3 below shows what cells are present during the different disorders that can be diagnosed (Pusterla et al., 2006).

Table 2.3: Cells present in disorders

Disorder	**Cells Present**
Acute inflammation	Neutrophils
Bacterial pneumonia	Neutrophils showing signs of degeneration
Credence	Intracellular bacteria
Fungal infection	Neutrophilic infiltration, large number of eosinophils and macrophages
Viral Infection	Increase in lymphocytes and epithelial cell injury
Nonseptic inflammation	Nondegenerative inflammatory cells with no evidence of etiologic agents

BAL is the most common sampling method used by veterinarians when testing for diffuse inflammatory disorders in horses. In this method, an endoscope is used to retrieve a sample of the fluid lining in the distal airways in the alveoli. This sample is then used in cytological examination or quantitative culture techniques. Quantitative culture techniques must be used so that contamination due to the nasopharyngeal bacteria can be ignored. The BAL sample cell distribution is compared to a normal cell distribution to determine the disorder (Pusterla et al., 2006). Veterinarians can use a similar method to diagnose the disease using the cell types listed in Table 2.3.

Thoracentesis can be completed quickly and easily with very little equipment, so it is a preferred method for many veterinarians. Once the sample is collected both culture and cytology analyses can be conducted. Additionally, the odor, color, and consistency of the sample is analyzed. A normal sample should be odorless, transparent, and slightly yellow. If the sample taken does not appear normal then there is an abnormal cell present, which means that culture and cytology examinations should be conducted. This sampling method can be used to easily and quickly diagnose disorders such as; pulmonary abscesses, pneumonia, chronic obstructive lung disease, pulmonary granulomata, equine infectious anemia, systemic mycosis, traumatic penetration of the thorax, and primary and secondary thoracic neoplasms. There are a few risks because it is an invasive procedure. These risks include the chance of pneumothorax, cardiac puncture, intercostal artery or vein laceration, and patient collapse due to rapid removal of large amounts of fluid. Although these results are very uncommon, they can occur, so this method is typically only used if other diagnostic methods do not work (Pusterla et al., 2006).

The last sampling technique used is the percutaneous lung biopsy. This procedure is extremely invasive and there are many complications that can be observed. These complications include epistaxis, pulmonary hemorrhage, tachypnea, respiratory distress, pneumothorax, collapse, and death. Since there is such a high risk for this procedure, it is typically a last resort and is only used when all less invasive diagnostic methods have failed to provide an accurate diagnosis. This procedure can be conducted in unsedated, standing horses, but it is much more commonly done on a chemically restrained horse in the stock. To try to reduce the risk of the complications, ultrasonographic evaluations are conducted before the procedure to map the major organs to avoid puncture while accessing the desired location. The percutaneous lung

biopsy is typically used to diagnose diffuse lung disease or undetermined etiology (Pusterla et al., 2006).

It is clear that sampling techniques allow for both sensitive and accurate results if contamination is taken into account, but all of the sampling techniques are invasive and have a risk of very serious complications, so veterinarians are trying to move towards less invasive methods that are just as sensitive and accurate. They do have some special laboratory diagnostic techniques that they can use, but they are only used for very specific disorders.

2.5.3 Special laboratory diagnostics

Special laboratory diagnostics are less commonly used than imaging and sampling, but they can be used when trying to diagnose very specific disorders or when imaging and sampling do not provide a clear diagnosis. The laboratory techniques commonly used with horses include hematology, immunodiagnostic testing, and molecular diagnostics.

Hematology is a very sensitive and time dependent method of determining if the disorder is infectious or noninfectious. This is determined by increases and decreases of cell types over time, but the changes are very small unless it is a chronic infection, so it is very hard to determine if the disorder is infectious from this analysis. It can be used to detect inflammation quite accurately though because inflammation is dependent on plasma concentration, which is easier to quantify than the small changes in the different cell types. Inflammation is present if there is an increase in plasma concentration. Based on this, hematology is commonly only used to determine if inflammation is present, but if records are kept well and the test is conducted very cautiously, information on the infectious versus noninfectious nature of the disorder can be determined (Pusterla et al., 2006).

Immunodiagnostic testing is a serologic test that is conducted to determine the presence of specific antibodies. The antibodies present are detected by using either enzyme-linked immunosorbent assay (ELISA), radioimmuno-assay, or immunofluorescence methods. This type of testing can be used to determine the disease progression, detect if the patient is a carrier of a disease, and to distinguish between vaccination, exposure, and disease. A limitation of this test is the veterinarian needs to have a good understanding of what the results mean. A positive test can mean an active disease, but it often does not. A negative result does not mean that the horse does not have the disease. Veterinarians need a strong understanding of the sensitivity and specificity

of the test to interpret results correctly. Another limitation is the age of the horse can affect the results. Since the test does not give clear results, it is difficult to use for accurate diagnoses and is not reliably repeatable (Pusterla et al., 2006).

Lastly, molecular diagnostics can be used to diagnose infections caused by pathogens that are difficult to cultivate. For this method, Polymerase Chain Reaction (PCR) is used to amplify the sample and ELISA is used to determine if antigens are present. This method is still in the development phase, but its applications have been increasing. For it to be widely used the ease of use, safety, cost efficiency, sensitivity, reproducibility, and automation need to be improved. The speed and reliability of molecular diagnostics are advantageous to other diagnostic methods, but the limitations currently outweigh the positives. The test often produces false positives because of PCR contamination. Once this is improved it will be more widely used.

These special laboratory diagnostic techniques are used primarily for infectious disease diagnostics. Infectious disease only makes up a very small portion of all pulmonary disorders in horses, so these methods are not used often, but if they are made easier and more reliable they may be applied more frequently in the future to determine if a horse is suffering from an infectious disease before testing for other disorders.

2.5.4 Additional methods

Many veterinarians have begun to use other less invasive methods for diagnosing equine lung function disorders. Some of these additional methods have become the gold standard for specific clinics. These methods can include conventional mechanics, flowmetric plethysmography, histamine challenge, bronchodilator challenge, and forced oscillatory mechanics.

The conventional mechanics method is considered the gold standard for lung function testing, but it is an invasive method. In this method, a balloon-tipped esophageal catheter is placed in the thoracic esophagus to measure the pleural pressure. This pleural pressure is measured at the same time as the flow at the nostrils. The flow at the nostrils is measured with a pneumotachograph. Software is used to find the resistance, dynamic compliance, and end expiratory work from the measured airflow, pressure, and respiratory rate. One limitation of this device is the invasiveness causes the horse to swallow frequently, causing pressure readings to be inaccurate. It also has low sensitivity, making it difficult to detect small airway obstructions.

The low sensitivity is due to low resistance in small airways at normal breathing and changes in resistance and compliance as frequencies change. This method is applied in severe cases, but can be made more sensitive when coupled with a histamine challenge (Mazan, & Hoffman, 2003).

The histamine challenge and the bronchodilator challenge are bronchoprovocation methods used to detect low-grade airway obstruction. Low-grade airway obstruction is difficult to detect with other methods, but it has been found that horses suffering from low-grade airway obstruction have airway hyperactivity. Airway hyperactivity means the airway is more responsive to a mild stimulus than an airway in a normal horse would be. There are many causes of hyperactivity, which include airway thickening caused by inflammation, mucus, hyperplasia of the epithelial cells, and high acetylcholine or defective neural response. Histamine challenges are conducted more frequently than bronchodilator challenges. In a histamine challenge, forced oscillatory mechanics (FOM) is used to measure the resistive friction (RRS). A baseline is set with FOM and then histamine is administered in 2 mg/mL doses until the RRS increases more than 75%. Table 2.4 displays the level of obstruction based on the histamine dosage reactivity occurs at.

Table 2.4: Airway Reactivity based on Histamine

Histamine dosage where 75% reached	**Airway Obstruction Classification**
less than 2 mg/mL	Severe reactivity, probably has signs of heaves
2 mg/mL - 4 mg/mL	Moderate airway obstruction
4 mg/mL - 6mg/mL	Mild airway obstruction
6 mg/mL	Considered healthy and normal

If a horse reacts to low doses of histamine a bronchodilator challenge is typically performed. This is done to measure the obstruction and to determine if a bronchodilator treatment is right for the horse. The bronchodilator used is typically albuterol (15-minute wait time) because it has a shorter wait time after administering, but Ipratropium bromide (45-minute wait time) can also be used (Mazan, & Hoffman, 2003).

Cummings School of Veterinary Medicine at Tufts University uses a combination of

flowmetric plethysmography and a Fleisch Pneumotachograph to quantify obstructions experienced by the horse. The benefit of this method is that it is a sensitive, non-invasive test method that provides an accurate diagnosis. This method and a similar forced oscillatory mechanics (FOM) method are described in significant detail in section 2.6.

2.6 Cummings School gold standard

Cummings School currently measures equine lung function with devices utilizing a Fleisch pneumotachograph. This is a flowmeter that makes accurate, linear flow measurements. The pneumotachograph is based off of Poiseuille's Law which states that under capillary conditions in a rigid tube, the flow is proportional to the pressure lost per unit length. Figure 2.3 shows a Fleisch pneumotachograph device during testing and a schematic of the current device.

A.

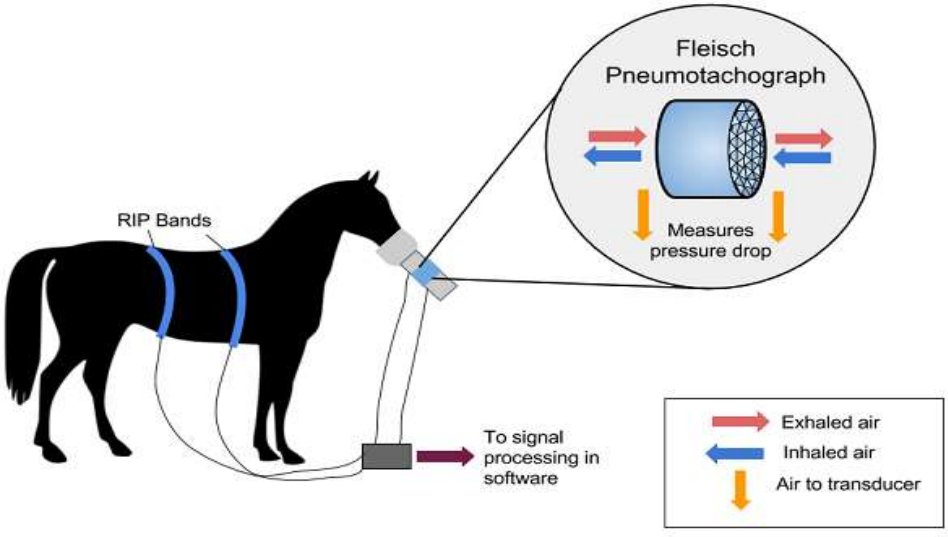

B.

Figure 2.3: A) A horse being tested with the passive Fleisch pneumotachograph device, B) A schematic of the current device and how it works

The arrows in 2.3 C represent the flow of air through the device. The red arrow represents the warmed exhaled breath of the horse. The blue arrow represents the flow of the room temperature into the horse as it inhales. Lastly, the orange arrows represent the flow of air to the pressure transducer. Air flows to the pressure transducer from before and after the capillary bed, so the pressure drop can be measured between these two locations. The pneumotachograph is calibrated by using a 3 L syringe to force a known amount of air through the system. The pressure loss, or difference in pressure between two points, creates a curve that represents velocity of the air flowing (Vitalograph, 2016). Several capillary tubes are added to prevent turbulent flow in the tube. A transducer is included in the device which collects a voltage signal from the pressure drop and converts it to a visible signal that is displayed using a software, Open Pleth, designed for the particular transducer used in the device. Along with the pneumotachograph, RIP elastic bands are wrapped around the thorax and abdomen to collect lung volume data as shown in Figure 2.4.

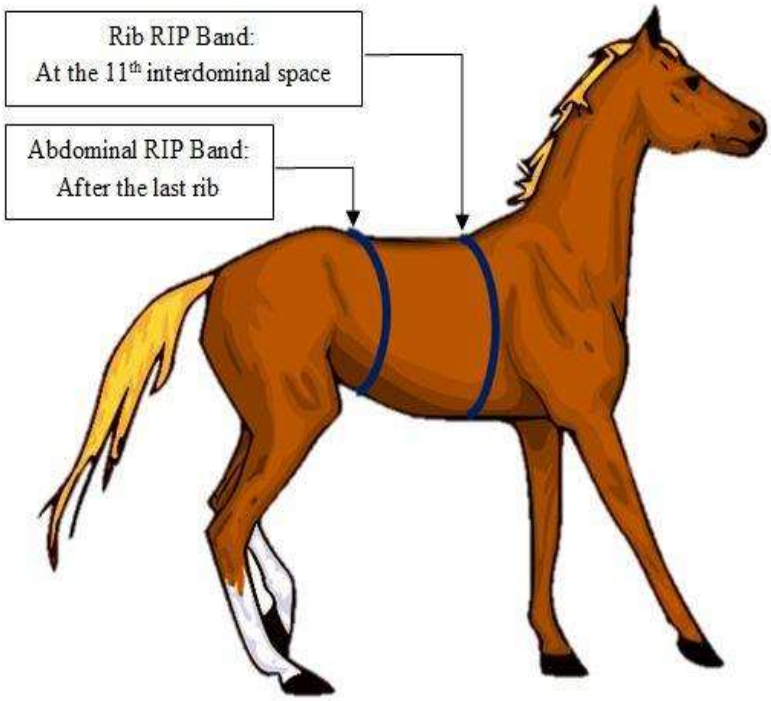

Figure 2.4: Placement of abdominal and thoracic RIP bands (Howell, 2011)

These bands are calibrated to the horse using the Fleisch pneumotachograph data and are at a voltage of zero when not moving. The bands will increase in voltage as the horse's body expands during breathing. The data from the pneumotachograph and the bands are collected simultaneously by a transducer, processed, and displayed on the same screen. The two signals are then compared to diagnose pulmonary disorders (Hoffman, 2002). An example of graphs used to diagnose disorders are shown in Figure 2.5, where the graph on top represents normal lung function and the one below it represents abnormal lung function.

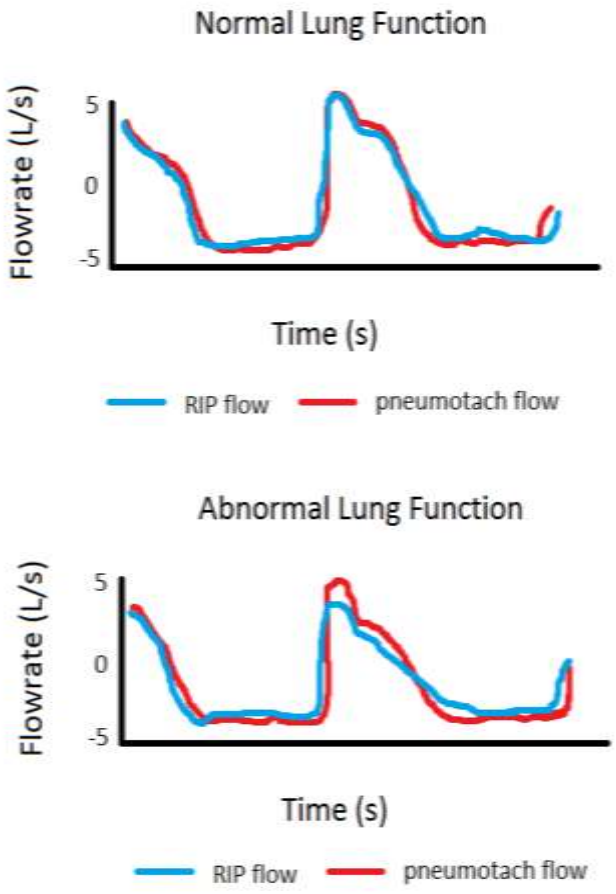

Figure 2.5: Examples of graphs used for diagnosis

The slight peak in the pneumotach flow in the lower image of Figure 2.5 represents a lower respiratory obstruction. A series of graphs displaying the data of both the RIP bands and the Fleisch pneumotachograph measurements are displayed in Figure 2.6.

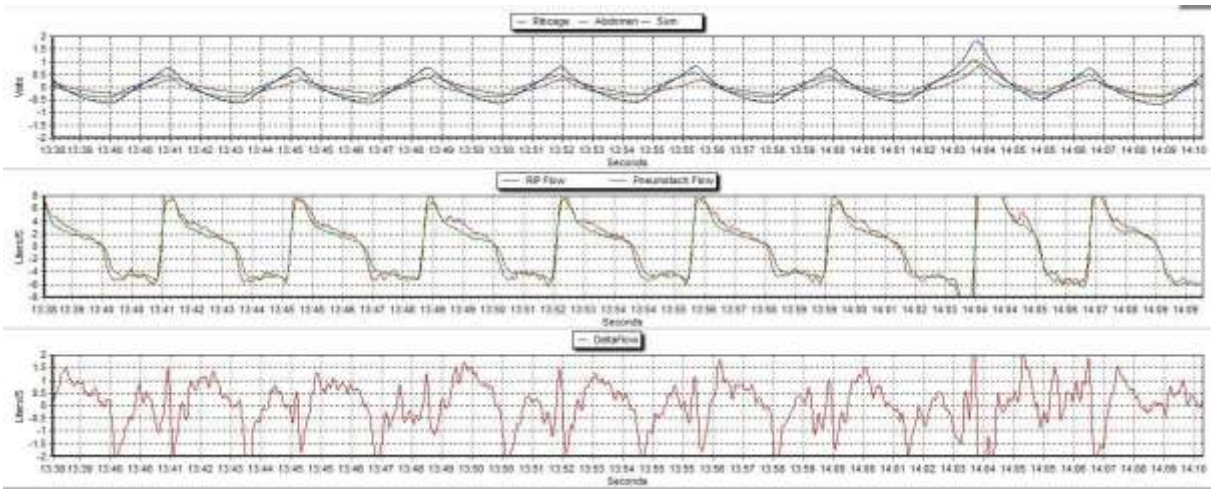

Figure 2.6: Representative data from the RIP bands and the Fleisch pneumotachograph in Open Pleth

The first graph is the voltage readings from the RIP bands. The second graph includes the conversion of the voltage data to volumetric flow data for the RIP bands, red, overlaid with the volumetric flow of the Fleisch pneumotachograph, green. The third graph is the difference between the volumetric flow rate data of the Fleisch pneumotachograph and the RIP bands.

An advantage of the Fleisch pneumotachograph is the minimum resistance to the horse's breathing during rest. This is beneficial because added resistance can result in less accurate results and larger pressure swings. However, the Fleisch pneumotachograph still provides too much resistance to breathing for a horse to use while exercising. Fleisch pneumotachographs are also capable of displaying collected data as a graph with a linear output. This makes analyzing the results and making diagnoses more efficient for the operator.

The device is attached to the horse using a facemask. For young horses or less affected horses, FOM is used when collecting data to show how the air moves through the respiratory system. From a compressed air tank, sinusoidal waves of air are directed into the horse’s nostrils and through the system which also creates sinusoidal pressure waves. The natural fluctuations from breathing are filtered out and the amplitudes of the FOM waves are analyzed as the lung function (Hoffman & Mazan, 1999). The main output of FOM is impedance which is the ratio of driving pressure to flow; the lesser the flow, the higher the impedance. Impedance signals will change based on resistance, elastance, and inertance. Elastance tends to contribute to impedance

at low FOM frequencies, whereas, inertance dominates at higher frequencies. In between frequencies is often solely resistance. There is also a revealing frequency value that can signify lung function abnormalities. A horse's normal revealing frequency is around 2.5 Hertz and will increase if there are obstructions (Hoffman & Mazan, 1999). FOM is advantageous because testing is not time consuming or invasive. Figure 2.7A shows the FOM device that Cummings School of Veterinary Medicine uses and a Figure 2.7B is a schematic depicting how it works.

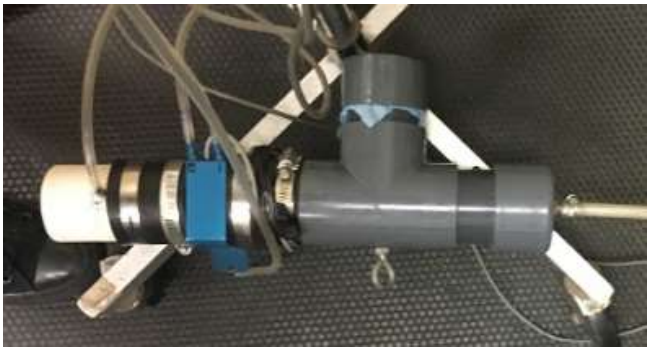

A.

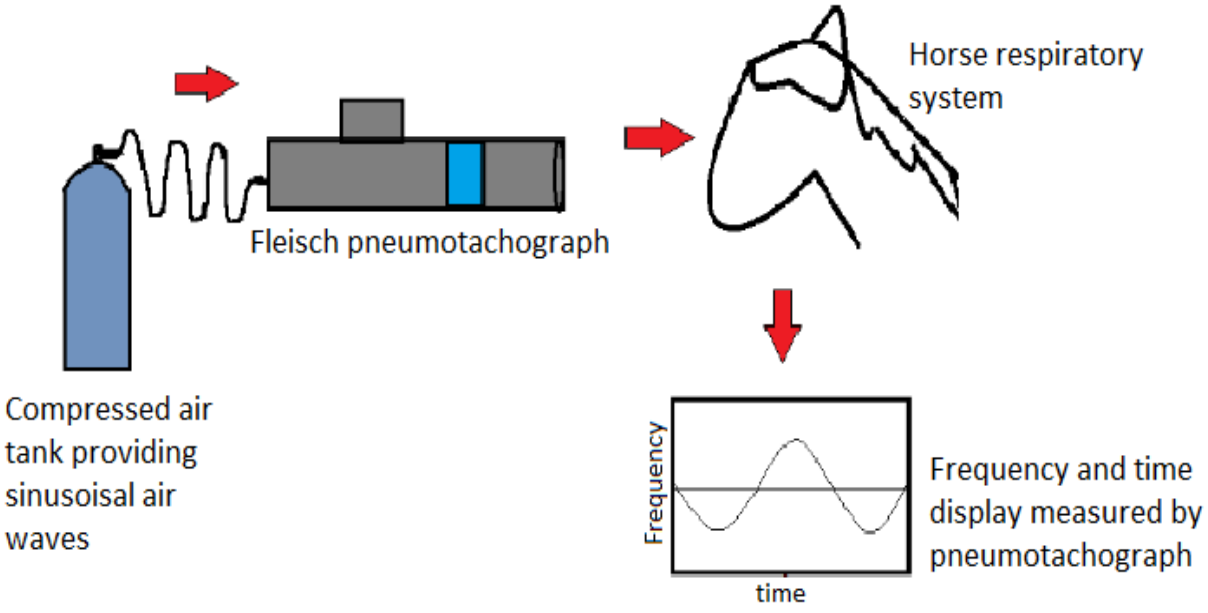

B.

Figure 2.7: A) Cummings School of Veterinary Medicine FOM device, B) Schematic of FOM method where sinusoidal air waves are forced through the pneumotachograph to the horse's respiratory system

If the horse is older or has a severe breathing disorder, the respiratory rate too closely matches the FOM signals. In this case, a similar device is used without any added sinusoidal air. The passive device can be used with healthy horses as well, but nebulized histamine is given to the horse to restrict the airways and increase the flow velocity so that the acquired signal can be read more clearly (M. Mazan, Personal Communication, September 30, 2016). This method is the most commonly used at Cummings School.

The device does have some disadvantages. Some problems with the current setup is saliva accumulating in the device, interfering with the working parts and altering the calibration, imbalance of the flow transducer, and small amounts of added resistance from the pneumotachograph (Hoffman, 2002). Another disadvantage with any signal collecting device is the potential for noisy data. To determine which breaths to actually analyze, inclusion criteria were developed by Dr. Andrew Hoffman to determine unusable data that is caused by things like sniffing or coughing. For example, if FOM is used, the data will filter out frequencies that are not between 5 and 30 Hz per minute, and inspiratory to expiratory volume ratios that are not between 0.7 - 1.3. Criteria can also be included that removes tidal volumes below 2 L and inspiratory flows less than 1 L/sec. The criteria will not filter out every unusable data point and some is still removed manually. The facemasks used on the horse can also cause irregular breathing and pressure swings. The application of the facemask and the testing process also causes a lot of anxiety for horses, often requiring sedation. A minimal amount of Xylazine must be used to avoid affecting the horse's tidal volume and ventilation (Hoffman, 2002).

2.7 Complications when dealing with horses

Horses are very large animals that can have behavioral problems such as crib biting, weaving, chewing wood, box-walking, and various other aggressive behaviors (Moore, Millar, Matsuda, & Buckley, 2003). Horses, when in human contact, can pose a serious threat due to these aggressive behaviors. Any humans dealing with horses, regardless of experience, can become victims of injuries such as bites and kicks because they can occur unexpectedly. Horse bites can be very serious as muscle rupture, fat necrosis, and severe hematoma can result (Moore et al., 2003). In a survey completed by 216 Swiss veterinarians, 75% of them were kicked by a horse at least once every year (Hausberger, Roche, Henry, Visser, 2008). A horse's instinctive response to new stimuli is random movements. These movements typically include stepping

sideways, swinging its head, or moving backwards. Being under sedation is a new environment for most horses, so they typically respond with these random unpredictable movements (McCall, 1990). This causes a dangerous situation for anyone in range of the horse's head or the device itself if it becomes a projectile during testing. Aside from their behavioral issues and unpredictable nature, horses are non-compliant, and thus will not breathe when told to do so. Therefore, invasive methods are more commonly used to measure lung function compared to non-invasive methods.

2.8 Significance of developing devices for horses

Horses that live in the northern hemisphere are usually fed hay that is preserved in humid environments during the summer (Robinson, Derksen, Olszewski, & Buechner-Maxwell, 1996). Moisture levels exceeding 20% promote microbial activity in hay, and therefore dry winters do not pose a concern in stimulating antigen growth (Knapp, Holt, & Lechtenberg, 1975). However, in the winter, dust is a concern as it worsens respiratory conditions and diseases. Hay is usually stored off the ground in stables in the winter, and over long periods, dust accumulates that can affect the surrounding environment. The humidity in the summer causes antigens such as thermophilic molds and actinomycetes to grow in the hay, and when horses breathe in these antigens, neutrophils attack the lung causing an inflammatory response. Specifically, both histamine levels in the bronchoalveolar lavage fluid and plasma levels of inflammatory mediators are increased. Chronic obstructive pulmonary disease (COPD) is therefore caused by the delayed hypersensitivity response that is caused from these antigens as the airways become obstructed and exhibit nonspecific hyper responses. Additionally, mucus accumulates in the airway, causing stabled horses to heave and cough (Robinson et al., 1996).

Equine lung function disorders are prevalent, as up to 80% of stable horses can be suffering from inflammatory airway disease (IAD) (Cumming Veterinary Medical Center, 2016). It is important to provide an early diagnosis and therapy treatment for young horses with IAD because it can lead to coughing, heaving, or even permanent tissue damage, especially in racehorses (Wood, Newton, Chanter, & Mumford, 2005). The performance levels of race horses with pulmonary disorders, especially in younger horses, significantly decreases (Sanchez, Couetil, Ward, & Clark, 2005). The race horsing industry is expensive, not only in the USA, but worldwide. Additionally, equine veterinary care is also costly; performance racehorses require

annual care that costs approximately $500 to $1,400 per horse (Gordon, 2009). In the state of Kentucky, the amount of money that is bet daily on horse races can rise up to $1.2 million, if not higher, for a single race track. As of 2009, a tax of 3.5% was issued on horse races, and therefore the government receives a significant revenue. Additionally, in 2010, Australian governments earned more than $289 million due to a 4% tax placed on gambling turnovers (McManus, Albrecht, & Graham 2013). Gambling turnover revenues are significant as they support governments, the racing industry, and charities. For example, the Hong Kong Jockey Club (HKJC), is a non-profit organization that donates a portion of their annual surplus to various charities, such as ones that support Autism disorders, and community projects (McManus, Albrecht, & Graham 2013). If horses are unable to perform at their best performance levels due to pulmonary disorders, a significant amount of money will be lost in the horseracing industry.

2.9 Conclusion

IAD and other pulmonary disorders can greatly impact the performance and health of all horses. Current diagnosis methods are complex, invasive, and expensive, making it challenging for horse owners to receive adequate diagnosis and treatment for their horses suffering from subclinical lung function disorders. The Cummings School of Veterinary Medicine at Tufts developed a non-invasive method to test for lung function abnormalities. This device has proven to be successful, but has some disadvantages as well. The device is heavy and protrudes far off the face of the horse, causing a risk of injury to the operator. The device also uses a Fleisch pneumotachograph component that is expensive and no longer produced. Our team was tasked with developing an improved method of measuring lung function of horses. In the following chapter, we discuss our design process to develop an improved method for measuring equine lung function.

3.0 Project strategy

3.1 Initial client statement

After speaking with our sponsor, Dr. Mazan, and reviewing literature on the topic of equine lung function testing, it was noted that lung function testing in horses is very difficult, and that there is no universal gold standard in place. Cummings School of Veterinary Medicine at Tufts' gold standard is the passive airflow device incorporating a Fleisch pneumotachograph. There are some concerns with this device including the risk to the human user, the cost, the accuracy, and the resistance it adds to the horse's normal breathing. Based on these concerns and the need for accurate equine lung function testing equipment, it was determined that the overall goal of the project was to develop a way to measure airflow in horses with inflammatory airway disease or other subclinical pulmonary obstruction disorders in order to detect and develop a treatment strategy in the early stages of the disease.

3.1.1 Stakeholders

The stakeholders of our project include equine patients that will be tested with the device, their owners, our team, Dr. Mazan, and other veterinarians who will use the device. Because the device will be directly used on horses, it is important that the device does not harm them. The horses and their owners, the clients, will benefit from the device because it will allow for early diagnosis of lung function disorders. When disorders are diagnosed early, treatment is often more successful and less expensive. In addition to the horses and clients, the veterinarians that will use the device are stakeholders. Dr. Mazan is the primary stakeholder because the device was designed specifically around her needs, but other large animal veterinarians' needs were also important to keep in mind during the design process. The critical thing to keep in mind was that many large animal veterinarians travel to their clients. Finally, our team is a stakeholder because we designed the device to successfully meet the needs of our sponsor and were ultimately responsible for its ability to meet her needs.

3.2 Technical design requirements

Our first task was determining the limitations of the current device. Figure 3.1 shows the current device labelled with its identified limitations.

Figure 3.1: Limitations of the current device

With these limitations in mind we developed a list of objectives that we wanted our design to meet. These objectives are explained in detail in the following section.

3.2.1 Objectives

Table 3.1 displays the objectives for our new lung function testing design. The rest of the section explains the objectives in more detail.

Table 3.1: Summary of our design objectives.

Objective Number	Objective Description
1	Accurately obtain lung function signals
2	Minimize resistance to horse's breathing
3	Cannot require compliant breathing
4	Minimize risk for human user
5	Less expensive than current device
6	Compatible with LabVIEW
7	Portable
8	Meets veterinary standards

3.2.1.1 Accurately obtain equine lung function signals (± 0.33%)

Currently, calibration of the device relies on a three-liter calibration syringe that provides a set volume. This is the standard way to calibrate an equine lung function testing device, but the particular syringe used can only calibrate the device to an accuracy of ± 3.33%. Our sponsor wanted an improved accuracy to better distinguish the signal differences between the flow rate measured by the RIP bands and airflow measured by the sensor.

3.2.1.2 Minimize resistance to the horse's breathing

Resistance causes inaccuracies in measurements and potentially results in discomfort for the horse. Increased resistance caused by the device can limit the amount of airflow measured by the sensors and therefore misrepresent the lung function of the horse. Also, if the resistance is high enough to physically impede the horse's ability to breathe, then the device would become hazardous to the horse's health. Dr. Mazan would like to perform tests while the horse is exercising. This is not possible with the current device because it is cumbersome to use with a moving horse and adds too much resistance, making it difficult for the horse to breathe. When resistance is sufficiently minimized, the device can be used during exercise. Resistance can be minimized by avoiding designs that create obstructions to airflow and/or block sensors from gathering measurements.

3.2.1.3 Cannot require compliant breathing

Currently, lung function testing in humans requires the patient to follow directions of when to forcibly exhale with maximum effort, which is considered compliant breathing. A horse is unable to follow these directions; therefore, the device must acquire measurements of airflow without compliant breathing.

3.2.1.4 Minimize risk for the human user

The current device is heavy, 3 lbs., and protrudes out from the horse's facemask approximately 12 in. This increases the risk to the human user because they need to be close to the horse during testing to support the device and horses often shake their heads. There have been documented cases of the current device causing harm to human users, such as concussion and sutured head wounds. Dr. Mazan felt that the risk of harm was an important issue to address with the new design of the device. Reducing this risk involved reducing the weight and the length of the device. One way to reduce the weight was to use lighter materials for the internal

components. The housing of the new device consists of a softer, more flexible material that reduces the risk of harm to the operator upon impact.

3.2.1.5 Less expensive than the current device preferably less than $1000

All the components required for the current device total $18,000. A less expensive device that is able to accurately measure lung function increases its accessibility for veterinary clinics. Dr. Mazan would like to standardize equine lung function testing, and in order to do that, small traveling veterinarian practices need to be able to afford the equipment. Based on this, and our available budget, it was determined that the newly designed device should cost no more than $1,000.

3.2.1.6 Compatible with LabVIEW software

Cummings School of Veterinary Medicine at Tufts uses the current device in conjunction with proprietary software that was designed for the transducer used in the system. The proprietary software, Open Pleth, provides data and graphs obtained from the current device, but the display is small and difficult to read. Our sponsor has access to LabVIEW software and is interested in the idea of developing a way to process the data through LabVIEW. LabVIEW allows more customization and provides an interface that is easier to understand. A clearer interface makes it easier for Dr. Mazan to explain the process to her clients.

3.2.1.7 Portable

The limitations of the current device include a setup that requires a lab space and multiple operators, making it difficult to be used in other locations, such as at a client's home or at the track. By creating a device that is able to be used onsite, access to lung function testing is increased. The key to making the device portable involved making a small device that required fewer operators.

3.2.1.8 Meets veterinary standards

The device was intended to be used on horses and should meet the veterinary standards required for medical devices. It was imperative to consider the safety and well-being of the horse when designing a device and conducting tests. Various standards exist in the medical device industry to ensure human safety, so it was important to research any parallel standards for veterinary medical devices.

3.2.2 Constraints

When developing a design to meet the objectives, there were many constraints that needed to be taken into consideration. One of the largest constraints on this project was the overall budget. Working within a budget of $1,000 limited what could be spent on prototyping and testing. Other constraints considered when designing the device were the veterinary standards for veterinary medical devices. Anything that is designed needs to meet these standards for it to be applied in equine clinical tests. Working with horses was also a constraint because they are large, non-compliant, and unpredictable animals which can cause a dangerous work environment and can lead to many complications during device development. The horse cannot give feedback on the device, so every component of the device needed to be tested to ensure compatibility and comfort for the horse. An additional constraint was the time frame of the project. A device needed to be designed, prototyped, tested, and validated in nine months. Lastly, a constraint for this project was the physical location of the current device and where we completed our design work on the device. Since Cummings School is the only location in the North East that owns the Fleisch pneumotachograph and uses the device frequently for research and clinical testing; the device had to stay on site at all times. The travel time between Cummings School and Worcester Polytechnic Institute (WPI) had to be factored in for all meetings and reduced the amount of time spent with the current device. In order to address these constraints, we planned our purchases carefully and used a lot of resources available to us at WPI. We researched veterinary standards ourselves and checked in frequently with our veterinarian sponsor to ensure our ideas were compliant with any standards. In order to work efficiently, we developed a timeline of different tasks and established deadlines. Several tasks could be completed on campus for when traveling to Cummings School was not possible.

3.2.3 Functions and means

Our new design was divided into four functional blocks to help ensure that we met the necessary objectives for our sponsor. Figure 3.2 displays the functional blocks we created. Table 3.2 elaborates on the functions given in Figure 3.2 by stating the different methods we brainstormed that can be used to complete each function.

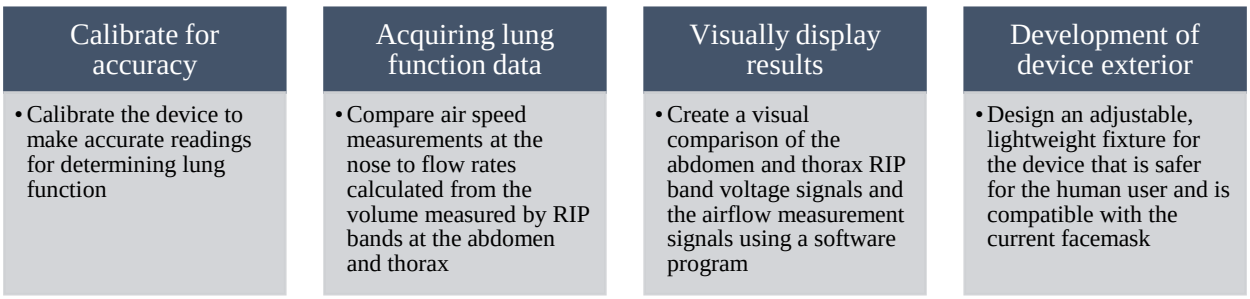

Figure 3.2: Functional blocks

Table 3.2: Functions and means chart

Functions	**Means**
Calibrate Device	● 3 L syringe is the current lung function testing standard for calibrating volume ○ Accurate to ± 3.33% ● Improve accuracy of syringe ± 0.33% ○ Could use linear encoder ● Have known flows to test with devices that measure flow rate directly ○ Use a calibrated flowmeter ○ Use a wind tunnel
Measure airflow of horse's breath	● Measuring pressure drop ○ Fleisch pneumotachograph ○ Lilly pneumotachograph ○ Venturi meter ● Measure temperature ○ Hot-wire anemometer ○ Silicon airflow sensor ● Measure RPMs ○ Three-cup anemometer with tachometer ● Measure deflection ○ Strain gauge
Display voltage signals into a readable display	● Graphical display ● Open Pleth software for equine lung function testing ● LabVIEW ● Arduino ● Transducers
Device exterior/ attachment to horse	● Facemask ● Nose inserts ● Adjustable straps ● Consider pressure points of horses

The first functional block focuses on the calibration of the device. Having a method to accurately calibrate the device is key to the device functioning accurately, so this was a critical component of the project. The standard calibration device is a 3 L syringe. The syringe on the market is $250-$400. Our team designed our own, inexpensive, calibration syringe using PVC piping and an aluminum piston that is 4.07 L. For sensors that measure airflow directly, volume will not suffice to calibrate the device. In this case, known flow rates must be used to create a calibration curve. Handheld flowmeters or a wind tunnel can be used for this application.

The second block includes various measurements that could be collected from the horse patient to measure their lung function. We had to choose a type of sensor to best collect these measurements and determined airflow within the desired accuracy. Various sensors or methods of measuring airflow directly or indirectly are given in Table 3.1 as the means for meeting the airflow measurement function. To complete this functional block, it was determined which sensors or combination of sensors would best measure the data we need. The advantages and disadvantages of different device concepts are further analyzed throughout Chapter 4, where we discuss the process used to determine our final design.

The visual display component of the design is the next block. This was done using software to collect voltage signals from a transducer and display it on a virtual interface. There ideally should be a linear relationship between the inputs and the voltage signals. It should also be clear to understand so veterinarians can explain the testing process to their clients. LabVIEW and Arduino are two options that can be used to acquire data from a sensor.

The fourth and final functional block is the device exterior. We wanted to design the housing of our device to be adjustable so that it can be stable and comfortable when attached to the horse. The material should minimize risk to the horse, the operator, and all personnel present in the testing room. To minimize this risk, the housing should be lightweight, no more than 1.5 lbs., and not protrude more than 6 in. from the horse’s face. These dimensions decrease the size of the device by 50%. We also considered how and where the device will attach, so that accurate measurements can be made and to ensure comfort, particularly avoiding pressure points that may irritate the horse if the device directly contacts them. The nose and lips are the most sensitive areas on a horse's face, so when designing a mask, direct contact with these areas needs to be avoided (Preuschoft, Witte, Recknagel, Bär, Lesch, & Wüthrich, 1999).

3.2.4 Specifications

Our design must meet certain specifications in order to provide accurate and useful data. Currently, the device is calibrated with a 3 L syringe that provides an accuracy of ± 3.33%. Our sponsor would like the new device to be calibrated to ± 0.33%, or the equivalent percentage of error, if possible. Not all sensor types can be calibrated with only a known volume, so depending on the sensor used, an alternative calibration technique will need to be determined. The device must also measure volume measurements from the horse. A horse's resting volume is approximately 5 L. The resting flow rate of a horse is 60 L/min and the galloping flow rate is 1,500 L/min. The device must accommodate these parameters. The device must also convert the collected measurements into a visible signal in order to analyze lung function. Visible signals include flow/volume loops and breaths over time. The weight of the entire new device should be less than the current device, which is approximately 3 lbs.

3.3 Design requirement standards and specifications

Different standards must be met for the design and operation of various components of our device. This includes standards related to the biocompatibility, the flow output, and the use of animals during testing.

The device design must consider the safety and comfort of the horses it will be used on. The material should be nontoxic and not cause any allergic reactions. Also, the device cannot prevent airflow in or out of the nose because horses are obligatory nose breathers. Methods to research and evaluate the effects of different materials should be developed to ensure the device meets the ISO 10993-2:2006 Biological Evaluation of Medical Devices standard (International Organization of Standardization, n.d.). Ideally, the device should also be designed to meet the ISO/IEC 17025:2005 standard for competence while calibrating in a laboratory setting, as well as the ISO 7066 standard which provides procedures for designing calibration curves when measuring flow rate. The standard also supplies ways for assessing the uncertainty in the calibrations (International Organization of Standardization, n.d.). IEEE 2700-2014 provides a framework for sensor performance, including units, conditions, and limits which should be considered when choosing a sensor for our new design (IEEE, 2014).

Our device was designed to be used for testing with multiple horses, requiring proper cleaning of the device. USP-NF 797 provides a procedure for properly sterilizing the device to

avoid the spread of infections (Pharmacopeia, U. S., 2014). The device was designed with this in mind so that the shape and materials are able to be sterilized properly. There is also a standard to be followed when administering drugs. To conduct lung function testing, the horse is often sedated. USP-NF General Chapter 1151 outlines the recommended dosage and quality requirements (Pharmacopeia, U. S., 2009). These standards are important to follow because an overly sedated horse could cause inaccurate results during testing due to a change in breathing pattern.

The device was designed specifically for horses. Testing this device on live horses requires approval by the Institutional Animal Care and Use Committee (IACUC). According to the American Veterinary Medical Association (AVMA), a Massachusetts law requires client records to remain confidential unless the client releases the veterinary records of their animal (American Veterinary Medical Association, 2015). This caused difficulty when trying to obtain samples of data from client owned horses, compared to research horses. Also, although veterinary medical device standards are not as comprehensive as human medical devices, the U.S. Food and Drug Administration (FDA) has a guideline in the compliance policy guide manual (CPG Section 607.100) addressing proper labeling and species designation to avoid device misuse (U.S. Food and Drug Administration, 1995).

3.4 Revised client statement

After developing a better understanding of the project through meetings with Dr. Mazan and researching the topics of equine lung function testing and the physiology of the equine respiratory system, it was determined that the need for this device was more prevalent than one may imagine. Due to the fact that up to 80% of horses can have a lung function disorder, there is a need to be able to test horses for pulmonary disorders on a regular basis, especially since many of the disorders are subclinical (Cumming Veterinary Medical Center, 2016). In result, the overall goal of the project evolved to be: to develop an improved device to measure equine lung function that can be used to detect abnormalities in airflow and diagnose horses with inflammatory airway disease or other subclinical pulmonary obstruction disorders. This improved goal placed our focus on developing a method to improve the airflow measurement component of the device because this would resolve many of the concerns with the Fleisch pneumotachograph.

3.5 Management approach

Our project approach was divided into three sections: identify, invent, and implement. This approach ensured that we would meet the objectives determined from discussions with our sponsor and properly follow the design process.

3.5.1 Identify

In the identify stage, the first step was to determine the need and significance of the project. This included discussions with our sponsor, research about the prevalence of lung function disorders in horses, and research into the benefits provided by the current device and similar devices. Characterizing the current device provided insight into the specifications for measuring lung function and limitations of the device that had to be improved upon. After this research was completed and the current device was characterized, the need and the design space for the new design was well-defined. Our project objectives were created and our constraints were discussed.

3.5.2 Invent

From characterizing the current device, we determined specifications of what our new design would need. We also designed a LabVIEW program to read and acquire data from our new device. Before creating a LabVIEW program for the new device, we developed a LabVIEW program to read in data from the current device. This allowed the team to test our understanding of the current device and the signal processing necessary to create the expected visual data output. Once a successful LabVIEW program was created for the current device, changes were made to the base program to accommodate the new device.

Next, a list of brainstormed possible devices to measure equine lung function was created based on research and a better understanding of the limitations of the existing device. These ideas were then further narrowed down to four alternative designs. A CAD model or an assembly for each of our alternative designs was created. Our final design was chosen based on research, advisor input, feasibility studies, and feedback as discussed in Chapter 4. Lastly, the final design was prototyped and tested.

Testing the different concepts is difficult because it is not practical to test each concept on a horse. Using human test subjects can be used to test some aspects of horse breathing, but humans cannot produce the volume or flow rates that a horse can produce, thus a testing

instrument needed to be designed that can accurately model a horse's breathing. The gold standard for calibrating and testing the Fleisch pneumotachograph is using a 3 L calibration syringe. We decided to use a similar device to model a horse and test our concepts. We chose to construct our own syringe because a 3 L calibration syringe can cost anywhere from $300-$500 depending on the manufacture and the desired accuracy. We used SolidWorks to design the components of our syringe and then we created a final assembly to make sure that there was no interference between parts when the piston was compressed and decompressed. Figure 3.3 displays an exploded view of the SolidWorks assembly.

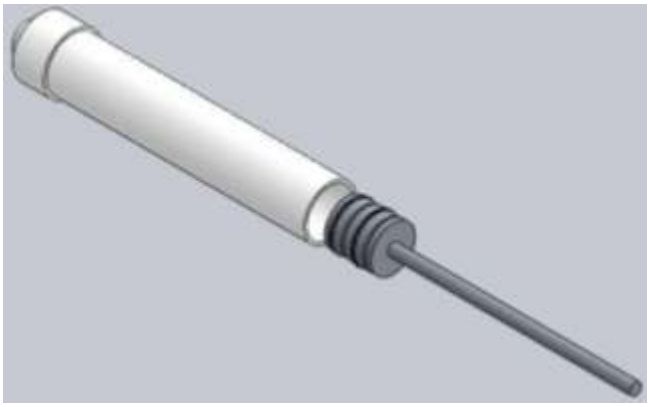

Figure 3.3: Exploded view of the SolidWorks calibration syringe model

We used this model to create a bill of materials and purchase the required parts. We specifically designed the syringe to use a standard PVC pipe size (4 in.-diameter) as the body and a standard reducer coupling as the nozzle (4 in. to 2.5 in.), so these parts were easily purchased at Lowes. The PVC piped purchased was 2 ft. in length. The only modification made to these parts was the inside edge of the PVC pipe was chamfered using a handheld chamfering tool and the internal surface was smoothed at the end where the piston was inserted. To manufacture the piston, a 4 in.-diameter 6 in. long stock of aluminum was purchased. Following the SolidWorks design, the piston was machined from the aluminum stock using a manual lathe. The overall diameter was decreased to approximately 3.85 in. and the surface on both ends was finished. O-ring grooves were then cut to accommodate 2-240 O-rings. Three O-ring grooves were cut to provide an air-tight seal. A band saw was used to remove the excess 3-in. of length. Lastly, a ¾ in. hole was drilled using the manual lathe and it was tapped, so that a wooden ¾ in.

dowel could be inserted as the handle. The handle was glued in place with gorilla glue. O-rings were placed in the first and last O-ring grooves and the piston was coated in silicon vacuum grease to guarantee a complete seal and also reduce the friction, thus allowing the piston to slide easier. Figure 3.4A shows the disassembled final product and Figure 3.4B shows the assembled, completely depressed syringe.

A. B.

Figure 3.4: A) Disassembled syringe with the body on the left and the piston and handle on the right; B) Assembled and depressed syringe

The volume of our syringe was calculated by finding the volume of the body and subtracting the volume of the piston. The volume was also measured by filling the syringe with water and then measuring the volume of water. From both of these methods it was determined that the volume of the syringe is 4.07 L.

3.5.3 Implementation

Before constructing and testing the new device, an analytical model was developed to simulate lung function testing. LabVIEW was used to construct an interface that displays the desired pressure and volume signals. The pressure drop that normally occurs across the pneumotachograph in the current device can be set as an input to generate a sample output. This helped us understand exactly what our device's output should look like.

After making a model, our new device was calibrated, tested, and compared with the model data. Once our experimental testing was determined to be accurate, the new device was used in a clinical setting to measure equine lung function.

3.5.4 Management tools

The work breakdown structure (Figure 3.5) displays the objectives that the team completed in order to create a successful project deliverable.

Figure 3.5: Work breakdown structure

In Figure 3.4 the completed tasks for each objective are clearly stated. The design phases of the work breakdown include brainstorming and modeling solutions to meet our objectives. We used materials that are durable, lightweight, biocompatible, and affordable, such as PVC and rubber, similar to the current device. The exterior materials are soft and flexible to minimize risk of injury to the horse and operators. Research was done on standards regarding veterinary medical devices and procedures to ensure that the materials chosen were acceptable to use in this application.

Our team developed Gantt Charts to manage the timeline of our tasks and milestones for the project. Three Gantt Charts display the team's tasks for each seven-week term (Appendix A). For each task, a time frame was allotted for it to be completed and the percentage complete was estimated and recorded at the end of each term.

3.5.5 Financial tools

Our team was supplied with a budget of $1,000. We managed our spending for the duration of the project by keeping a detailed budget in an EXCEL spreadsheet. The budget was organized based on project component or design. For example, all of the items used in our final design were grouped together. We limited our spending by using resources available to us already. When having to purchase items, we carefully considered the costs and benefits beforehand and avoided buying excess items. A spreadsheet of our total spending is located in Appendix B. Our final amount spent was $662.74 with $337.26 remaining.

4.0 Design process

4.1 Needs analysis

Our team was fortunate enough to be given a specific project statement from the beginning. After meeting with our sponsor only a few times for clarification, the final objectives for our new device design were developed. These objectives are displayed in Table 4.1 as a reference. The objectives highlight what our new design must incorporate for it to be useful to our sponsor. Some of our main focuses included minimizing risk of injury to the human users and making the device more cost effective.

Table 4.1: List of project objectives

Objective #	Objective Description
1	Accurately obtain lung function signals
2	Minimize resistance to horse's breathing
3	Cannot require compliant breathing
4	Minimize risk for human user
5	Less expensive than current device
6	Compatible with LabVIEW
7	Portable
8	Meets veterinary standards

In order to determine which objectives were required for a successful design and which were desires of our sponsor, the importance of each was ranked by both the team and our sponsor. Table 4.2 shows each objective and its rankings for each party with an overall average. The overall average of each objective was then used in a pairwise table (Table 4.3) to compare the significance of the objective to each other.

Table 4.2: Objective rank comparison

Objective #	**1**	**2**	**3**	**4**	**5**	**6**	**7**	**8**
Team Rank	3	4	5	4	3	2	1	5
Sponsor Rank	5	5	5	5	4	3	5	5
Weight	4	4.5	5	4.5	3.5	2.5	3	5

Table 4.3: Pairwise objective comparison

Objective #	**1**	**2**	**3**	**4**	**5**	**6**	**7**	**8**	**Total**
1		-1	-1	-1	1	1	1	-1	-1
2	1		-1	0	1	1	1	-1	2
3	1	1		1	1	1	1	0	6
4	1	0	-1		1	1	1	-1	2
5	-1	-1	-1	-1		1	1	-1	-3
6	-1	-1	-1	-1	-1		-1	-1	-7
7	-1	-1	-1	-1	-1	1		-1	-5
8	1	1	0	1	1	1	1		6

After comparing our team's rankings and our sponsor's rankings, we were able to determine which objectives were classified as needs and which were classified as wants. Table 4.4 separates the objectives into these two different categories.

Table 4.4: Needs and wants

Needs	Wants
● Lighter than 1.5 lbs. ● Does not require compliant breathing ● Biocompatible ● Measures flow both ways ● Airflow and RIP band measurement needs to be synced ● Non-invasive ● No more than 6” of protrusion	● Accuracy (± 0.33%) ● Cost (less than $1000) ● Compatible with both foals and horses ● Compatible with LabVIEW ● Portable

The main size constraints for the device are protrusion of no more than 6 in. and a weight of no more than 1.5 lbs. These values were identified as a need because they will greatly reduce the risk to the human user, by decreasing the overall size and weight of the device by at least half.

4.2 Concept of designs and further testing

4.2.1 Concept map

The concept map displayed in Figure 4.1 was developed based on our brainstormed ideas. This concept map displays the connection of different components of our final desired design and potential solutions for measuring airflow either directly or indirectly. By developing a concept map to organize our potential solutions, we were able to more easily identify the most suitable design. The team brainstormed eight alternative device concepts which are listed in Table 4.5.

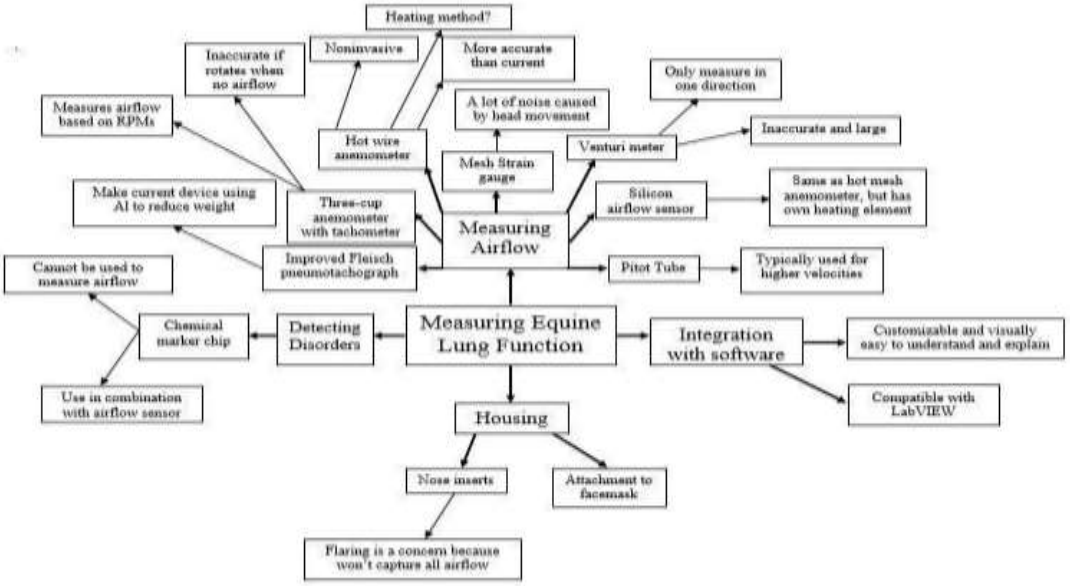

Figure 4.1: Concept map based on the functions of the design

Table 4.5: List of conceptual designs

Design #	Design Ideas
1	Improved Fleisch pneumotachograph
2	Three-cup anemometer
3	Hot-wire anemometer
4	Mesh strain gauge
5	Venturi meter
6	Chemical marker chip
7	Pitot tube
8	Silicon airflow sensor

These were brainstormed through initial research on the concept of measuring wind speed and testing for respiratory disorders. The next step in the process was determining which of the concepts were feasible for measuring equine lung function and narrowing down the list to allow for a more in depth analysis to be completed on a few potential concepts. To narrow down the list of potential designs, we presented the ideas to our advisors and sponsor to get their feedback on the feasibility of each concept and then conducted research based on their feedback.

4.2.2 Advisor feedback

Each concept was discussed with our advisors and they provided feedback based on their knowledge of the method or sensors. The main concern with the first concept, the improved Fleisch pneumotachograph, was the machinability of a bed of capillaries made from aluminum. Our mechanical advisor suggested brazing small thin sheets of metal to create the capillary bed. However, he cautioned that making an improved Fleisch pneumotachograph would be a manufacturing project not a design project. Due to our limited machining knowledge, our advisors believed it was impractical for us to machine (Robert Daniello, Personal Communication, September 23, 2016).

The main concern our mechanical advisor had for the three-cup anemometer was the accuracy. The turbine will have a delay in starting and stopping because of inertia and this delay could produce inaccuracies when overlaying the RIP band data with the sensors. Overall, he believed that the accuracy could be corrected with software and thus was not a major deterrent from pursuing the design further (Robert Daniello, Personal Communication, September 23, 2016).

Our mechanical advisor agreed that the hot-wire anemometry would work, but he had concerns about the varying moisture concentration between the flow in and out. He believed using a calibration factor would account for the moisture content since all horses should have a similar moisture concentration in their breath (Robert Daniello, Personal Communication, September 23, 2016).

There were many concerns with the original idea of a mesh strain gauge. One concern was the sensitivity of the strain gauge. Another potential concern was that the sensor would be very fragile, which is not ideal for a device being used on a horse. Lastly, any temperature changes or quick movements could convolute the signal causing a lot of noise that will make the desired data difficult to analyze. Also, our mechanical advisor had many questions on the fixation of the inert wire scaffold that the strain gauges would be mounted on. The fixation method is key to reducing noise, but must not reduce the sensitivity of the gauge (Robert Daniello, Personal Communication, September 23, 2016).

Through discussions with our mechanical advisor, we determined a venturi meter would not work for this application. One issue with this concept is that venturi meters are typically

designed for larger pressure drops, which would not be sensitive enough to measure the pressure drop caused by a horse breathing. Another concern is the potential high resistance to breathing the venturi meter would cause for the horse. Venturi meters can only measure flow in one direction and for this application we need to be able to measure the flow in both directions to capture the horse's inspiration and expiration. Lastly, there are major concerns about the size of the venturi meters. Venturi meters are often quite large to increase their sensitivity, but since one of the main goals of the project is to make the device smaller and safer, this method would not be ideal (Robert Daniello, Personal Communication, September 23, 2016).

The major limitation of a chemical marker chip is that it needs to be used in combination with another airflow measurement device because it detects chemicals in the air, not the flow data that is desired (Robert Daniello, Personal Communication, September 23, 2016). It is also very difficult to design, as it requires small scale circuitry and a chemical that can detect particles that are characteristic of lung diseases. Another constraint of the chemical marker chip is that it would not be sensitive to all pulmonary diseases, however, it will act as a verification for the ones that it can detect (Marsha Rolle, Personal Communication, September 27, 2016).

A pitot tube works better for higher velocities and is frequently used for transient flow. The velocity of a horse's breath is significantly slower than the airflow over an airplane wing, which is the typical use of a pitot tube. This will cause it to not be sensitive enough for the lower velocity applications. Measuring laminar flow would be more ideal than measuring transient flow because it has known equations and can be more easily processed. Our mechanical advisor believes horses' airflows can be simplified to laminar flow (Robert Daniello, Personal Communication, September 23, 2016).

The silicon airflow sensor operates similar to hot-wire anemometry, as it measures airflow using the change in temperature of a heated component. Discussions with our advisor revealed that the silicon airflow sensor had potential as a concept because moisture did not affect its measurements like hot-wire anemometers. The silicon airflow sensor, however, is very small and could be too fragile for this application. The technology is also relatively new and sensors are expensive with minimal options available to work with (Robert Daniello, Personal Communication, September 23, 2016).

4.2.3 Literature and research

4.2.3.1 Improved Fleisch Pneumotachograph

After our mechanical advisor mentioned brazing metal being an option for producing an improved Fleisch Pneumotachograph, we researched the different techniques to evaluate if they were within our technical background. Each brazing technique follows the idea of welding metal in the presence of a filler material. Torch brazing utilizes a torch that produces a steady flame to heat the metal to the right temperature and is typically used for small volume pieces. The capillary bed might be too large for the torch brazing technique and it requires operator skill, which the team does not possess. Furnace brazing has a range from medium to large volume pieces that are raised to high temperatures by convection. This technique does not require any operator skill and would be sufficient for the capillary bed (Schwartz, 2003). However, the team does not have access to a furnace which could braze.

4.2.3.2 Three-cup anemometer

To address our advisors concerns about the accuracy of this concept, we researched real world applications of three-cup anemometers. Three-cup anemometers are commonly used as reliable wind sensor instruments for weather stations, which indicates others were able to overcome the accuracy issues. Through experimentation, researchers concluded that three-cup anemometers can be simplified to a linear relationship between wind speed and revolutions as well as follow mathematical models that account for the effect the mass has on the device rotating faster or slower than the actual wind speed (Kristensen, Hansen, & Hansen, 2014; Saylor Academy, 2011).

4.2.3.3 Hot-wire anemometry

The main concern determined for proceeding with the hot-wire anemometry concept was the effect humidity can have on the sensing element. Standard practice for hot-wire anemometry when used to measure air is to neglect the humidity's effect (Durst, Noppenberger, Stil, & Venzke, 1996). Research shows that not incorporating humidity will result in an error in the velocity reading of 1-5%. To adjust for humidity, there is a correction factor to Nusselts number using Reynold’s number and temperatures as shown in Equation 4.1.

$$\mathrm{Nu} = (0.24 + 0.56\mathrm{Re}^{0.54})[\frac{\mathrm{T_f}}{\mathrm{T_a}}]^{0.17}[1 + \mathrm{Ax} + \mathrm{Bx}^2] \text{ (Eq. 4.1)}$$

Despite humidity being the major concern of our mechanical advisor, the literature illustrates that humidity is not a concern for hot-wire anemometry measurements and provides an equation to correct for humidity. The literature provided the team with the ability to pursue this design by addressing the major concern of our mechanical advisor.

4.2.3.4 Mesh strain gauge

After further research on the mesh strain gauge, it was determined that the mesh would either need to be very stiff to reduce the fragileness of the material or it would need to be adhered firmly to the walls of the housing. Both of these solutions will decrease the sensitivity making it harder to read the small changes the horse's breath will cause. Without making the mesh stiffer, the device will be too fragile and there will be a lot of noise in the readings. While researching this concept, another similar concept was found that was not as fragile, so it would be better for our application. This new design concept was strain gauges on hair like structures. This design has been used in the past to measure low wind speeds and is based on a biological function of some insect hair that is used to determine wind speed (Ozaki, Ohyama, Yasuda, & Shimoyama, 2000). Another concern with strain gauges in general were also uncovered during our literature review, such as the effects of temperature and creep on the readings. Because a horse breath is at a different temperature than the ambient air, the effect of temperature may be a major concern. However, it can be calibrated for. Other than the temperature concern, the strain gauges on hair like structures are a viable design that will be analyzed further (Omega, n.d.).

4.2.3.5 Venturi meter

The Venturi meter was determined to not be a feasible option for this project after speaking with our advisor and no further research was conducted. The Venturi meter would be too large to use on a horse and the application of the meter would not be stable enough to obtain accurate results.

4.2.3.6 Chemical marker chip

A chemical marker chip must comprise of two main components, which are a sensor that can detect the desired analyte and a reader that can interpret the results. One drawback of a chemical marker chip is that multiple tests must be performed if quantitative data is desired.

Running a lung function test multiple times is not optimal. Also, to interpret the results, a visual feedback system is required which is often difficult to read. On the other hand, binary data is not as difficult to acquire and interpret, however, the severity of a certain disease cannot be determined using this method (Erickson et al., 2014). Therefore, a chemical marker chip can verify that a horse has a pulmonary disease, but it cannot distinguish the severity of the disease. Also, with the chemical marker chip, flow data cannot be determined, and an alternative airflow measurement device is needed in conjunction with the chip.

4.2.3.7 Pitot tubes

After researching the applications and functions of pitot tubes, the team determined that laminar fluids are difficult to measure with pitot tubes. This is because a Reynold's number of greater than 3,150 is necessary to measure flow, and at this point the flow is turbulent. For low Reynold's numbers, pitot tubes require correction factors (Bailey et al., 2013). Also, pitot tubes are ideal for measuring high velocities, like the wind speed over an airplane wing, which are much greater than that of a horse's breath. A device that measures pressure must be attached to the pitot tube, typically a manometer. For low velocity airflows, using a manometer to measure pressure drop can create inaccurate readings by the human user. Additionally, smaller pressure measurement devices such as a hot-wire are more ideal to work in conjunction with the pitot tube.

4.2.3.8 Silicon airflow sensor

It was believed that a silicon airflow sensor functions similarly to a hot-wire anemometer, but its readings are not affected by moisture, making it more ideal. However, we learned that humidity does not have the effect it does on the hot-wire anemometer because it is adjusted for using a correction factor. This correction factor removes the concerns with the humidity of the horse's breath (Durst, Noppenberger, Stil, & Venzke, 1996). The silicon airflow sensor is more expensive, and has a limited sensor selection compared to a hot-wire anemometer. Additionally, silicon airflow sensors are a newer technology, posing a concern that it may be difficult to operate. With these drawbacks, we decided to conduct further research on our original hot-wire anemometer idea and rule out the silicon airflow sensor from our final design considerations.

4.2.4 Final alternative design selection

After conducting further research and speaking with our advisors, we narrowed down the eight design ideas to the four most feasible: the improved Fleisch pneumotachograph, the three-cup anemometer, the hot-wire anemometer, and the strain gauges on hair-like structures. These four alternative designs were then further analyzed regarding our project objectives.

4.2.5 Predictive models

Different models were used as an initial method to test and analyze our design concepts. We first created a LabVIEW program to model the software used for the current device. Data was collected from the current software, Open Pleth, and loaded into the LabVIEW program we developed. This was done to better understand how the current device collects and processes data from the pneumotachograph and RIP bands.

Next, we completed flow simulations in SolidWorks for each of the four chosen concepts. These were done using the flow simulation add-in in SolidWorks 2016. After each model was created using SolidWorks, it was opened with the flow simulation add-in. As we went through the setup wizard, each model was setup using internal, laminar flow of air with an inlet flow rate of 65 L/min, the average resting flow rate of a horse. Initial boundary conditions were then set for each model. The inlet flow rate was set to 65 L/min and the static pressure was set to standard pressure of 101 Pa. The flow calculations were then completed and velocity and pressure cut plots were made from each model.

4.3 Alternative designs

After reviewing the original eight concepts, we narrowed down our design concepts to the four most feasible for measuring equine lung function. These ideas are discussed in more detail in this section.

4.3.1 Improved Fleisch pneumotachograph

An alternative Fleisch pneumotachograph model could be designed using lighter and less expensive material compared to the original model. Aluminum capillary tubes could be used to mimic the stainless-steel capillary bed of the original Fleisch pneumotachograph, as they can align on top of one another inside plastic tubing that will act as a casing. This design will minimize resistance to the horse's breathing if the capillary tubes are aligned precisely. The diameters of the aluminum capillary tubes should be between 2.2-5.0 mm and their wall

thicknesses should be between 0.2-2.5 mm. Grades 1050, 1060, 1070, or 3003 of aluminum can be used. The material of the plastic tubing can either be polypropylene, polycarbonate, polyurethane, polyethylene, or polyvinyl. Compared to stainless-steel, aluminum is much lighter as its density is between 156-181 lb./ft^3 compared to 474-506 lb./ft^3 of stainless-steel (Granta Design Limited, 2016).

Using a different material than the original model is advantageous because it makes the device lighter and shorter thus reducing the risk of injury to the operator. The aluminum capillary tubes can be brazed in place to prevent dislocation. They should be cut into 1.5 in. lengths, to mimic the length of the original pneumotachograph device, and be placed inside a 3-in. plastic tube. When the capillary tubes are aligned on top of one another, they will create circular and triangular tubes (Figure 4.2), resulting in a more accurate pressure drop.

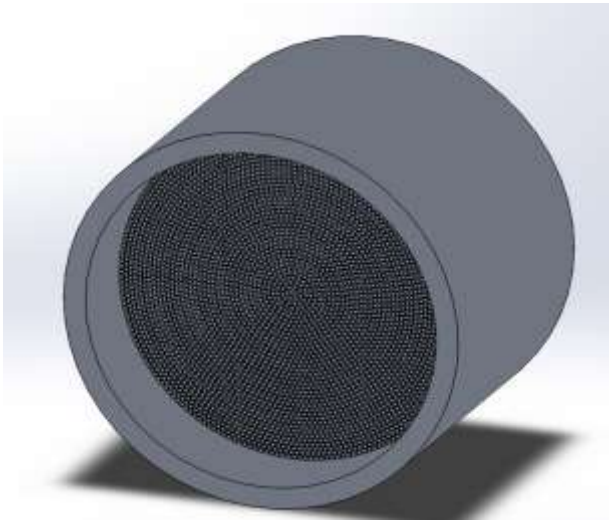

Figure 4.2: SolidWorks model of an improved Fleisch pneumotachograph

However, if the capillary tubes are placed compactly with no spaces in-between them, the pressure drop will be exceptionally high thus increasing the resistance to the horse's breathing. After counting how many of each tube type is present in the system, the pressure drops for each tube were calculated. The pressure drop across the circular tube was calculated using Equations 4.2 and 4.3 (Young, Munson, Okiishi, & Huebsch, 2011). The number of tubes were multiplied by their corresponding pressure drops and added together to get a final pressure drop reading across the device.

$$Q = \frac{\Pi R^2 v_c}{2} \text{(Eq. 4.2)}$$

Q is the flow rate
V_c is the maximum velocity
R is the radius

$$Q = \frac{\Pi D^4 \Delta P}{128 \mu l} \text{(Eq. 4.3)}$$

Q is the flow rate
D is the diameter
ΔP is the pressure drop
l is the length

This device could be incorporated inside a longer piece of tubing that attaches to a facemask. A 3 L calibration syringe could be used to calibrate the device and to accurately obtain lung function signals from equine patients. Similar to the current model, this device can connect to a pressure transducer that will relay the collected data into LabVIEW Software. The pressure transducer will reside in a data acquisition box (DAQ box). Additionally, this device can be used onsite, however, it must be connected to a computer to display the data. With this improved Fleisch pneumotachograph, fluid can flow in two directions, and the device is compatible with passive breathing. In regards to the price, this improved pneumotachograph would be less expensive than the current device because aluminum is less expensive than stainless-steel. Table 4.6 highlights the pros and cons of this improved Fleisch pneumotachograph design. This design would meet veterinary standards if biocompatible materials are used for the connection to the horse's muzzle and proper sterilization procedures are followed.

Table 4.6: Pros and cons of the improved Fleisch pneumotachograph design

Improved Fleisch Pneumotachograph	
Pros	Cons
● Lightweight ● Less expensive than original model ● Linear relationship	● Pressure drop can be inaccurate if not properly constructed ● Limited strength ● Tedious construction

4.3.2 Hot-wire anemometry

Hot-wires are a type of anemometer that measures the flow of a gas or liquid. Hot-wires are often used in internal combustion engines or industrial process control applications, making them affordable and easy to acquire. The sensor will determine the flow velocity by measuring the rate at which heat is removed from the wire by the flowing fluid. Equation 4.4 shows the governing equation of hot-wires. E is the thermal energy stored in the wire which is expressed in Equation 4.5. W is the power generated from heating in joules given by Equation 4.6. H is the heat transferred to the surroundings determined by using an energy balance of the convection to the fluid, conduction to the supports, and radiation to the surroundings (Funda, 2010). The electrical energy needed to maintain the wire's temperature is proportional to gas flow which can then be displayed as a voltage signal (Shiner & Steier, 2012). The signal could then be displayed using a software like LabVIEW.

$$\frac{dE}{dt} = W - H \qquad \text{(Eq. 4.4)}$$

E is the thermal energy stored in wire
W is the power supplied to the wire
H is the heat transferred to surroundings

$$E = C_w T \qquad \text{(Eq. 4.5)}$$

C_w is the heat capacity of wire
T is the temperature.

$$W = I^2 R_w \qquad \text{(Eq. 4.6)}$$

I is the current
R_w is the resistance of hot-wire which is temperature dependent

Hot-wire anemometers can be wires, meshes, or films; wires are often made of platinum, but tungsten, glass tubes, silicon films, and quartz wires can also be used. The material used should have a high temperature coefficient of resistance to increase sensitivity to velocity variations and an electrical resistance low enough that the wire can heat up at a reasonable voltage and current level. The material should also be strong enough to withstand stresses from flow velocities (Funda, 2010).

There are constant current and constant temperature hot-wire anemometers. Constant temperature hot-wires are used more frequently because they are an accepted standard, are easier

to use, and produce lower noise (Funda, 2010). Figure 4.3 shows the basic circuit used when building a constant temperature hot-wire anemometer. The circuit design utilizes a Wheatstone bridge to determine an unknown resistance. R_1 and R_2 are fixed resistors, R_3 is a variable resistor, and R_w is the hot-wire. R_w completes the bridge and is a function of temperature. R_3 adjusts to the R_w starting point. As airflows over R_w, the temperature, and therefore the resistance, change. The flow generates a voltage difference between points 1 and 2 which is recognized by the amplifier. The amplifier then adjusts the feedback current to keep the wire temperature and resistance constant by rebalancing the bridge (Advanced Thermal Solutions Inc., 2007). Over the years many advancements have been made to hot-wire anemometry. The sensors are reliable, sensitive, have a fast response time, and can even be made on a miniature scale to measure single point flow measurements (Chen, Wang, Zhang, Chen, & Chen, 2012).

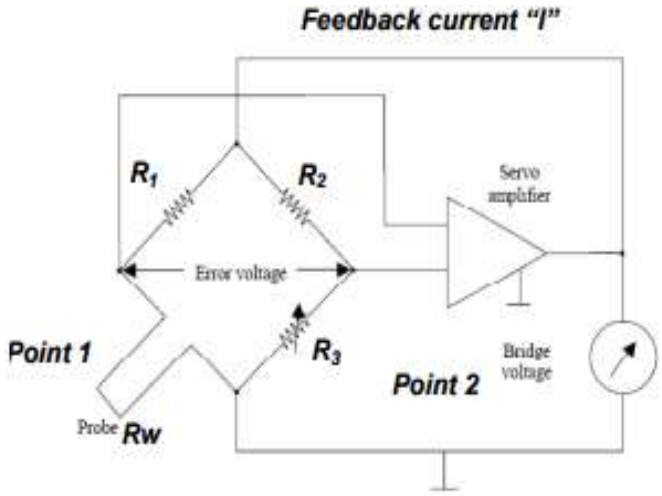

Figure 4.3: Basic hot-wire anemometry circuit including a Wheatstone bridge (Advanced Thermal Solutions Inc., 2007).

Hot-wire anemometry has potential to be used for lung function testing because of its accuracy and reliability. In addition, the fluid can flow both ways through a hot-wire system with two wires installed in series (Kramme & Schlegelmilch, 2011). The sensor would also work with passive, non-compliant breathing and has low noise levels. Hot-wire anemometry has been successfully used in measuring infant lung function; the Florian neonatal respiratory function monitor (RFM) is the most common hot-wire anemometry device used for lung function testing

which has an accuracy of ± 8% (Verbeek, Zanten, Vonderen, Kitchen, Hooper, & Pas, 2016). Horses would require an even less sensitive sensor because their expiratory flow rates are larger than an infant's. Hot-wires also exhibit less resistance during lung function testing than pneumotachographs since they are smaller devices that can be placed in open tubes rather than a tube divided into many tiny capillaries (Araujo, Freire, Silva, Oliveira, & Jaguaribe, 2004). Figure 4.4 shows a basic design of a hot-wire anemometer that could be used for a lung function testing device.

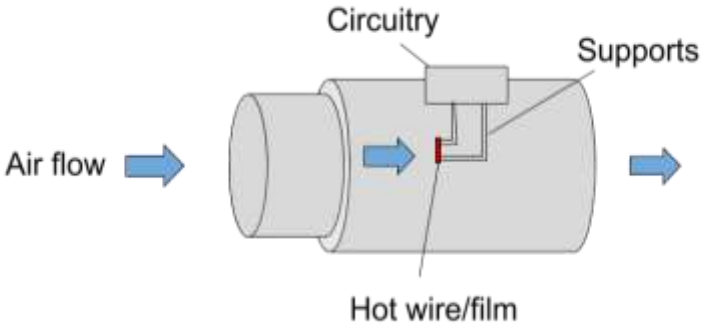

Figure 4.4: Basic schematic of a hot-wire anemometer device.

A smaller sensing element would result in a lighter and more compact lung function testing device, allowing easier attachment to the horse and minimizing the risk to the operator. Additionally, hot-wire anemometers are able to meet calibration and flow standards when calibrated using known flow rates, as well as be housed in an exterior made of biocompatible materials. Table 4.7 includes a summary of the pros and cons of using a hot-wire anemometer for our new lung function testing device.

Table 4.7: Pros and cons of using a hot-wire anemometer in our lung function testing device.

Hot-Wire Anemometer	
Pros	Cons
• High accuracy • Sensitive to rapid changes in velocity • Minimal resistance • Small/ lightweight • Air can flow both ways	• Sensitive to contaminants and moisture • Complex circuitry • Difficult to clean

4.3.3 Three-cup anemometer with tachometer

An alternative design to the current device with a Fleisch pneumotachograph is a three-cup anemometer with a tachometer. This type of anemometer is a common wind speed measurement instrument, particularly in weather stations (Kristensen, et al., 2014; Saylor Academy, 2011). Having the anemometer consist of three hemispherical cups allows the design to respond more quickly to wind speed changes compared to the four-cup design (Kristensen, et al., 2014). For the project, the main focus of this design is to measure airflow more directly by measuring the revolutions per minute (RPM) rather than indirectly, such as the current device with a pressure drop. Airflow in this design is meant to move the three hemispherical cups of the three-cup anemometer at the same speed as the airflow, which describes a linear relationship between airflow speed and the hemispherical cups rotational speed (Saylor Academy, 2011). The tachometer sends a signal that reflects off of the reflective tape on one of the hemispherical cups. The tachometer senses when the signal is sent back from the reflective tape, which is equivalent to one revolution, and has a timing module to sense elapsed time to produce the display of RPM.

The three-cup anemometer with tachometer accomplishes the objectives set by our sponsor in a different way than other alternative designs. There is a potential that the tachometer's accuracy will not be within the desired ± 0.33%. However, because the accuracy objective is not weighted as a requirement, it does not disqualify the design from consideration. There is the potential for the three-cup anemometer hemispherical cups to continue moving due to inertia caused by their mass rather than to the airflow, which would cause inaccurate readings of airflow. This phenomenon is commonly referred to as overspeeding; moves faster than the actual wind speed (Kristensen, et al., 2014). Also, based on the angle of the hemispherical cups, the anemometer can underspeed. Underspeeding is when there is a delayed reaction to the change in wind speed, which causes the hemispherical cups to move slower than the actual wind speed. However, a three-cup anemometer more easily overspeeds due to an increase than a decrease in wind speed (Eq. 4.7; Kristensen, et al., 2014).

$$K_{+}(U - rS) > K_{-}(U + rS) \text{ (Eq 4.7)}$$

S = angular velocity

r = rotor radius

U = wind speed

K_{+} = Cup(s) experiencing acceleration

K_{-} = Cup(s) experiencing deceleration

There are equations that account for the three-cup anemometer overspeed and underspeed bias (Kristensen, et al., 2014). Due to the size of the three-cup anemometer, the design as a whole is expected to offer minimal resistance to the horse's breathing. A CAD model of the three-cup anemometer is seen in Figure 4.5**.**

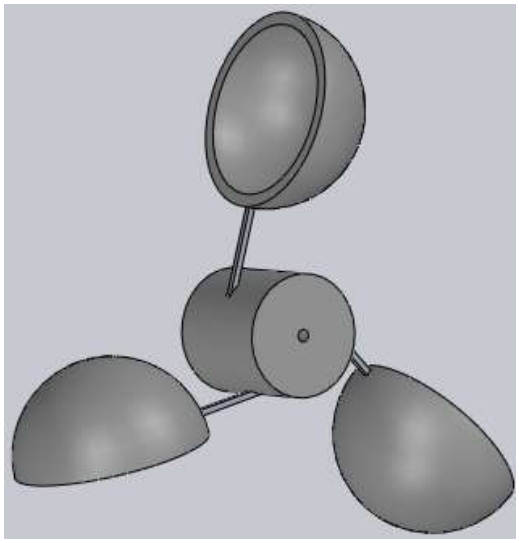

Figure 4.5: SolidWorks model of the three-cup anemometer component of the design

The three-cup anemometer moves in response to any airflow force and therefore is compatible with passive breathing. This means that the design does not require compliant breathing. Part of the intent with the design is to minimize the risk for the human user. This objective is satisfied by the three-cup anemometer with tachometer design because the housing is a 5-in. diameter by 4 in. length pipe, which protrudes less than the current device. The diameter of the housing makes the design not compatible with the current horse facemasks. The SolidWorks model of the housing can be seen in Figure 4.6.

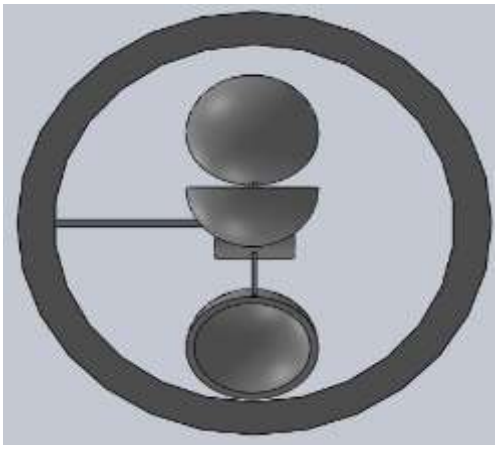

Figure 4.6: SolidWorks model of the housing for the three-cup anemometer design

Material selection can also reduce the risk to the human user by incorporating lighter materials such as, aluminum or polycarbonate (PC), for the three-cup anemometer component (Granta Design Limited, 2016). To compare, the current device weighs 3 lbs. The cost of all the materials for the three-cup anemometer with tachometer is within the budget and satisfies being less expensive than the current device. This design can be compatible with LabVIEW if the tachometer has an encoder that converts pulses to a voltage signal. The encoder's wires would be stripped to connect either to alligator clips or soldered to longer wires, which would attach to a data acquisition box (DAQ box). Satisfying the portability objective is dependent on the amount of equipment veterinarians are willing to bring to house calls, but this design can operate onsite. The equipment necessary for testing lung function with this design is the horse mask, three-cup anemometer with tachometer unit, DAQ box, and a computer. Most veterinary standards are considered as guidelines and recommendations for performing care. Based on the information gathered about veterinary standards, this design would fulfill this objective by consisting of biocompatible materials, not cause harm to the horse, and adhere to proper sterilization procedures.

The three-cup anemometer with tachometer also has different means that satisfy the functional blocks, which set it apart from the other alternative designs. The calculate airflow functional block contains different means that accomplish this goal, but the three-cup anemometer with tachometer design is unique with attempting to calculate volumetric flow rate

through measuring RPMs. To accurately calculate volumetric flow rate for this design, the shape of the three-cup anemometer must be accounted for as described in simplified terms in Equation 4.8 and 4.9 (Gudmundsson, 2013; The Engineering Toolbox, n.d.).

$$\mathrm{CFM} = \mathrm{RPM} * \mathrm{p} * \pi * (\frac{\mathrm{D}}{2})^2 \quad \text{(Eq. 4.8)}$$

RPM =revolutions per minute
p =pitch (ft.)
D =diameter (ft.)
CFM =cubic feet per minute

$$\text{Air Volumetric Flow Rate} = \mathrm{CFM} * 0.0328^3 * 10^{-3} \quad \text{(Eq. 4.9)}$$

The functional block regarding signal display has three means and the three-cup anemometer with tachometer is compatible with two of the three means. The three-cup anemometer with tachometer design was discussed earlier to be compatible with LabVIEW to display voltage signals. Due to the linearity relationship of voltage to RPM from the encoder, an Arduino is another viable option to display the voltage signals. An additional benefit of using an Arduino is the design would be more likely to be portable because of the size of the Arduino compared to the current device's pressure transducer box. The envisioned device exterior is a cylinder, 5 in. diameter, which is attached to the existing facemask. Calibration for the three-cup anemometer with tachometer would be achieved by using the calibration syringe. With the calibration syringe supplying a known volume, the airflow can be predetermined and expected as the output. Table 4.8 summarizes the pros and cons of the three-cup anemometer with tachometer alternative design.

Table 4.8: Pros and cons of the three-cup anemometer with tachometer design

Three-cup anemometer with Tachometer	
Pros	**Cons**
● Lightweight ● Less expensive ● Protrudes a max of 4in.	● Accuracy errors ● Tachometer must have an encoder to connect to LabVIEW ● Difficult to use onsite

4.3.4 Strain gauge on hair-like structures

Another alternative design for measuring airflow is using strain gauges on a hair-like structure. Using strain gauges to measure airflow was developed from a study of insect hair because they can measure very slight airflows based on the strain of their hairs. Most strain gauges can measure microstrains and large strains, so are beneficial to use on large ranges of airflows (Ozaki, et al., 2000). The horse will breathe through a tube that has the hair-like structures in the center. The hair-like structures will deflect with the airflow and the strain gauges will measure the output and produce a voltage reading. This device could measure airflow in both directions because the hair-like structures can deflect in both directions. One strain gauge would be required for each hair-like structure and at least two hair-like structures would be required to make accurate measurement.

There are many mathematical models for the airflow related to the strain that can be used to find the velocity of the airflow. Equation 4.10 is the equation used to calculate drag of a cylinder perpendicular to flow. Equation 4.11 is the calculation for moment of inertia of the wire. Finally, Equation 4.12 is the equation used to calculate the amount of deflection the hair-like structure experiences.

$$D = Cd * \frac{1}{2} * \rho_{air} * U^2 * A \quad \text{(Eq. 4.10)}$$

D is Drag

Cd is the drag coefficient that can be determined based on Reynolds number and length/diameter

ρ_{air} is the density of air (kg/m^3)

U is the velocity (m/s)

A is the area (m^2)

$$I = \frac{(\frac{0.0036784546}{1000} * d^2)}{2} \quad \text{(Eq. 4.11)}$$

I is the moment of inertia

d is the diameter of the hair-like structure (m)

$$\text{deflection} = \frac{D * L^4}{8 * (6.063 * 10^9) * I} \quad \text{(Eq. 4.12)}$$

D is drag calculated in Eq. 4.10

L is length (m)

I is moment of inertia calculated in Eq. 4.11

The strain gauges and hair-like structures can be incorporated into a system that attaches to the current facemask, but it would only extrude approximately two inches from the horse's face rather than the current 12 in. of the Fleisch pneumotachograph. The weight can also be significantly reduced because two narrow wires and small strain gauges can be used instead of a large stainless-steel component. The wire can be any thin, long wire, so aluminum could be used because it is less expensive and lighter than many other metals. Since this new device is using the same facemask as the current device, it will still be biocompatible and the system can be cleaned effectively as long as care is taken with the strain gauges. This means the device meets the primary veterinary standards that are in place. The overall device would weigh less than 1.5 lbs., which again is significantly reduced from the current 3 lbs. By improving both the protrusion and the weight, the device will be significantly safer. A model of the alternative design can be seen in Figure 4.7.

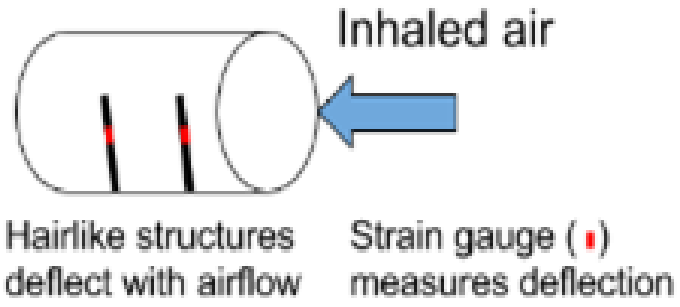

Figure 4.7: Schematic of strain gauges on hair-like structures design

Since the horse is breathing through a large cylinder containing only two thin wires, the pressure drop is negligible. Thus, reducing the resistance to a negligible amount would allow the strain gauge and hair-like system to be used while the horse is at full exertion. The deflection will also occur as the air flows over it, so the horse just needs to breathe as it naturally would, which means this device does not require compliant breathing. The strain gauge used needs to experience the same deflection as the wire it is on. Omega's bonded resistance strain gage could be used for this application because it can be used in a wide range of temperatures, it has a range of sizes, it is highly sensitive, and it can be used in dynamic conditions. The desired size of the strain gauge would be 0.008 in. because it needs to experience the strain of the 20 gauge wire it

is adhered to (Omega, n.d.). The main concern about the accuracy of the device is the noise caused by the horse's movements during testing. Any movement of the horse's face will cause deflection of the hair-like structures leading to noise that needs to be filtered out in order to produce accurate measurements. Once calibrated with the calibration syringe that simulates the airflow of a horse at a known volume and flow rate, the overall system will be more accurate than the current device because it can differentiate at such a small interval. Lastly, strain gauges can be combined into most circuitry systems and produce an output voltage signal, making it compatible with LabVIEW and portable if a computer or other data acquisition device is connected. In LabVIEW, this voltage signal can be converted to airflow, which can then be synced and displayed in time with the RIP band measurements.

Table 4.9 summarizes the pros and cons of the strain gauge method for measuring airflow using the hair-like structures.

Table 4.9: Pros and cons of hair-like structures on strain gauges

Hair-like structure on a strain gauge	
Pros	**Cons**
● Lightweight ● Protrudes less than 3 in. ● Resistance is negligible ● Cost < $40	● Accuracy affected by noise due to horse movement ● Delayed measurement can cause syncing to RIP bands difficult

4.4 Final Design Selection

Table 4.10 shows a design matrix of our four alternative designs for an equine lung function testing device. This matrix was created after further researching our four alternative designs discussed in section 4.3. The design concepts are labeled in the top row and the criteria that the designs should meet to be successful are in the left-most column. Ratings of -1,0, and 1 were given to each concept if they did not meet the criteria or were worse than the current device, matched the current device, or were better than the current device, respectively. Each criterion was weighted between a 1 and a 5 based off the results of Table 4.3, which compared each objective to each other based on the averaged weighting between Dr. Mazan and the team.

Table 4.10: Design matrix of alternative designs

	Weights	Improved Fleisch	Three-cup anemometer	Hot-wire anemometry	Strain gauge
Accurately obtain lung function signals (± 0.33%)	3	1	-1	1	-1
Minimize Resistance to breathing	4	-1	-1	1	1
Cannot require compliant breathing	5	0	0	0	0
Minimize risk for human users (<1.5 lbs. and <6 in.)	4	0	1	1	1
Less expensive (<$1000)	2	1	1	1	1
Compatible with LabVIEW	1	-1	1	1	1
Portable	1	0	0	1	1
Meets veterinary standards	5	0	0	0	0
Rank		0	0	15	9

4.4.1 Aluminum Fleisch pneumotachograph

4.4.1.1 Cost

When comparing the aluminum Fleisch pneumotachograph to the current device, there is a noticeable difference in their costs as the aluminum Fleisch pneumotachograph is significantly less expensive. Aluminum capillary tubes and plastic tubing are the materials needed to assemble the pneumotachograph. A 3-pack of 12 in. aluminum capillary tubes costs between $1.00-$1.50. Approximately 500-1,000 1.5 in. aluminum capillary tubes are needed in the device, which means approximately 60-125 12 in. capillaries need to be purchased (Midland Hardware, 2016). A 3-in. piece of plastic tubing costs approximately $5, resulting in an overall total of no more than $68 for the materials. Factors such as time and manufacturing will add to the cost of the aluminum Fleisch pneumotachograph. However, it is expected that this device will be less expensive than the current pneumotachograph at $8,000 after manufacturing and time costs.

4.4.1.2 Accuracy

The accuracy of the aluminum Fleisch pneumotachograph is dependent on how well the capillaries are assembled inside the tubing. The capillaries must be assembled in such a way that triangular tubes form between their gaps. Additionally, the capillaries should not be able to shift in direction under any circumstance. Assuming that these conditions are met, the aluminum Fleisch pneumotachograph can serve as an accurate model for reading a pressure drop. When completing flow simulations on the entire pneumotachograph model, the data that was acquired was not expected nor meaningful. This is because the fluid boundary layers were not completely defined. Therefore, flow simulations were completed on a single circular and triangular capillary to determine if a pressure drop was present across the tube and to determine if there was a standard velocity profile. Figures 4.8, 4.9, 4.10, and 4.11 display the measured pressure drop and velocity profiles for both a single circular and triangular capillary.

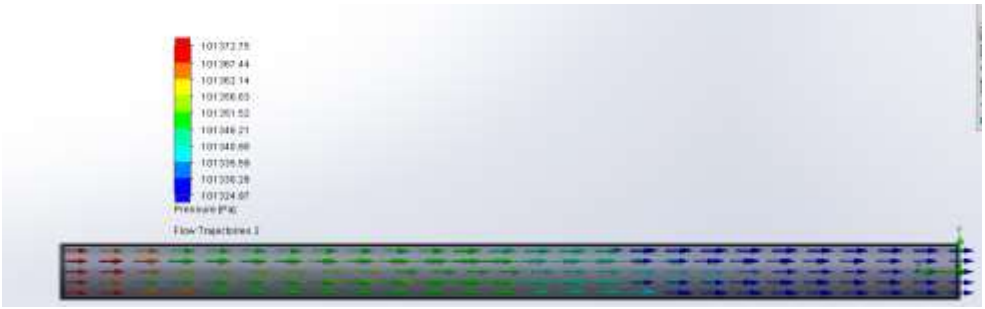

Figure 4.8: SolidWorks flow trajectory pressure profile for a circular capillary

Figure 4.9: SolidWorks flow simulation velocity cut plot for a circular capillary

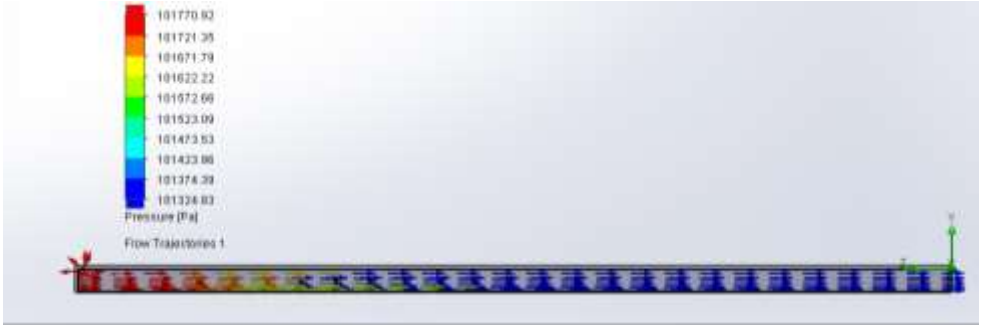

Figure 4.10: SolidWorks flow trajectory pressure profile for a triangular capillary

Figure 4.11: SolidWorks flow simulation velocity cut plot for a triangular capillary

The pressure drops across the circular and triangular capillaries were calculated in SolidWorks to be 47.78 Pa and 446.09 Pa respectively. The team's calculated pressure drop across a single circular capillary was calculated to be 41.44 Pa using Equations 4.13 and 4.14 below. When creating the velocity profiles, the normal resting flow rate of a horse's breath of 65 L/min was used as the inlet velocity for both capillaries. The velocity was constant throughout the length of the tube in both instances, which was expected because the flow is laminar.

$$Q = \frac{\Pi R^2 V_c}{2} \text{(Eq. 4.13)}$$

Q is the flow rate
V_c is the maximum velocity
R is the radius

$$Q = \frac{\Pi D^4 \Delta P}{128 \mu l} \text{(Eq. 4.14)}$$

Q is the flow rate
D is the diameter
ΔP is the pressure drop
l is the length
μ is viscosity

4.4.1.3 Feasibility

Regarding the feasibility of the aluminum Fleisch pneumotachograph, manufacturing was a main concern. The success of the pneumotachograph reading a correct pressure drop is dependent on how well the capillaries are assembled. Ultimately, circular and triangular tubes need to be present in the model to create an accurate pressure drop reading. Brazing the aluminum capillaries can secure the capillaries in place to prevent any shifting of the tubes. However, manufacturing requirements would be complex, time consuming, and expensive for the device.

Pressure drop calculations were performed to verify that the aluminum Fleisch pneumotachograph was a feasible design. The pressure drop across both circular and triangular tubes were calculated. This pressure drop is equal to the pressure drop across the entire device..

4.4.1.4 Prototype

A prototype of the aluminum Fleisch pneumotachograph was constructed to verify that the device would produce a pressure drop. To read the pressure drop, a double-sided manometer was also constructed using plastic tubing and a piece of wood. For the pneumotachograph prototype, coffee stirrers were cut into 1.5 in. lengths and were sanded down to even their surfaces. Using rubber bands, the stirrers were secured into a 3-in. circular shape and placed inside a 3-in. long plastic bottle. The plastic bottle was then punctured once in an area before the straw pneumotachograph model and once after the model. These punctures acted as inserts for the rubber tubing of the manometer. One side of the manometer read the pressure before the air flowed into the straws and the other side read the pressure right after air passed through. Using these readings, the pressure drop was determined. A constant stream of air was provided by an air regulator on a compressed airline.

4.4.2 Hot-wire anemometry

In section 4.3.2 a hot-wire anemometry concept was discussed as a potential design for equine lung function testing. This method uses thermal sensing to measure airflow. This section further discusses its cost, accuracy, and overall feasibility for our project.

4.4.2.1 Cost

Using a method of thermal sensing to measure airflow has the potential to be significantly cheaper than the current device. Mass airflow sensors utilize a hot-wire and can be found for

around $35.00 from Premier Farnell Ltd (Farnell Ltd, 2016). Hot-wire anemometers can also be made from scratch using materials like tungsten or platinum wire. Tungsten or platinum wire can be obtained for $50.00-$200.00 from chemical suppliers like Sigma-Aldrich (Sigma-Aldrich, 2016). Thermistors can also be used to measure airflow by thermal sensing similar to hot-wire anemometry when wired in a specific way. A thermistor is a resistor whose resistance increases when cooled, in this case from a horse breath. A thermistor with all the embedded circuitry necessary to measure air speed can be purchased for $17.00-24.00 dollars from Modern Device (Modern Device, 2016). These sensors were financially the best option for thermal sensing, so each was purchased to determine which was most technically feasible.

4.4.2.2 Accuracy

Our hot-wire anemometry design contained a cylinder with two open ends for the air to pass through and a sensing element protruding into the cylinder to catch passing air. The top of the cylinder contains housing for the necessary circuitry that the sensing element requires. Flow simulations were done to determine the velocity profile and if there was any major pressure drop. A figure of the measured pressure drop and a figure of the velocity profile for an inlet flow rate of 65 L/min (the average resting rate of a horse) are displayed in Figure 4.12 and Figure 4.13, respectively.

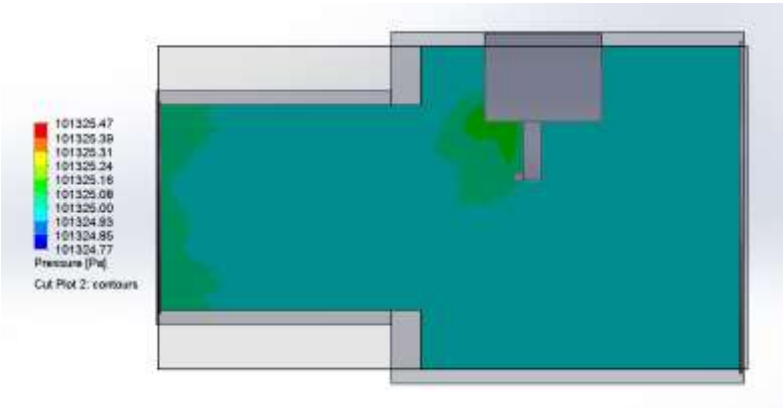

Figure 4.12: SolidWorks flow simulation pressure cut plot for the hot-wire anemometry concept

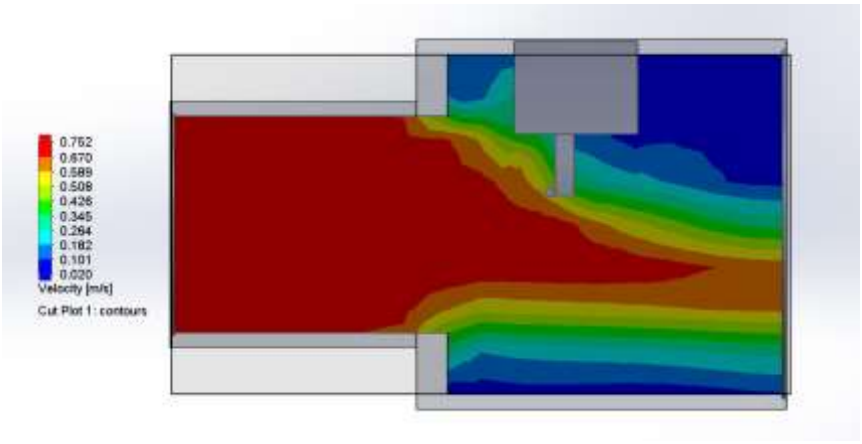

Figure 4.13: SolidWorks flow simulation velocity cut plot for the hot-wire anemometry concept

There was a slight pressure drop in the cylinder which was expected since the cylinder increases in size where the sensing element is located. This drop-in pressure should not affect the results as it is negligible, in ranges close to only 1 Pa, suggesting there is hardly any resistance within the device. The velocity profile displays a higher velocity in the mid-section of the cylinder as the flow continues to develop. This is also expected and the flow is laminar as desired. The sensor's placement is in the midrange of the velocities present, which is also ideal.

The Rev P Wind Sensor (Figure 4.14A) itself is capable of measuring wind speeds of 0-150 mph, speeds well above what we require the device to measure, has ambient temperature compensation, and can display temperature values. The Rev P has also been improved from an earlier wind sensing model to have a maximum output voltage of 3.3 V and high precision resistors (0.1%) in the embedded circuitry (Modern Device, 2016). Another sensor, the Rev C Wind Sensor (Figure 4.14B), was developed before the Rev P and does not have ambient temperature compensation. It works the same way as the Rev P does. However, it was designed for use with lower flow speeds and operates using a lower voltage (Modern Device, 2016).

A. B.

Figure 4.14: A) Modern Device Rev P Wind Sensor; B) Modern Device Rev C Wind Sensor

4.4.2.3 Feasibility

The hot-wire anemometry concept is a feasible option for testing equine lung function. Specifically, The Rev C Wind Sensor, is a highly feasible option because it is extremely affordable at $17.00 and it includes all the necessary embedded circuitry. Assembling our own hot-wire circuit posed a challenge because components could be expensive and our team's skill set is mostly mechanical. Having a sensor requiring minimal circuitry made it much more intuitive to calibrate and conduct testing on. The Rev C Wind Sensor is also small in size which made it easier to incorporate into a small design. This resulted in a safer device for operators and more comfortable for the horses. The sensor is also compatible with LabVIEW which made it easy for us to conduct various experiments with the sensor using LabVIEW software we had access to already. Additionally, the sensor requires a 5-10 V supply voltage which is easily obtained with a 9 V battery, laboratory regulated power supply, a regulated wall adapter, or using a data acquisition box programmed in LabVIEW (Modern Device, 2016).

4.4.3 Three-cup anemometer

In section 4.3.3 the three-cup anemometer was considered as an alternative design for equine lung function testing. This design uses a tachometer to record the revolutions per minute of the hemispherical cups to measure airflow. This section focuses on the cost, accuracy, and overall feasibility of the design in the context of our project.

4.4.3.1 Cost

There is a significant price difference between the actual cost of the Fleisch pneumotachograph and the projected cost of considering the three-cup anemometer with a tachometer design. As stated throughout the report the Fleisch pneumotachograph itself costs $8,000. Based on the CAD model of the three-cup anemometer when the design is created out of aluminum the corresponding mass for the design is 0.18 lbs. When the CAD model is created out of polycarbonate (PC) the corresponding mass for the design is 0.07 lbs. Aluminum is approximately $1.15/lb. and PC is $1.84/lb. (Granta Design Limited, 2016). Knowing the approximate mass and cost per mass allows for a general estimate of the cost of the three-cup anemometer design. If the three-cup anemometer is machined out of aluminum, it will cost around $0.20 or if it is machined out of PC it will cost $0.13. However, those estimates are based solely on the mass of the design, not the amount of stock material required to create the design.

In addition to the three-cup anemometer, the design requires a tachometer instrument that is compatible with the design. One type of suitable tachometer instrument was found on McMaster-Carr and costs around $158 (McMaster-Carr, 2016). PVC pipe is required for the housing of the design and PVC typically costs around $10. Adding the costs of all of the components and materials necessary for the three-cup anemometer design gives an approximation of the total cost of pursuing the design, $170.

4.4.3.2 Modeling

Flow simulations were done using a fluid flow simulation in SolidWorks to evaluate the design, the three-cup anemometer was housed in a circular tube and a steady state, fully developed, laminar flow rate 65 L/min, the average resting flow rate of a horse, was generated at the inlet of the circular tube. The velocity profile of the three-cup anemometer at these conditions is displayed in Figure 4.15. As the flow interacts with the three-cup anemometer, it begins to curve in an eddy, which means the fluid flow is beginning to flow in the opposite direction. Eddies cause inaccuracies because they oppose the flow. This means that the tachometer will be reading velocities different than the actual airflow. Additionally, eddies pose a hazard to the horse by increasing the pressure drop and adding to the overall resistance.

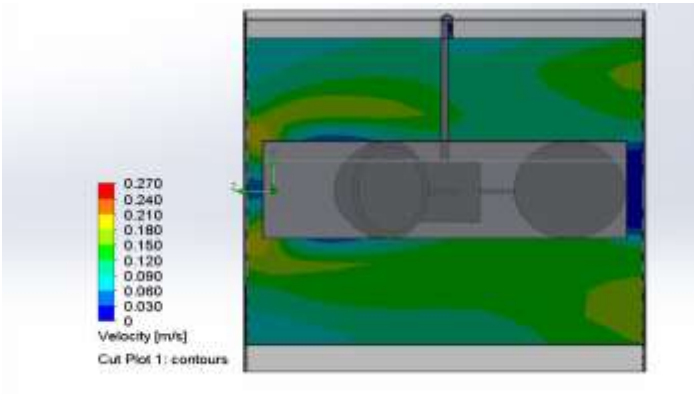

Figure 4.15 SolidWorks cut plot of flow velocity profile for the three-cup anemometer design

The pressure drop of the airflow through the three-cup anemometer design was also simulated using SolidWorks (Figure 4.16). The pressure drop was small and would not contribute significantly to the resistance of the device.

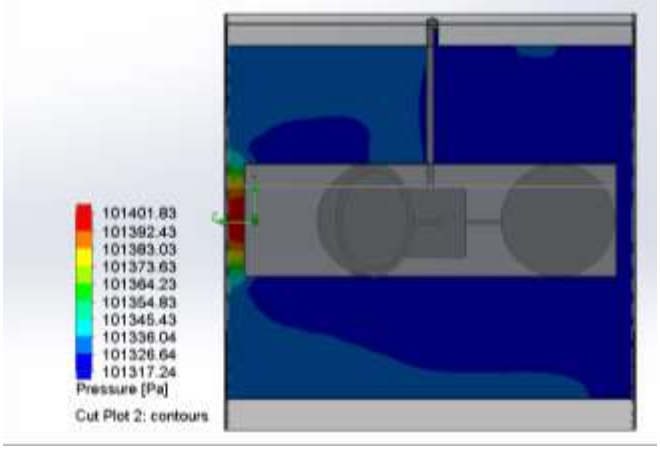

Figure 4.16: SolidWorks flow simulation pressure cut plot for the three-cup anemometer design

4.4.3.3 Feasibility

In terms of manufacturing, the three-cup anemometer would not be a feasible design due to our limited manufacturing background and difficulty to machine. The small design would require precise cuts on a lathe to create the cup shapes. Cutting the inner and outer diameter of the cup would be difficult. The shape of the cup requires the inner diameter to be cut first and then the piece needs to be removed from the chuck and flipped around in order to cut the outer diameter. This flipping of the cup piece may also pose a concern because the chuck may not be able to secure such a small component that has already been cut.

Another deterrent from pursuing the three-cup anemometer design is potential restriction it poses against the horse's breathing. A design cannot cause harm to the horse and the eddies present from the SolidWorks simulations demonstrates that the three-cup anemometer can greatly restrict the horse's breathing at a level that can harm the horse.

The overspeeding of the device leads the design to be considered infeasible. PhD candidate conducted several experiments on different three-cup anemometers for his doctoral dissertation. His work illustrated a variety of three-cup anemometers overspeeding for an average period of two seconds after being subjected to wind speeds of 15 m/s, 10 m/s, and 5 m/s (Chen, 2016). His work displays three-cup anemometers having a tendency to overspeed as discussed in 4.3.3. Based on horses' resting flow rate and maximum exertion flow rate it was determined that the corresponding wind speeds would be in a range of 0 to 5.5 m/s. Therefore, a three-cup anemometer subjected to horses' wind speeds should also expect an average time of

two seconds of overspeeding. Horses breathe at an average rate of twelve breaths per second, which is equivalent to five seconds per breath with 2.5 seconds of inspiration and 2.5 seconds of expiration (Erickson, 2004). Theoretically two seconds of overspeeding would occur after the end of expiration, because during expiration the three-cup anemometer would be increasing speed. Inspiration is flow in the opposing direction to expiration, effectively acting as a decelerator for the three-cup anemometer. The three-cup anemometer would only be able to respond accurately to the last 0.5 seconds of inspiration. Missing two seconds of inspiration wind speed data for each breath would make it impossible to accurately report a horse's lung function.

With the simulations and equations considered for this design, we have deemed it unfeasible, but more simulation would be needed to fully understand the other factors of modeling turbomachinery and their effects on accuracy.

4.4.4 Strain gauges on hair-like structures

As described in chapter 4.3.4 the idea of using hair-like structures to measure airflow is developed from the knowledge that insects use the hair on their bodies to determine wind speed and direction based on its deflection. This concept has been adapted to work with wire and strain gauges to measure deflection caused by airflow, which is a potential method for measuring equine lung function.

4.4.4.1 Cost

Using strain gauges to measure airflow has the potential to cost significantly less than the current device. This design is drastically less expensive than $8,000. An appropriate strain gauge for this application costs on average $70. As discussed in section 4.3.4, the 0.008 in. bonded resistance strain gauge would work best for this application because it would strain with the twenty-gauge wire (Omega, n.d.). The twenty-gauge wire can be a simple aluminum wire, which can be purchased for $2 to $6 from various online retailers. Also, an epoxy that does not creep is required to ensure that the strain gauge's accuracy does not change over time. An appropriate epoxy can be purchased at any hardware store and will cost $5 to $10. Lastly, the hair like structures will need to be housed in tubing with a 3-in. diameter and no more than 2 in. long. A PVC pipe with these dimensions can be purchased at any hardware store and costs less than $10. An estimated overall cost to construct this device is $96. This is significantly improved from the cost of the Fleisch pneumotachograph.

4.4.4.2 Accuracy

There are a few concerns with the accuracy of the strain gauges for this application. Strain gauges are very sensitive to small changes in strain, which may pose a problem when being used to measure a transient flow such as a horse's breath. There are also concerns with the delay in response time. Since the wire deflection does not occur instantaneously, there will be a delay in the strain gauges reading. This delay would be almost imperceptible, but when the timing with another device is critical such as in this system where timing with the RIP bands is critical this delay could cause a drastic visual shift in the data from the band readings producing an undesired result.

In order to determine if the flow would react differently in this device causing inaccurate readings, flow simulations were conducted using the fluid simulation add-in in SolidWorks. These flow simulations were completed to make sure that the system had a normal laminar flow velocity profile and experienced a minimal pressure drop. The boundary conditions set were a static pressure at the outlet and an inlet flow of 65 L/min, which is the average resting rate of a horse. Figure 4.17 shows the velocity profile for the strain gauge design. The hair like structures caused no disruption in the flow, so a standard laminar flow velocity profile was seen as expected. As expected, the maximum velocity occurred in the center of the housing and was 0.488 m/s, which is approximately the same as the maximum velocity for the other designs including the existing Fleisch pneumotachograph model. Matching that maximum velocity between the designs is ideal.

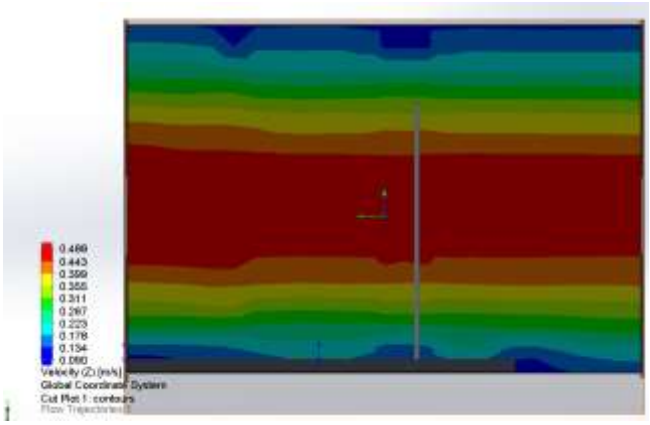

Figure 4.17: SolidWorks flow simulation velocity cut plot for the strain gauge design

Pressure drop is a very important parameter to consider when designing a device for non-invasive equine lung function testing because a higher-pressure drop applies more resistance to the horse's breathing. If the resistance is too high, the horse could suffocate because it would be unable to breathe. Due to the open profile of this design, the pressure drop is minimal which is shown in the pressure cut plot in Figure 4.18.

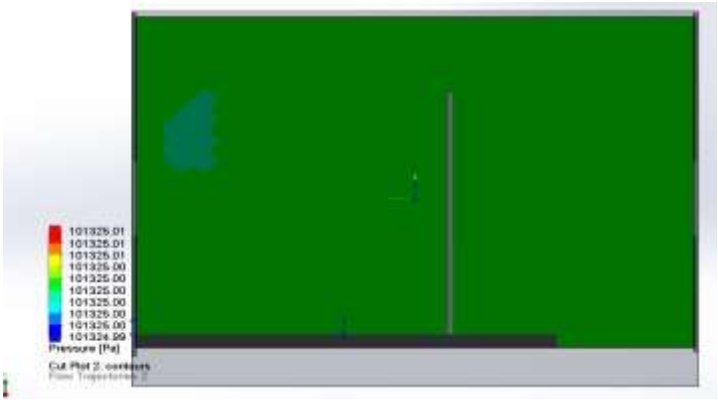

Figure 4.18: SolidWorks flow simulation pressure cut plot for the strain gauge design

As seen in Figure 4.18 the pressure is very consistent throughout the housing. The maximum pressure drop experienced is 1.00 Pa, which is significantly lower than the current device thus improving the resistance the horse experiences during testing.

4.4.4.3 Feasibility

There are a few concerns about the feasibility of this design for our team. As mentioned before, we all have a mainly mechanical background, so working with and designing circuits is outside our area of focus. Since the strain of the wire needs to be detected, a microstrain gauge would need to be positioned on the wire appropriately to measure that deflection. Using equation 4.9 through 4.11 the drag, moment of inertia, and deflection were calculated to be $2.72 * 10^{-6}$N, approximately 0 Kg*m^2, and 0.308 nm respectively. Due to the size of the wire and the strain calculated for the average flow rate produced by a horse, the strain gauge used would need to be extremely small and sensitive. Strain gauges of this size and sensitivity are not readily available, so we would have to design and construct a strain gauge specifically for this purpose, which would require an electrical engineering background. Strain gauges also require a lot of signal processing, which requires a deep understanding of data analysis and computer science. Due to

our inexperience in the required fields to create this design and interpret the results, it was determined that it was not feasible for us to pursue this design further.

4.4.5 Overall sensor selection

After researching, modeling, and conducting simulations for our four alternative designs, we chose the hot-wire anemometry concept to incorporate into our final design. Specifically, we chose to perform testing with the Rev P and Rev C Wind Sensors from Modern Device because they were affordable, small, and had all necessary circuitry and code embedded.

The Rev P Wind Sensor was designed to work with an Arduino Uno. The Arduino code was provided with the device and included calibration curve equations for the conversion of the raw data to the temperature and wind speed. Equation 4.15 displays the calibration equation for the temperature and Equation 4.16 shows the calibration equation for the wind speed.

$$T = \frac{((\frac{RawT*5.0}{1024.0})-0.400)}{0.0195} \text{(Eq. 4.15)}$$

T= temperature (^{o}C)
RawT= value proportion of bits output

$$\text{Wind Speed} = (\frac{RawW-264.0}{85.6814})^{3.36814} \text{(Eq. 4.16)}$$

Wind Speed= speed (MPH)
RawW= value proportion of bits output

The Rev C Wind Sensor is also produced by Modern Device, the same manufacturer as the Rev P sensor, but it is an earlier model. The Rev C does not have ambient temperature compensation built into its circuitry, but does have an adjustable calibration factor within the supplied code, making it simpler to calibrate. Like the Rev P, the Rev C measures temperature changes that it converts to wind speed in MPH. The sensor is designed to work with an Arduino Uno and the code with the calibration equations was provided. The sensor was originally calibrated by Modern Device with a 5 V source, but the zeroWindAdjustment factor built into its calibration code can be changed based on the voltage used. Equation 4.17 is the calculation of zeroWind in Arduino units, Equation 4.18 is the conversion of that value to zeroWind in voltage, which is where the zeroWindAdjustment factor is used, and lastly Equation 4.19 is the conversion to WindSpeed in MPH.

$$\text{zeroWindADunits} = (-0.006 * \text{TMPThermADunits}^2) + (1.0727 * \text{TMPThermADunits}) + 47.172 \text{ (Eq. 4.17)}$$

TMPThermADunits=temperature of the thermistor on the wind sensor in Arduino units
zeroWindADunits=the velocity measured at zero wind in Arduino units

$$\text{zeroWindvolts} = (\text{zeroWindADunits} * 0.0048828125) - \text{zeroWindAdjustment} \text{ (Eq. 4.18)}$$

zeroWindvolts=the velocity measured at zero wind in volts
zeroWindAdjustment=0.2 at 5V

$$\text{WindSpeedMPH} = \left(\frac{(\text{RVWindVolts} - \text{zeroWindvolts})}{0.2300}\right)^{2.7265} \text{ (Eq. 4.19)}$$

RVWindVolts=measured wind speed converted from Arduino units to voltage
WindSpeedMPH=final output of wind speed in MPH

After calibrating and testing each, we determined the Rev C was most feasible for our device. Chapter 5 covers our experimental plan and how we verified our choice of thermal sensing to measure airflow.

4.4.6 Final Design

This section discusses the housing, attachment, and software options that we chose for our final sensor selection.

4.4.6.1 Housing

An appropriate housing needed to be chosen to contain the sensing element. The housing for the sensor had to be shorter than the current 12 in. long device and be softer or more flexible than the current combination of stainless-steel and PVC. These specifications were decided on because they would make the entire device safer for the operators and personnel in the room during testing. The wind sensor is made up of an embedded circuit, which should have minimized exposure to the humidity of the horse's breath. To accomplish this, the circuitry was surrounded by a protective box within the housing of the device, so that only the thermistor sensing element is exposed to the horse's breath.

We developed three different designs of how the sensor should be attached to the horse in order to capture the horse's breath. The first and simplest to implement was an attachment to the current facemask. The second idea was to 3D print a more streamlined facemask that covered less of the horse's face. Our last design was a mask that connected to a standard bridle that just

covered their nostrils.

4.4.6.2 Attachment to facemask

Cummings School currently has a facemask that attaches to the pneumotachograph device, so the simplest way to integrate our sensor was to make it attachable to the existing facemask. The facemask that they use fits over the horse's entire muzzle, so that all air is captured from their breathing. An image of the mask can be seen in Figure 4.19.

Figure 4.19: Current facemask used for testing

The connection on this mask to the current device is 2.5 in. in diameter, so the new design needed to have the same dimensions on the portion that connects to the mask. Ultimately, the new design needed to be shorter and lighter than the current device to address safety concerns.

4.4.6.3 Streamlined facemask

By inverting and 3D printing a mold of a horse's face, we could produce a shorter and less bulky mask that would not sit so far back on the horse's face. It would also sit closer to the sides of their face rather than protruding out on each side. This could reduce cost and increase safety for the user and comfort for the horse.

4.4.6.4 Bridle incorporated mask

Since horses are obligatory nose breathers and are used to wearing bridles, we initially assumed they would be comfortable with wearing a modified bridle for the test. A mask that just covers their nostrils could be developed to connect to the bridle, so that their entire face did not have to be encased in a plastic mask for the test. The sensor would be inserted into a small

opening in the mask with the electrical components above. This design would be lightweight, more comfortable for the horse, and would protrude significantly less than the current design. These modifications would significantly improve the safety of the overall device for the human user and increase the comfort for the horse being tested. However, after discussing this idea with our sponsor, we learned horses have high sensitivity around their mouth and nose. Therefore, a bridle incorporated mask may cause discomfort for the horse.

4.4.6.5 Final housing

We chose to make an attachment to the current facemask. The overall length of the housing is approximately 3.5 in. making it significantly safer for the veterinarians using the device. It only protrudes 2.5 in. from the mask and weighs 0.32 lbs. The wires that connect from the DAQ box to the sensor are 8 ft. long, to connect the device to the DAQ box at a sufficient distance away from the horse and extend through the top of the housing for easy access. Figure 4.20 shows the final housing in the mask with the sensor inserted.

Figure 4.20: Final housing and Rev C sensor in current facemask

4.4.7 Software

The current software used for real time data acquisition during testing is called Open Pleth. This program is designed to work with the pressure transducer and circuitry contained within a box that Ambulatory Monitoring Inc. made specifically for the Fleisch pneumotachograph system. Since our device does not work based on the pressure drop across the

sensor, as the Fleisch pneumotachograph does, Open Pleth software does not work. This software could not be edited to meet the needs of the new sensor, so a new program needed to be developed to interface with the bands and the new sensor.

The new program was written in LabVIEW because we all had prior experience programming in it and Dr. Mazan prefers the ability to access the block diagram, or code for the program in case changes need to be made. LabVIEW can be used to collect data in real time from most sensors when coded correctly for the input data to be processed. The cost for a new user to buy the full edition of LabVIEW is $2,999 and an additional $149 is required for the National Instruments' USB-6000 data acquisition box required for data collection (National Instruments, 2016a; National Instruments, 2016b). The new program will have similar graphs, user controls, and output data as the Open Pleth system. Some of the features in Open Pleth that were not ideal will also be improved upon such as the color scheme of the graphs.

5.0 Design Verification

To verify that the design met the required needs of the client, multiple tests needed to be completed, but first, the sensor needed to be calibrated. The sensor was calibrated at a zero-point to ensure that the values were read accurately. After calibrating the sensor, the functionality at high and low speeds was determined to verify the sensor's ability to work appropriately for the specified application. Lastly, the sensor was tested in a clinical setting to prove proper function on a horse.

5.1 Calibration of the thermal sensors

The two thermal sensors we purchased had to be calibrated to perform correctly and obtain accurate results. If the sensor could not be properly calibrated then it was deemed infeasible for this application and further testing was not continued.

5.1.1 Arduino to LabVIEW

Both the Rev P and Rev C sensors from Modern Device were designed to work with an Arduino Uno. In order to make the sensors compatible with other components of our device and meet the objective of being compatible with LabVIEW, the equations in the Arduino code were recreated in LabVIEW. Equations 4.15 and 4.16 are the wind speed and temperature equations for the Rev P sensor that we recreated in LabVIEW (Appendix C). Equations 4.17, 4.18, and 4.19 are the wind speed equations for the Rev C sensor that we recreated in LabVIEW (Appendix D). These equations needed to be converted to perform the same operation in LabVIEW as they did for the Arduino. The Arduino works in portions of bits, but LabVIEW reads voltage directly. The Arduino used was a 10 bit Arduino Uno with a resolution of 2^{10} (or 1024) values and a maximum voltage output of 5 volts. The values are divided by the maximum voltage to get a conversion factor of 204.8 values/volts. To account for this difference in the LabVIEW program, the acquired voltages were multiplied by 204.8 before using the Arduino equations to process the data. Once the data was properly converted and the appropriate equations were written, a zero-point test was used to calibrate the sensor.

5.1.2 Zero-point test

A zero-point test was conducted with both the Rev P and Rev C sensors to calibrate each device. The Rev C sensor had a zero-wind adjustment factor that was used to ensure that the value read at a known 0 MPH flow rate was, in fact, 0 MPH. The Rev P did not have this

correction, so it had to accurately read 0 MPH without correction. To guarantee there was a solid connection between the DAQ box and the sensor, wires were soldered directly to the four required pins on the sensor and then were inserted directly into the proper ports on the DAQ box. Each sensor was powered with an appropriate wall wart that provided a consistent voltage. The Rev C was powered with a 5 V wall wart and the Rev P was powered with a 9 V wall wart. To ensure that the sensor was in a zero-wind environment for this test, a glass bowl was placed over the sensor, only leaving a small gap between it and the table to allow for the wires to connect to the DAQ box. Figure 5.1 displays the experimental setup for this test. Both sensors were tested using the same setup.

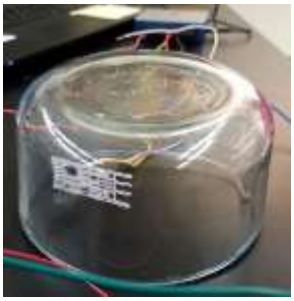

Figure 5.1: Rev C sensor covered by a glass bowl to simulate a known zero-wind environment

Using the test setup seen in Figure 5.1 with the Rev P sensor we conducted a zero-point test with a 9V power supply. When tested, the Rev P sensor produced an average reading of 0.0179 MPH (Figure 5.2).

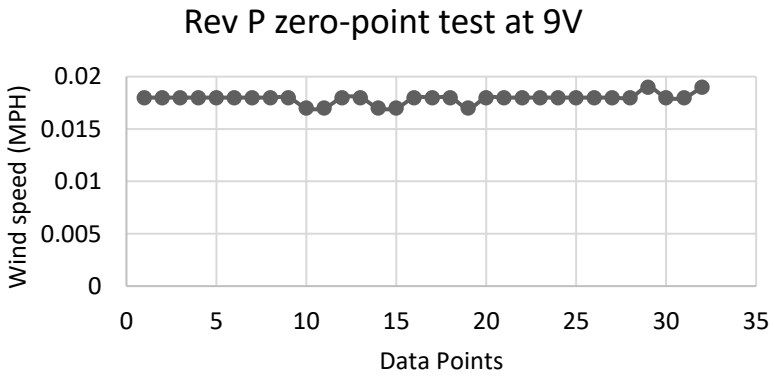

Figure 5.2: Graphical representation of the results of the 9 V zero-point test with the Rev P sensor

Using the setup shown in Figure 5.1, the Rev C sensor was originally tested with a 4.7 V excitation voltage using a power supply and it was found that with a correction factor of 0.05 the sensor read consistently at 0.001 MPH. Figure 5.3 shows the speed in miles per hour on the y-axis and the sampled data points on the x-axis. This graph clearly shows that the wind speed readings were consistent throughout the length of the zero-point test.

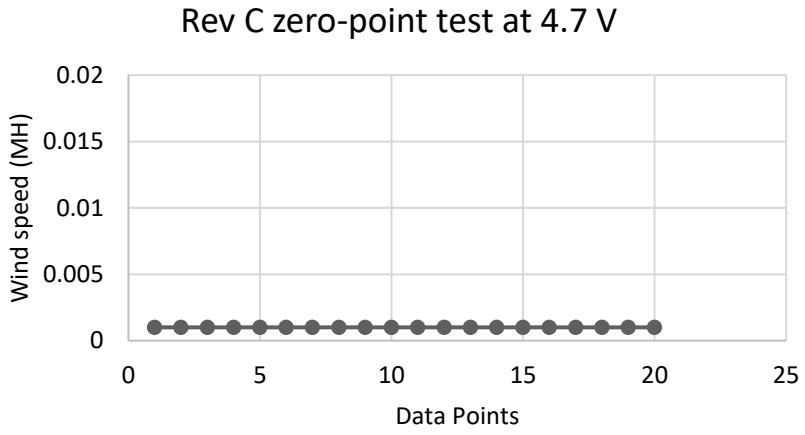

Figure 5.3: Graphical representation of the results of the Rev C zero-point test at 4.7 V

For the Rev C, we found that the correction factor required to get a 0 MPH reading at a known 0 MPH flow was dependent on the environmental conditions and the excitation voltage. A calibration LabVIEW program was created that would automatically find the correction factor that resulted in a reading less than 0.0005 MPH (Appendix E). This program consistently finds a correction factor within the range of 0.25 to 0.39 for a 5 V excitation voltage depending on the ambient temperature of the room. If run repeatedly in the same room, it will find a value within ±0.01 every time. This proves that the Rev C calibration is repeatable and reproducible making it ideal for further testing.

5.2 Sensor function verification

After verifying that both sensors read reasonably close to 0 MPH after the zero-point calibration test, the sensors' abilities to read higher wind speeds needed to be verified. First a high-speed wind tunnel was used to verify the sensors' abilities to accurately display the same wind speed as the set wind tunnel speed values. Also, high wind tunnel testing determined which sensor, the Rev P or the Rev C, was more accurate so that our focus was directed towards one

sensor. After choosing which sensor to pursue, we had to develop a different method to verify the sensor results at low flows that are more representative of a horse's breath. This was done by developing our own wind tunnel specifically for low flows. Finally, we tested on multiple horses to verify the total system's functionality.

5.2.1 High speed wind tunnel test

The wind tunnel in WPI's Aerospace department was used to verify both sensors accurately measured high wind speeds. The wind tunnel is calibrated based on reading a large water manometer that experiences changes in the water height due to the speed of airflow through the pitot tube in the wind tunnel. Visual changes in the water height do not occur below approximately 20 MPH and above this the change in height is still very small, so the calibration is approximate and assumed linear from 0 to 100 MPH even though the low speeds cannot be verified. Eq. 5.1 is the current calibration equation for the wind tunnel.

$$\mathrm{V(m/s)} = \frac{45}{56.5} * \mathrm{f(Hz)} \text{ (Eq. 5.1)}$$

Equation 5.1 was used to determine what frequency to set the wind tunnel to in order to test at the desired speeds. We laser cut an acrylic part (Figure 5.4) that attached to the common metal fixture (Figure 5.5) to hold the sensor steady in the flow stream.

Figure 5.4: Laser cut acrylic fixture for holding Rev P and Rev C sensors for high speed wind tunnel testing with a slot for wire insertion and hole for screw connection to the metal fixture (Figure 5.5)

Figure 5.5: Common fixture for attaching the test object in the high-speed wind tunnel

Figure 5.6 displays the final test setup for the wind tunnel test with the sensor in the wind tunnel attached to the laser cut piece and the standard metal fixture.

Figure 5.6: Rev P sensor held in flow stream by the laser cut acrylic piece

We first tested the Rev P sensor at wind speeds of 0, 2, 5, 8, and 12 MPH assuming that the calibration was actually linear at these low speeds. These speeds were chosen because the average flow rate of a horse, 65 L/min, is approximately 0.2 MPH assuming a diameter of 3 in. for the housing and the maximum flow rate of a horse, 1500 L/min is approximately 12 MPH assuming the same 3 in. diameter for the housing. Testing from 0 to 12 MPH ensured that we were testing across the entire possible range that a horse could produce. The first test was completed using the original equation, Equation 4.16, and then from this data five other equations were created for testing in order to determine which equation produced the best results. The five alternative equations were two linear equations (Equations 5.2 & 5.3), two polynomial equations (Equations 5.4 & 5.5), and one additional power equation (Equation 5.6).

$$\text{mph} = 0.126 * \text{values} - 36.965 \text{ (Eq. 5.2)}$$
$$\text{mph} = 0.1302 * \text{values} - 38.557 \text{(Eq. 5.3)}$$
$$\text{mph} = 0.0004 * \text{values}^2 - 0.1546 * \text{values} + 11.521 \text{(Eq. 5.4)}$$
$$\text{mph} = 0.003 * \text{values}^2 - 0.0492 * \text{values} - 7.6893 \text{(Eq. 5.5)}$$
$$3 * 10^{-19} * \text{values}^{7.5712} \text{ (Eq. 5.6)}$$

A LabVIEW program for each of these equations was created to increase the ease of testing, Appendix F displays the block diagram for each of these programs. We did not obtain the expected readings using any of these equations, but we did find that Equation 5.2 was the best fit for wind speeds below 2 MPH and that Equation 5.6 was the best fit for wind speeds above 2 MPH. The graphical results for each of these low flow tests with the Rev P sensor are displayed in Appendix G.

Since the Rev P sensor did not respond well to the low flow test in the wind tunnel we developed other methods for testing at low speeds, but we tested both the Rev P and Rev C sensors at higher speeds in the wind tunnel to guarantee that they responded to the known calibration speeds correctly. Both were tested at high speeds using their original Arduino equations in LabVIEW. Figure 5.7 is the graphical results for the Rev P and Figure 5.8 is the graphical results for the Rev C.

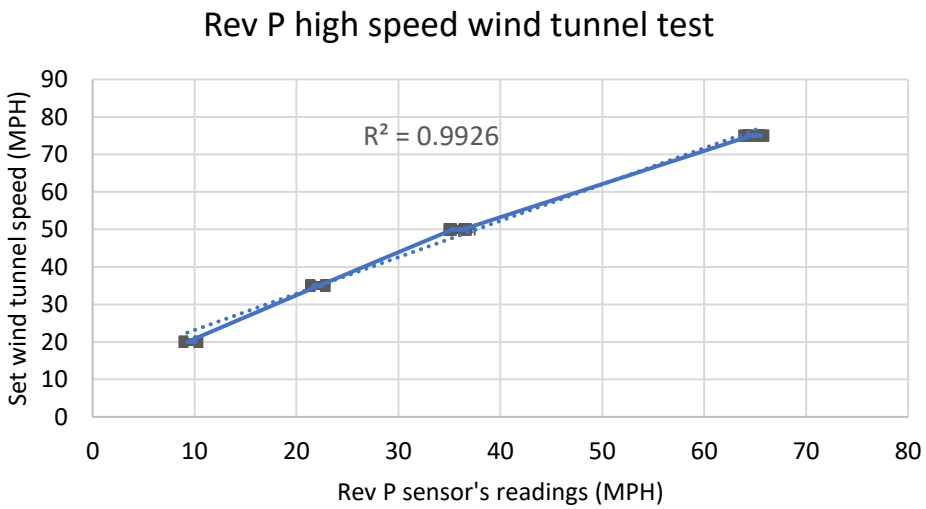

Figure 5.7: High speed wind tunnel test of the Rev P wind sensor with linear regression

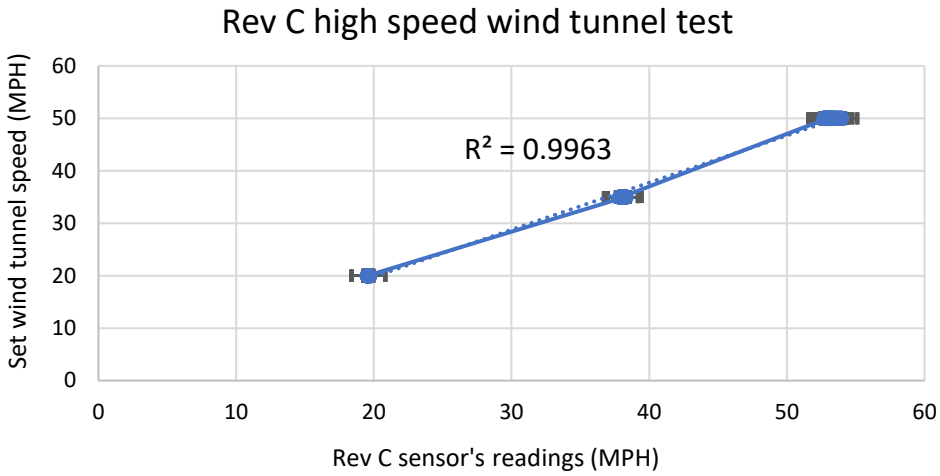

Figure 5.8: High speed wind tunnel test results of the Rev C wind sensor with linear regression

As seen in Figure 5.8, the Rev C sensor responded linearly to the increase in speed. It also read very close to the known calibration value, whereas the readings from the Rev P sensor were linear, but did not read within an acceptable range of the known value as seen in Figure 5.7. The Rev P was reading close to 10 MPH at 20 MPH, whereas the Rev C read 20 MPH at 20 MPH. Due to the low speed readings and inability to properly calibrate the Rev P sensor, all additional testing was continued with just the Rev C sensor to further verify its functionality.

5.2.2 Low flow wind tunnel test

After testing in the high-speed wind tunnel, we designed and constructed our own low flow wind tunnel for testing at speeds closer to what horses produce while breathing both at rest and during exercise. We created our low flow wind tunnel using two 2 ft. 3-in. diameter PVC pipes connected by a coupler, an air regulator, an on/off ball valve, 6 ft. of airline tubing, and 5 PVC reducers to go from 3-in. diameter PVC to ¼-in. NPT, a bundle of coffee stirrers, and a compressed airline. The coffee stirrers were cut to 1.5 in. lengths and then bundled using rubber bands to form a 2-in. diameter flow straightener. This was placed at the end of one of the PVC pipes closest to the regulator. The air regulator was connected to a compressed airline and the flow rate was controlled using the regulator and ball valve. A rotameter device was placed at the start of the tunnel connected directly to the ball valve and then the wind tunnel. This was used to measure initial flow rate. The sensor was attached 4 ft. from the regulator at the end of the other PVC pipe to ensure that the flow was laminar when it reached the sensor. Appendix H has

detailed instructions on how to properly setup and use the low flow wind tunnel. Figure 5.9 shows the overall setup of the low flow wind tunnel.

Figure 5.9: Low flow wind tunnel test setup showing the Rev C wind sensor wires connected at the end of the tunnel (left), the Testo 405i hot wire probe held at the open space at the end (left), and the rotameter (right) used to determine the set pressure of the ball valve

This wind tunnel was used with a variety of tests comparing to three different calibrated devices to verify that the Rev C sensor accurately measured low wind speeds. First, the Rev C sensor, which was taped inside of the PVC pipe to keep the sensor in the center of flow, was compared to the Hold Peak handheld anemometer. Appendix I is a standard operating procedure (SOP) for the use of the Hold Peak handheld anemometer. The handheld anemometer was held at the end of the wind tunnel just past where the sensor was. Many different orientations and locations were tried, but the handheld anemometer did not respond to the airflow because the airflow was too low to overcome the friction of the anemometer shaft.

Since the Rev C sensor's functionality could not be verified using the Hold Peak handheld anemometer we purchased a Testo 405i hot wire anemometer smart probe. The hot wire probe was held at the end of the PVC, so that the hot wire portion was in the center of the flow. Data was recorded using a Testo app (Smart probes). The data was then saved as an EXCEL file and compared to the sensor's readings. Appendix J includes a SOP for using this device. Figure 5.10 shows the two sensors speed readings in m/s graphed over the data points of each. Figure 5.11 shows the results of the same test, but compares the two sensor's speed readings directly with the Rev C sensor's readings on the x-axis and the Testo 405i hot wire probe's readings on the y-axis.

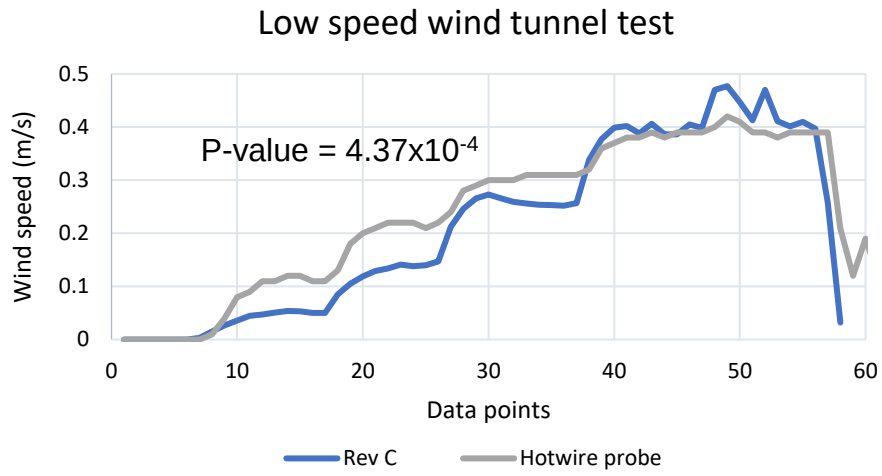

Figure 5.10: Overlaid signal from the Rev C and Testo 405i hot wire probe

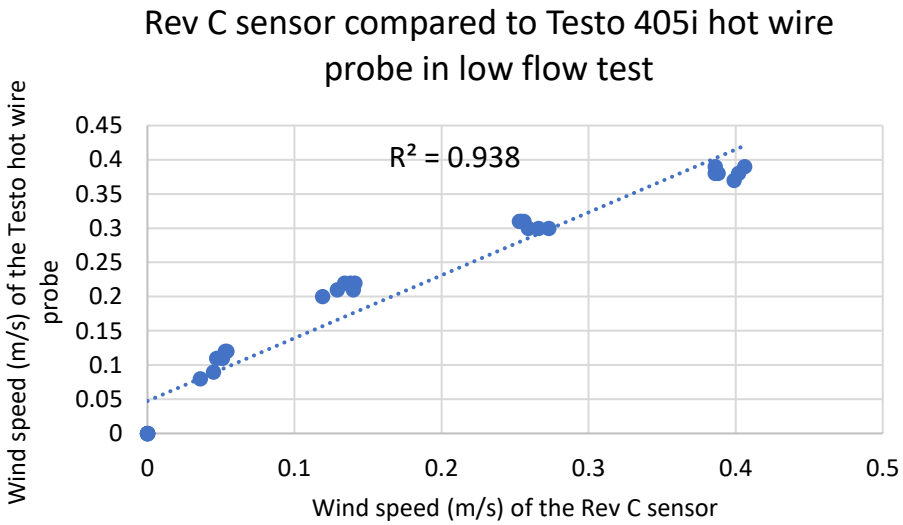

Figure 5.11: Linear regression analysis of the Rev C wind sensor compared to the Testo 405i hot wire probe in low flow wind tunnel test

As Figure 5.10 shows, the hot wire anemometer produces similar readings to the Rev C sensor at flows below 0.5 m/s. Above this speed the Rev C sensor's readings began to drift higher than the hot wire probe's readings. A one sample T-test was conducted between the differences of the two data sets with a null hypothesis of $\mu \neq 0$. The test had a p value of 0.000437, much less than an α of 0.05, so the null hypothesis was rejected. This showed that there was no

significant different between the hot wire probe and Rev C data sets, thus verifying that the Rev C sensor is calibrated and functions correctly in the range that would be expected for a horse at rest. Figure 5.11 further justifies that the Rev C sensor accurately reads low wind speeds because it is linearly comparable to the Testo 405i hot wire probe. This is shown by the R^2 value of 0.9369, which is close to 1, meaning the line is almost perfectly linear.

Lastly, the Rev C sensor was compared to the Fleisch pneumotachograph in the low flow wind tunnel to verify the readings from each were comparable. The Fleisch pneumotachograph was first connected to Open Pleth and calibrated using the 4.07 L syringe we constructed. After reaching an appropriate calibration factor from the calibration, the device was attached to the low flow wind tunnel along with the Rev C sensor. Very quickly we realized that the low flow wind tunnel would not be appropriate for testing the pneumotachograph because the pneumotachograph finds the volumetric flow rate using integration. Since the low flow wind tunnel provides a consistent flow rate the integration resulted in a zero reading at all constant speeds. To get a proper integration factor that can be compared to the flow rate measured by the Rev C sensor the flow needs to be cyclic so other test methods were used to compare the two devices.

5.2.3 Syringe test

We used the 4.07 L syringe that we designed and constructed to test the wind sensor's response to cyclic airflow. The syringe produced airflows between 0.6 and 1 MPH based on readings from the handheld anemometer. The Rev C sensor responded as expected, producing cyclic peaks and valleys with maximums close to those measured by the handheld anemometer. Figure 5.12 shows the wind speed in MPH measured by the sensor over the data points.

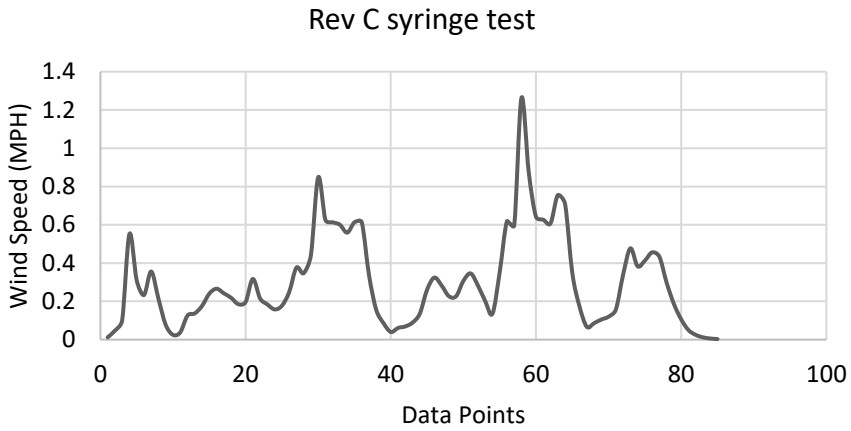

Figure 5.12: Rev C wind speed readings of cyclic flow produced by team created 4.07 L syringe

After determining how the Rev C sensor responded to cyclic flow, the syringe was used to produce a cyclic flow through both the pneumotachograph and the Rev C sensor simultaneously. Data for the Rev C sensor was collected using LabVIEW and data from the pneumotachograph was collected in Open Pleth. After five to ten cycles the programs were stopped and the data was exported to EXCEL. The flow rate data from both were compared by graphing. Figure 5.13 displays the flow rate comparison of the two devices during the syringe test.

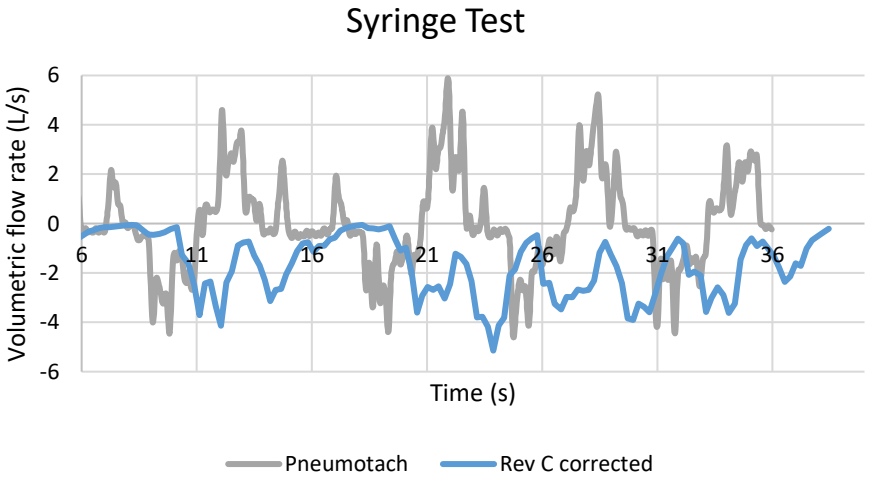

Figure 5.13: Graphical comparison of corrected Rev C data and Fleisch pneumotachograph data during syringe testing with the team designed 4.07 L syringe

There was a delay between the start of the two programs used to collect the data to produce the graph seen in Figure 5.13, resulting in a misalignment of the data. The Rev C sensor responds with the proper shape and amplitude to the cyclic flow, but all values it reads are positive. In order to correct for this the signal needs to be inverted, so that inspiration is negative and then shifted so that the graphical signal crosses zero as the veterinarian expects to see. This data manipulation does not change what the data represents, but instead puts it in a form the veterinarian is used to seeing, so it is easier for them to understand and compare to other methods they use for testing. Human breathing tests were used to better compare the performance of both the Rev C and pneumotachograph because breathing is more controlled and easier to compare than the irregular movement of the syringe.

5.2.4 Human breathing test

Humans and horses produce a similar shaped curve just with different amplitudes, so breathing tests on human subjects provide a good representation of how the sensor will respond on a horse. These breathing tests were performed to determine if the temperature change between inspiration and expiration would have an effect on the sensor's performance. We were also trying to determine if humidity would impact the sensors function. Breathing tests were performed following the same method as syringe tests. The sensor was adhered to the end of the pneumotachograph with the sensor in the center of the airflow. One of the team members breathed through a funnel attached to the pneumotachograph for 25 seconds. Data was collected using LabVIEW for the Rev C sensor and Open Pleth for the pneumotachograph. After the test was complete, the data was exported to LabVIEW from each program and the results were compared in EXCEL. Similar data manipulation techniques were used for the Rev C results to better display the relationship of the data from both. This manipulation included negating the data and shifting it up by a factor to ensure that it had both positive and negative readings where appropriate. Figure 5.14 displays the overlaid pneumotachograph and Rev C data from a breathing test after manipulation of the Rev C data.

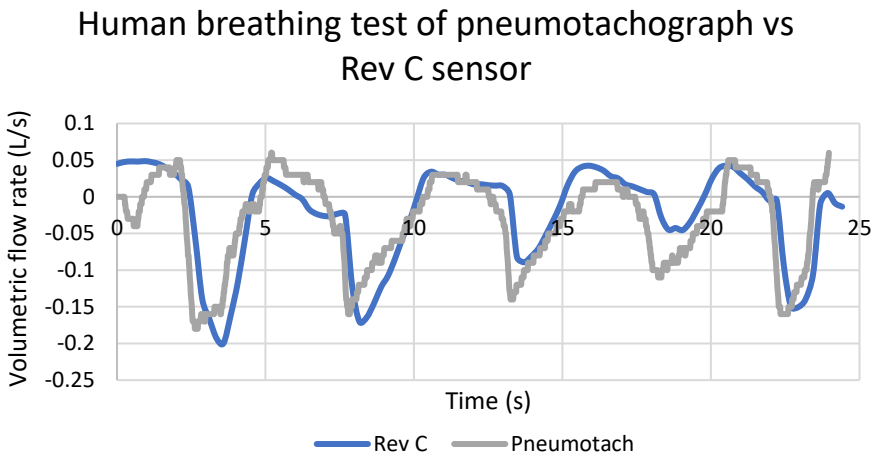

Figure 5.14: Overlaid pneumotachograph and corrected Rev C data for a human breathing test

Figure 5.14 shows that the curves of each device overlap very well. From these results, it was determined that temperature and humidity do not affect the Rev C sensor's functionality. The breathing tests also further verified that the pneumotachograph and the Rev C sensor produce readings that are within an acceptable range of error from one another confirming that both the pneumotachograph and the Rev C had a similar response to breathing.

5.3 Clinical testing on horses

We designed a simple housing that interfaced with the current facemask and housed the sensor exposing the sensor to the center of the airflow as shown in Figure 4.20. We also designed two different LabVIEW programs for clinical testing. The first incorporated a single calibration program that found the zero-wind adjustment factor using the method described previously. This zero-point was then automatically updated in the test program using global variables. This was executed using a case structure controlled by the ringer, so that the veterinarian using the program could easily control which program was running without having multiple files open. It also guaranteed the proper correction factor was entered into the test program removing the chances of human error with the transfer of the correction factor between programs. Appendix K displays images of both the front panel and the block diagram for this program. Appendix L is an SOP for how to use this program for a clinical test. The second program incorporates a second calibration program that is run after the zero-point calibration. This calibration finds the shifting factor that is required to automatically manipulate the data to display the data with both the

negative and positive values as would typically be seen in a breathing test. This program was written to shift and integrate the signal on each iteration until the integration equals the average dead space of a horse (2.5 L). Once this value is reached within a specified range of error, the program stops running and the shift factor is automatically incorporated in the test program. Appendix M displays images of the block diagram and front panel of this program and Appendix N is an SOP for using this program for clinical tests.

Three different horses, Oliver, Missy, and Ginger, were tested using the one-step calibration program. Oliver and Missy were both tested unsedated in stables in the hospital. Ginger was tested in the lung lab and was slightly sedated because of an earlier procedure. Before each horse was tested, the mask and housing were wiped down with an antiseptic, the sensor was zeroed to the room, placed in the housing, and the mask was put on the horse's muzzle by Dr. Mazan. The test program in LabVIEW was run on each horse for approximately a minute and the data was saved to EXCEL. Figure 5.15 shows the final device being used in a clinical test.

Figure 5.15: Final device being used during clinical testing

The flow rate versus time data was visually displayed during testing for each horse. After testing was complete, the saved data for each horse was manipulated in MATLAB to display the proper positive and negative readings, and was then graphed in EXCEL in order to analyze the results and compare to past test with the pneumotachograph. Figure 5.16 shows the graphical results from each horse.

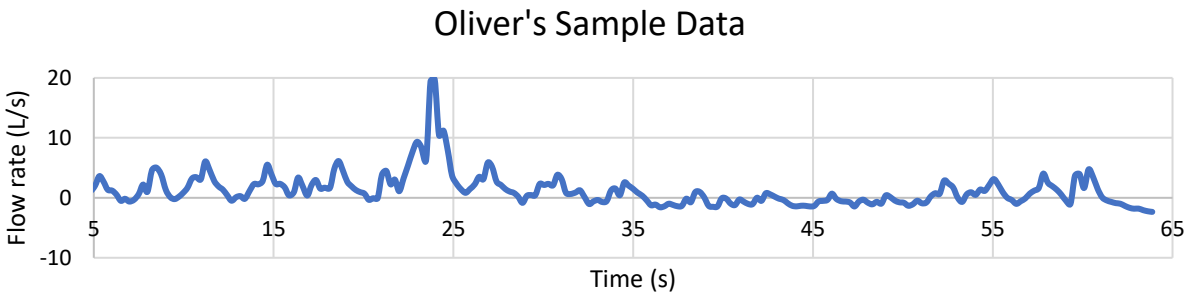

A.

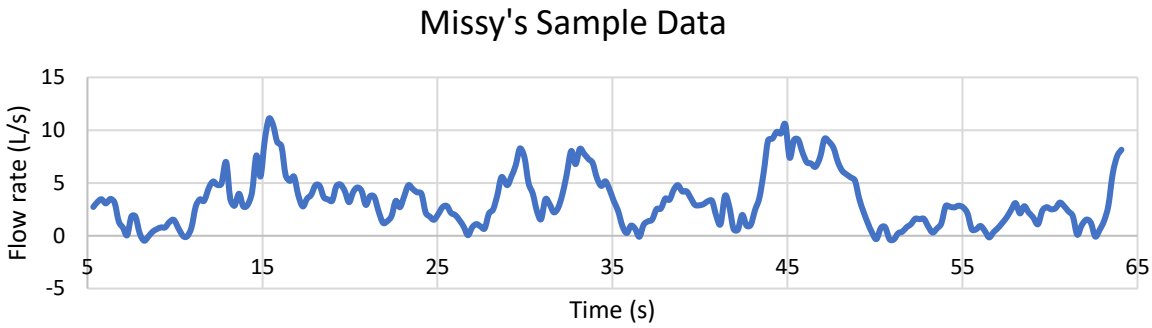

B.

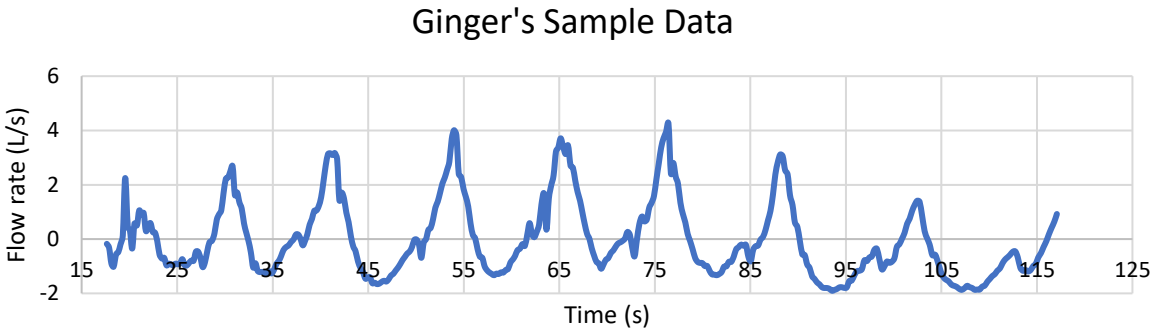

C.

Figure 5.16: A) Oliver clinical test results after manipulation in MATLAB; B) Missy test results after manipulation in MATLAB; C) Ginger test results after manipulation in MATLAB

Oliver was the first clinical test subject. His breathing provided the cyclic patterns and peaks expected in a horse's respiratory pattern, but he was frightened by other horse's in the area causing him to whinny (spike at 23 seconds). His respiratory rate was also fast and irregular compared to a sedated horse's patterns. Missy was a smaller pony compared to Oliver and Ginger, thus her lung capacity was smaller. She had lower peaks in her flow rate which was

expected, but the data was also noisy due to the misalignment of the sensor in the housing during testing. Lastly, Ginger had an ideal set of sample data. She was tested in the lung lab and was slightly sedated, so she had a very consistent respiratory rate. Her resulting flow rate maximums were comparable to past data from other horses of her size.

6.0 Final Design and Validation

6.1 Design validation

Our final functional design included several different components. Each working component required separate testing and verification to determine success. This section discusses how the testing for each component contributed to the overall functionality of the device and how our objectives were met.

6.1.1 Calibration of the sensors

The first major component of our design was the calibration of the sensing element we used to measure the airflow from the horse's lungs. Successful calibration was essential because it allows for accurate measurements to be made. The ISO/IEC 17025:2005 standard was incorporated while calibrating the Rev C wind sensor for accuracy. This international standard describes the requirements that calibration laboratories must follow to ensure competent testing. It focuses on technical requirements that determine whether or not calibration tests are reliable and correct, as well as management requirements that determine if a customer's requirements have been met (International Organization of Standardization, n.d.). Our sensor was calibrated by performing a zero-point test. This placed the sensor in an environment with no airflow and gave us our first point for a calibration curve. The zero-point test was also used to determine an adjustment factor that is automatically incorporated into our LabVIEW test program.

6.1.2 Measuring airflow from breathing horse

Another important component to the success of our project was measuring airflow from a breathing horse. These measurements are needed to analyze the lung function of a horse for potential disorders. We measured airflow directly using the Rev C wind sensor from Modern Device. The wind sensor measures air speed from the change in temperature that the horse's breath causes as it passes over a thermistor incorporated into the sensor.

After successful calibration, multiple tests were performed to confirm the wind sensor's function. The first was a basic test that involved blowing on the sensor to prove that it registered the change in airflow. After confirming the sensor's responsiveness, our zero-point testing was done again to prove that our calibration was correct. Zero-point testing provided a no airflow environment to change the adjustment factor in our LabVIEW program so the sensor reads correctly at 0 MPH of wind. After zero-point testing was successful, high flow wind tunnel

testing was done so that known wind speed values could be compared with the sensor's readings. This testing allowed us to confirm the sensor was reading airspeed correctly at higher speeds because the wind tunnel was calibrated linearly for wind speeds above 20 MPH. The wind tunnel testing also showed the consistency of the sensor's readings. To confirm the sensor could read lower wind speed values, closer to those of a horse's breath, we constructed a smaller scale wind tunnel using a compressed air regulator. We were able to conclude that the sensor can read at low flow speeds below 0.5 m/s. Additionally, we conducted breathing tests with human subjects that compared the Rev C to the pneumotachograph, simultaneously. This further confirmed the Rev C's function at low wind speeds, as well as its ability to read cyclic data that breathing produces. After manipulating the sensor data from wind speed to flow rate and accounting for the negative inspiratory flow, the graphs for both devices aligned with each other, showing the similarities between the readings. These tests verified that the Rev C can correctly read lower speeds similar to that of a horse at rest and during exercise.

After testing was completed to determine the sensor's function, the sensor, along with the entire system, was ready to be validated by testing on horses. Three horses were tested with our device. Two of the three horses were tested while unsedated in the stables of the hospital and the last was mildly sedated because of a previous test. This is an improvement from the Fleisch pneumotachograph which requires full sedation. Only one operator was required to perform these tests compared to the multiple required for tests with the Fleisch pneumotachograph. The results of these tests were comparable to past data collected in Open Pleth in terms of maximum flow rate experienced and respiratory rate.

6.1.3 Displaying the lung function data

The last main component of our new device is the data acquisition and display. Collecting and displaying data proved our sensor was working properly. LabVIEW was used to acquire the data from the sensing element and to also display the data graphically. A simple virtual interface developed in LabVIEW successfully allowed us to collect and save data during our calibration and measuring phases. Our team was also able to successfully account for both inspiration and expiration by manipulating the data in MATLAB after testing was complete because the sensor only collects positive readings. Improvements were made during the course of the project and our final program is able to not only collect and save data, but displays a graph of

the unmanipulated flow rate over time. Flow rate (L/s), speed in MPH and m/s, and volume (L) data points are also displayed while the program is running. All of this data is exported and saved in EXCEL for further signal manipulation after testing is complete.

6.1.4 Attachment of the device to the horse

Our team wanted to develop an improved attachment method for our new device design. The pneumotachograph attaches to a bulky, plastic mask that goes almost half way up the horse's muzzle. The sensor we used was capable of having a significantly smaller housing than the pneumotachograph. The housing used in our prototype is a simple, cylindrical rubber coupling that is 1.5 in. in diameter and 3.4 in. in length. An insert for the Rev C was cut into the coupling and a rubber stopper was attached to the coupling so that the sensor would rest in the stream of airflow. The coupling inserts into the current mask and protrudes only 2.5 in., decreasing the overall size by 80%. The housing also decreased in weight by 90%, weighing only 0.32 lbs. This design worked successfully in holding the sensor and attaching to the current mask while also decreasing the overall weight and size.

6.2 Impact of Device

6.2.1 Economics

Horses are expensive; they require special accommodations and veterinary care. Respiratory disorders are a common occurrence in horses and having a less expensive and easy way to test pulmonary function could save a horse owner's money. A less expensive option also makes the device more available to practicing equine veterinarians. Currently, Cummings school is one of few facilities that has access to the Fleisch pneumotachograph device. By creating a less expensive and easy to use device, the market would expand to other veterinarians around the country, potentially resulting in more diagnoses and higher treatment rates for horses with pulmonary disorders. The market for pulmonary testing could also expand beyond race and sport horses who often receive top of the line veterinary care. As an economic downside, however, a non-invasive and less expensive device could make invasive methods less common, taking business away from specialists that perform those kinds of procedures.

6.2.2 Environmental Impact

Compared to invasive methods to test an equine's lung function, our non-invasive device would produce less medical waste. Traditionally, an esophageal balloon is placed in the esophagus to measure pleural pressure to diagnose pulmonary disorders. The balloon and small tubing that are used in this method are then disposed of after the procedure is complete. Another common lung function testing procedure, Bronchoalveolar Lavage (BAL), utilizes a bronchoscope that is placed in the lungs and fluid samples are collected and analyzed. The fluid collected from this procedure must be properly disposed of, creating biohazardous waste. The waste generated from these invasive procedures would negatively impact the environment. Our device, however, minimizes waste because it is non-invasive, sterilizable, and reusable, reducing negative environmental impacts. Additionally, our device is much smaller than the current Fleisch pneumotachograph, therefore less chemicals are required to clean the device.

6.2.3 Societal Influence

A non-invasive and less expensive pulmonary testing device for horses could result in healthier horses. Currently, sport or race horses might receive more diagnoses and treatments for respiratory disorders because they are expected to perform well and their owners can easily afford or prioritize veterinary care. With a new device, more horse owners could have access to improved care and a healthier horse.

6.2.4 Political Ramifications

Our product not only can be used for lung function testing in equines, but for non-compliant humans such as those in emergency cases or infants. By expanding from veterinary use, the global market would be positively influenced because of the increase in potential users around the world. Looking at the veterinary market specifically, we performed a marketability study, where we asked veterinarians and horse owners a list of questions about respiratory disorders in horses and their willingness to pay and or use a non-invasive testing device. Appendix O includes a list of questions we asked horse owners and Appendix P includes the questions we asked veterinarians. From this study, we found that 30% of horse owners have had a horse with a respiratory disorder and a majority of horse owners were willing to pay over $150 for equine lung function testing if they thought their horse may have a respiratory disorder. Appendix Q shows the complete results of this study in pie graph form. The respondents were

limited to horse owners we knew and people they passed the survey onto, so this study had fewer respondents from a smaller region compared to the veterinarian study.

The veterinarians, who were surveyed around the country, also responded positively about their willingness to use the device, but most were not willing to spend a significant amount of money on the device. This need for less expensive diagnostic tools is one objective that our device will meet, thus making it more accessible to veterinarians, especially individual travelling veterinarians or small practices who have limited financial resources. Appendix R shows the overall results of the veterinarian survey, Appendix S displays the results broken down by region.

For both the veterinarian and horse owner surveys, some questions used the scale of 1 to 5 in terms of time, where 1 was never and 5 was weekly. These surveys did prove that there was a market for a non-invasive device in the United States, but it also suggested the device needs to be significantly less expensive than the current device to make it more available. We did not survey any veterinarians outside of the United States, but other countries that regularly practice equine sports could also benefit from improved veterinary diagnostic equipment. This would expand the market for our device globally and improve the standard of equine veterinary care as well.

6.2.5 Ethical Concerns

Our device could aid in diagnosing pulmonary disorders in racehorses. This could help improve the care and lives of horses performing at high levels. However, our device could also be indirectly linked with the horse racing industry. Although horse racing is designed to be elegant and showcase a horse's skill, there are some ethical concerns associated with the sport including drug abuse, injuries, and slaughter of horses.

6.2.6 Health and Safety Issues

Compared to the original Fleisch pneumotachograph, our device is physically smaller and lighter with a more secure attachment method, decreasing the probability that it would become a projectile during testing. This decreases the risk of serious injury of all personnel in the testing room. Additionally, because our device requires non-invasive techniques for operation, the complications and pain that the horse might experience during invasive tests are minimized.

6.2.7 Manufacturability

The final design, in terms of manufacturability, can be streamlined due to easily accessible components. There are two basic components: electrical and housing. The electrical component consists of the wind sensor and wires. The assembly process for the electrical component only requires one step because of the wind sensor's established circuitry; solder four wires onto the sensor. The final cylindrical housing would be rapid prototyped to incorporate the desired diameter and length as well as a slot for the sensor.

6.2.8 Sustainability

In an effort to promote sustainability with our design, we have chosen to use electricity at a low voltage to power our device, at only 5 volts. In addition, we have chosen to use a rubber coupling for our housing that can be repurposed later on if the device is disposed of. Our final device also creates minimal waste as described in 6.2.2, and can be reused for testing on horses. Due to the durability of the materials chosen and its multi-use design, the final device should last a long time and under proper use should not require frequent part replacements.

7.0 Discussion

Our project was designing a prototype of a new, non-invasive, small, lightweight, low cost, and accurate equine lung function testing device. The current gold standards for equine lung function testing are invasive, complicated procedures that most veterinarians perform as a last resort. The only non-invasive device in New England includes a Fleisch pneumotachograph that measures pressure drop across a 2.5 in. diameter and 1.5 in. length, stainless-steel, capillary bed. This device is heavy (3 lbs.) and extends off the horse's muzzle approximately 12 in. It also provides too much resistance to the horse's breathing to be used during exercise. Our design improves upon the size, weight, availability, and resistance of the current device.

7.1 Choosing an appropriate sensing element

The first task was to choose a feasible way to measure airflow from a breathing horse that would be more accurate than the current device, but also smaller and significantly less expensive. A new sensing element would improve the device's availability and safety for the user. The hot-wire anemometry concept, specifically using a thermistor-based Modern Device Rev C Wind Sensor, was determined to be the most feasible design choice because of its ability to measure low airflow rates, compared to alternative designs we considered. Measuring low flow rates was important because horses breathe at flow rates lower than most calibrated flowmeters are capable of measuring. Most flowmeters on the market claim to measure in ranges that include low flow rates, but are calibrated at higher speeds, resulting in inaccuracies at the lower speed ranges. This made testing our sensing element at lower speeds critical to determine its feasibility for our final device.

The Rev C sensor was also a good choice for our design because it was significantly smaller and lighter than the Fleisch pneumotachograph used in the current device. The Rev C measures approximately 0.7 in. by 1.6 in., largely contributing to our ability to reduce the size and weight of our new design.

7.2 Sensor calibration

In order to ensure the device could accurately measure low wind speeds, it was calibrated at a range of flows. All initial tests were conducted at 0 MPH, achieved by covering the sensor with a glass bowl, to ensure that the sensor read the appropriate value. Modern Device created the sensor with a corresponding calibration equation. The calibrated equation included a zero-

wind adjustable correction factor to ensure the sensor accurately read 0 MPH. This correction factor is based on the environmental conditions the sensor is in. Without changing the adjustment factor, the sensor initially read slightly above 0 MPH. We believe this is due to a combination of air movement in the room that seeped through a gap between the bowl and table and the voltage used to initially calibrate the sensor during manufacturing. From the results of the zero-point test, we were able to determine what the correction factor should be at various voltages so the sensor read 0 MPH. We then programmed a calculation for this correction into the final program so that it did not need to be manually changed for each test. Calibration is an important process to ensure that the results obtained are accurate. The calibration method for our device is more consistent than the current device's calibration which relies heavily on a known volume supplied by a human operated 3 L calibration syringe. Our device uses an automated program which removes sources of potential human error, decreases the amount of time needed for calibration, and improves repeatability between tests.

7.3 Sensor function verification

Since a device cannot be fully calibrated with a single datum point, additional data was required for our initial calibration. We thought that testing in the Aerospace department's wind tunnel would be an ideal way to calibrate the sensors at varying known wind speeds, but when we performed initial tests with the Rev P sensor, we found large discrepancies in the reading between the wind tunnel and the Rev P sensor. We believed the discrepancy in the Rev P sensor compared to the wind tunnel readings may be due to the inaccurate calibration of the wind tunnel at low wind speeds. The wind tunnel was calibrated using a water manometer and at low wind speeds no change in height of the water can be detected. There is no discernible change until the wind tunnel is set above approximately 20 MPH. The calibration for the wind tunnel is assumed to be linear, since it is linear in the high speed measurable region, but this may not be accurate for lower speeds. We created several calibration equations from the collected data and conducted another wind tunnel test with the Rev P, but it still did not read the values accurately.

However, when testing the Rev C in the wind tunnel, it was able to accurately read the set high wind speed values and had a strong linear fit. Like the Rev P, the Rev C was not able to accurately read lower flow values, agreeing with our hypothesis about the wind tunnel's calibration not being linear at lower speeds. Because the Rev C matched with the higher speed

values, we pursued testing with that sensor over the Rev P.

Since the calibration is unknown at these low wind speeds and there was no readily available way for us to accurately prove the wind tunnel's calibration, we were still left with the problem of needing more than one known datum point for proper calibration of the sensors. To produce these known low wind speeds, we constructed a low flow wind tunnel to produce a steady, fully developed, laminar flow environment of different wind speeds depending on the regulated pressure. To compare the Rev C's reading, both a hot-wire anemometer probe and a Hold Peak handheld anemometer were used during testing. The handheld anemometer was inconsistent and unable to measure the low flows. We tested the Rev C against the hot-wire probe and obtained comparable readings with both sensors for flows less than 0.5 m/s. This data confirmed that the Rev C functioned at low speeds, similar to what a horse's breathing would produce.

The device not only needs to be able to accurately measure low wind speeds, but also differentiate between inspiratory and expiratory flow. This cyclic flow pattern was modeled with a 4.07 L PVC syringe. The sensor accurately produced peaks within the range of the handheld anemometer's readings and it had both valleys and peaks that corresponded to the cyclic movement of the syringe.

After verifying the sensors response to low flows and cyclic flows we compared the Fleisch pneumotachograph and Rev C simultaneously with a breathing test to verify that the Rev C sensor is not affected by the temperature differences between inhaled and exhaled breaths or the moisture content. The results of this breathing test showed the Rev C and pneumotachograph function was similar suggesting that the Rev C is not significantly affected by the unique properties of breathing.

Through the verification of the Rev C sensor, we were able to prove that it can accurately read low wind speeds and differentiate between inspiratory and expiratory flow, which is critical for a properly functioning equine lung function testing device. Accurate calibration and function testing are not sufficient to prove that the device operates properly in a clinical environment, so clinical tests were conducted to validate the sensor's function in this setting.

7.4 Clinical testing

To ensure the device was reduced in length and weight, both the new device and the Fleisch pneumotachograph were measured and weighed. It was determined that the new device was approximately 90% lighter and 80% shorter than the current. This proved that we met the sponsors need for a shorter and lighter device to improve the safety for the human operators. This decrease in size also minimizes the number of people required to perform the test, making it more accessible to small veterinary clinics that lack the necessary staff Cummings School has available to perform a test with the Fleisch pneumotachograph.

The test that ultimately proved our device met all of our sponsor's needs and functioned properly was a clinical trial on horses. After testing our device, we determined that the Rev C operates properly because it produced a cyclic flow pattern and the peak flow rates it collected were between 3 and 5 L/s, as expected for a horse based on previous data acquired in Open Pleth. In addition, our device was tested on unsedated stabled horses with no concerns, unlike the Fleisch pneumotachograph. Also, while testing our device, only one operator was required to hold it, compared to multiple people required to hold the Fleisch pneumotachograph. During our test an operator had to hold the device because the straps on the horse's facemask were not available. If the straps were available there is the potential our device would not require any operators to hold it. This saves both time and money for the veterinarian and for veterinary clinics.

7.5 Limitations

Our team was able to successfully meet most of our design objectives. However, even with all of these improvements, the device still has limitations. Currently, the LabVIEW software the sensor interfaces with needs to be directly connected to the sensor via a DAQ box, so the device cannot be used on an exercising horse unless it is on a treadmill. The long wires cause a potential tripping hazard for the human operators and horse. The requirement of an external power source for the device limits its portability and ability to be used onsite. Another limitation for usability onsite are the unforeseen weather conditions (rain, snow, fog, high winds) and its effect on the circuitry. Currently part of the wind sensor rests outside of the attachment and raises a durability concern as it is possible that the sensor could sustain permanent damage and fail to function. Additionally, the LabVIEW software for data acquisition is potentially too

expensive for small veterinary clinics to afford, which reduces the device's accessibility. Another limitation is the difficulty to diagnose with just the wind sensor because the current diagnostic method depends on the comparison between the RIP band signals and the Fleisch pneumotachograph and our device does not include the RIP bands.

8.0 Conclusions and Recommendations

8.1 Conclusions

Using Modern Device's Rev C Wind Sensor housed in a rubber coupling, a National Instruments DAQ box, and LabVIEW, we were able to successfully prototype an improved non-invasive device to measure equine lung function, detect abnormalities in airflow, and diagnose horses with subclinical pulmonary obstruction disorders. Our device provided an improved alternative to the current device that uses a Fleisch pneumotachograph because ours is much safer for the human operators. The design met our objectives of being less expensive, smaller, and lighter than the Fleisch pneumotachograph, therefore minimizing risk of injury for the human user. Additionally, our device is non-invasive, compatible with non-compliant breathing, and minimizes resistance to the horse's breathing. It also remained non-invasive which is safer and more comfortable for the horses being tested with the device. We created a LabVIEW program that acquires and displays flow and volume data, and we created a MATLAB program that accounts for inspiratory and expiratory flow. This was necessary because most anemometry devices require more than one sensor to measure flow in two directions. The whole system proved feasible through clinical testing on horses. Additionally, our device significantly reduces the cost of pulmonary testing, making it accessible to equine veterinarians beyond the ones at Cummings School.

Initially, four alternative design concepts were developed and their feasibility were assessed using velocity and pressure cut plots created in SolidWorks' Flow Simulations. Additional calculations were completed to further assess each design concept. Three out of the four alternative designs were ruled out either because they would drastically increase resistance, cause significant eddying and have a delayed response time that limits accuracy, or cannot accurately measure lower wind speeds similar to a horse's breath. With further research, we decided that thermistor-based sensors were most feasible. They work similarly to the hot-wire anemometer concept, one of our four alternative designs, only they are less fragile and less likely to be affected by moisture. Therefore, both the Rev C and Rev P wind sensors from Modern Device were purchased. However, the Rev C proved to be more accurate at lower wind speeds and was further pursued.

Zero-point testing on the Rev C was completed to properly calibrate the sensor so that it

could consistently and correctly measure data. After we verified that the sensor was functional at higher speeds using a high-speed wind tunnel and functional at lower speeds using our low flow wind tunnel; breathing tests from human subjects were completed to compare the pneumotachograph reading to the sensor's reading. Results from this test also verified that the Rev C was capable of working at lower wind speeds. After sensor verification testing, we moved to clinical testing on horses. This testing confirmed our device worked as desired and meets our main objectives described above.

Overall, our device can successfully measure equine lung function. However, our team did face a major setback when trying to verify our sensing element, costing us time we could have spent improving other aspects of our design. This setback was due to the limited availability of flowmeters calibrated to read low flow rates. Our team had to purchase or acquire multiple types of flowmeters before finding one that read accurately at low flows and could be used to calibrate and help verify our sensor's readings. Eventually, we were able to move past this roadblock and focus on other aspects of our design so the device could be used for clinical testing.

8.2 Recommendations

Due to time constraints and limited resources, there were a few recommendations our team had to further improve our device. These concepts are discussed in the following sections.

8.2.1 Improved sensor housing

Currently, the sensor circuitry is exposed outside of the housing. This exposure can cause the sensor circuitry to not function as intended due to external environmental factors and it increases the likelihood of damage. We recommend a protective covering for the sensor circuitry consisting of rubber with a slot for the sensor to be inserted and removed from that can close during testing. The protective covering would be attached to the current rubber housing. Additionally, rapid prototyping a housing with a more precise slot and wire rest would be ideal to ensure the sensor does not move during testing. The protective covering mentioned above could also be incorporated into this design. This would make the housing a more rigid, but still lightweight, one-piece device that would be less fragile and would support and protect the sensor better.

8.2.2 Improved mask design

The pneumotachograph attaches to a transparent plastic mask with rubber components that slides onto the horse's muzzle and covers approximately half of the horse's face. Our device is housed in a 1.5-inch diameter rubber coupling that attaches to the current mask. However, the current mask is bulky, large, and has a protrusion off the front to attach the pneumotachograph. Due to a lack of time our team could not create a new mask, but CT scans of a horse's head were obtained. These scans could be used to design a mask that fits the horse's face better and directly incorporates the Rev C sensor. The current mask's protrusion could easily be eliminated with the new sensor, given its small size. We recommend an improved mask be made to better accompany the Rev C sensor and to continue increasing comfort for the horse.

8.2.3 Improved signal processing

The Rev C sensor only produces positive wind speed readings, so the flow rate versus time graph it produces, although correct, does not display in a way that is easily understandable for veterinarians because it is not what they are used to seeing when making diagnoses. This data can be manipulated in MATLAB after testing is complete, but ideally it would be processed real-time, so the running display can be used for diagnosis. In order to do this, a second functioning calibration program would need to be incorporated into the software. This program would find the appropriate shift factor for the horse being tested and then automatically incorporate it into the test program, using the same method as the zero-wind adjustment factor.

In addition to correcting the flow rate over time display, the veterinarians would like a display of a flow-volume loop that has the expected butterfly shape horse breathing generates. This would require making the XY chart used for the flow-volume loop dependent on time without time being an axis of the graph. If this graph is dependent on time, the data can be viewed over the same time interval as the flow rate over time graph thus showing only a given segment of the graph. This would allow the proper shape to be seen because a smaller scale would be analyzed at a time. The current display appears to be a straight line, but there are changes in the data that cannot be seen because of the scale. After making this graph time dependent these changes should produce the expected shape because the y-scale will be more appropriate for viewing the change.

Lastly, a table of critical values should be displayed during testing. This table should

include the start and end time of each breath, the breathing rate, the dosage of histamine administered, the delta flow, the tidal volume, theta (the angle between the abdomen and thorax signal produced by the RIP bands), the peak inspiratory flow, the peak expiratory flow, the inspiratory time, and the expiratory time. Further data processing will need to be programmed into the LabVIEW program to produce these values and display them in a table form. Others such as histamine dosage will need to be incorporated as a user input during testing. Lastly, theta cannot be found until the RIP bands are incorporated into the program and the voltage of both are graphed against each other with abdomen on the y-axis and ribcage on the x-axis.

8.2.4 Incorporating RIP bands

Veterinarians are able to diagnose pulmonary disorders with the current device from overlaying signals of the Fleisch pneumotachograph and the RIP bands. Currently the RIP bands are not integrated within our LabVIEW program, which means a veterinarian would have difficulties diagnosing pulmonary disorders with only our device. To integrate the RIP bands, we recommend a RLC (resistance-inductance-capacitance) circuit following the design in US-4,308,872 patent (Watson, Sackner, & Stott, 1982). The LabVIEW test program would also have to be updated to incorporate acquired signals from the RIP bands. This updated should include the overlaying of the RIP band and Rev C flow rate over time signals and a delta graph that shows the difference between these signals over time.

8.2.5 Wireless sensing

Our device is much smaller and provides less resistance to breathing than the current device, making it more ideal for use with exercising horses. Unfortunately, our device still incorporates wires to power the device and acquire the data from the sensor. In the future, we would like the device to be made completely wireless, using battery power and wireless data collection, so that veterinarians can easily use the device at barns or on racetracks. This could make the horses feel more comfortable if they are being tested at home. A wireless device could also be a better diagnostic tool because it could be used on exercising horses as well as resting horses, allowing veterinarians to compare lung function at different levels of exertion.

8.2.6 Improved test program

LabVIEW is used with the device we designed. LabVIEW allowed for easy customization when going through the process of building our data acquisition program, but

could be expensive for some veterinarians to acquire. Also, LabVIEW is a proprietary software that requires compliance with their license agreement in order to distribute and sell our device with our LabVIEW program. Due to their restrictions, we recommend that a software program be developed using a different platform than LabVIEW that is less expensive, able to sell without restrictions, and has improved user interface features. It would also be ideal if the software program is adaptable for mobile applications which would work well with a wireless device and enhance portability.

8.2.7 Continued clinical testing

Clinical testing was done on three horses with our device. Although our results suggested the device worked properly, more testing would help confirm its functionality. We suggest that the clinical tests include comparing our device to the Fleisch pneumotachograph on the same horses in the same conditions to confirm our device is comparable to the pneumotachograph. Further testing would also provide us with more data which could be used to better determine the accuracy of our device.

8.2.8 Humidity/moisture study

One concern we had with using a thermal-based sensing element was the effect that humidity and moisture could have on the sensor's readings. This is especially a concern since a horse exhales humid air that will condensate on the sensor. During our testing on horses, the sensor's readings did not appear to be affected by the moisture in the horses' breaths. However, conducting a study to specifically control for the effects of humidity on Rev C sensors would be beneficial to further confirm that humidity does not affect the readings of the sensor. If it is determined that humidity has a significant effect on the sensor's performance, a correction should be incorporated into the LabVIEW program to account for this effect.

8.2.9 Veterinarian feedback

Our team had hoped to interview multiple veterinarians after they used the device. Due to time constraints this did not happen, but would be beneficial to do in the future. Veterinarian feedback would provide insight to parts of the device that function well or make it easy to use as well as areas that are difficult to use or are not working as expected. This information would highlight improvements that would benefit the veterinarians using the product.

References

Advanced Thermal Solutions Inc. (2007). Understanding Hot Wire Anemometry. [Pamphlet]. Norwood, MA: Thermal Solutions.

American Lung Association. (2016). How lungs work. Retrieved from http://www.lung.org/lung-health-and-diseases/how-lungs-work/lung-capacity-and-aging.html?referrer=https://www.google.com/

American Thoracic Society. (2009). Lung Function Studies: Methacholine Challenge Test. *Am J Respir Crit Care Med*. *180* (3-4).

American Veterinary Medical Association. (2015). *Confidentiality of veterinary patient records*. Retrieved from https://www.avma.org/Advocacy/StateAndLocal/Pages/sr-confidentiality-patient-records.aspx

Araujo, G. A. L., Freire, R. C. S., Silva, J. F., Oliveira, A., & Jaguaribe, E. F. (2004, May). Breathing flow measurement with constant temperature hot-wire anemometer for forced oscillations technique. *In Instrumentation and Measurement Technology Conference, 2004. IMTC 04. Proceedings of the 21st IEEE* (Vol. 1, pp. 730-733). IEEE.

Bailey, S. C. C., Hultmark, M., Monty, J. P., Alfredsson, P. H., Chong, M. S., Duncan, R. D., ... & Nagib, H. M. (2013). Obtaining accurate mean velocity measurements in high Reynolds number turbulent boundary layers using Pitot tubes. *Journal of Fluid Mechanics*, *715*, 642.

The British Horse Society. (2011). Advice on horse respiratory health. [Leaflet] Warwickshire, England.

Chen, T., Wang, Q., Zhang, B., Chen, R., & Chen, K. P. (2012). Distributed flow sensing using optical hot-wire grid. *Optics express*, *20*(8), 8240-8249.

Chen, Y. R. (2016). Characterization of cup anemometer dynamics and calculation of the acoustic noise produced by a nrel phase VI wind turbine (Doctoral dissertation, Case Western Reserve University). Retrieved from https://etd.ohiolink.edu/!etd.send_file?accession=case1459427530&disposition=inline

Crabbe, B. (2007). The comprehensive guide to equine veterinary medicine. Sterling Publishing Company.

Cummings Veterinary Medical Center. (2016). Melissa Mazan DVM, DACVIM. Retrieved from

http://vetprofiles.tufts.edu/doctor/melissa-mazan.

Davis, S. (2013). How does the Equine Respiratory System Work. *FlexinebTM North America*.

Erickson, D., O'Dell, D., Jiang, L., Oncescu, V., Gumus, A., Lee, S., ... & Mehta, S. (2014). Smartphone technology can be transformative to the deployment of lab-on-chip diagnostics. *Lab on a Chip*, *14*(17), 3159-3164.

Erickson, H. H., Goff, J. P., & Uemura, E. E. (2004). *Dukes' physiology of domestic animals* (Vol. 512). W. O. Reece (Ed.). Ithaca, NY: Cornell University Press.

Farnell Ltd. (2016). FS5.0.1L.195 innovative sensor technology. Retrieved from http://uk.farnell.com/ist/fs5-0-1l-195/sensor-flow-gas/dp/1778049

Funda, D. (2010). Hot wire measurements [PDF document]. Retrieved from http://ocw.metu.edu.tr/course/view.php?id=66

Gordon, J. (2009). The horse industry contributing to the Australian economy. A report for the Rural Industries Research and Development Corporation, RIRDC publication 01/83 RIRDC project no CIE-9a.

Granta Design Limited. (2016). CES EduPack [Computer software]. Cambridge, United Kingdom.

Gudmundsson, S. (2013). *General aviation aircraft design: Applied Methods and Procedures*. Butterworth-Heinemann.

Hausberger, M., Roche, H., Henry, S., & Visser, E. K. (2008). A review of the human–horse relationship. *Applied Animal Behaviour Science*, *109*(1), 1-24.

Hoffman, A. M. (2002). Clinical application of pulmonary function testing in horses. *Equine respiratory diseases international veterinary information service Ithaca, Document No B, 3040802*.

Hoffman, A. M., Mazan, M. R. (1999). Programme of lung function testing horses suspected of small airway disease. *Equine Veterinary Education,* 11(6), 322-328.

Howell, D. (2011). Horse clip art. Retrieved from http://orig12.deviantart.net/bcc9/f/2011/152/f/a/horse_clip_art_by_soulhavennz-d3hr8sk.png

IEEE, (2014). *2700-2014 - IEEE Standard for Sensor Performance Parameter Definitions*. Retrieved from http://ieeexplore.ieee.org/document/6880296/

International Organization of Standardization. (n.d.). *ISO- International Organization of Standardization.* Retrieved from http://www.iso.org

Knapp, W. R., Holt, D. A., & Lechtenberg, V. L. (1975). Hay preservation and quality improvement by anhydrous ammonia treatment. *Agronomy Journal*, *67*(6), 766-769

Kramme, R., Schlegelmilch, R. M., (2011). Springer Handbook of Medical Technology: Pulmonary Function Testing. Berlin: Springer.

Kristensen, L., Hansen, O., Hansen, S. (2014). The working of the cup anemometer. Retrieved from http://www.windsensor.com/application/files/8814/2694/4640/The_Working_of_the_Cup_Anemometer_20140619.pdf

Kusano, K., Ishikawa, Y., Kazuhiro, S. E. K. I., & Kusunose, R. (2008). Characteristic of inflammatory airway disease in Japanese Thoroughbred racehorses. *Journal of equine science*, *19*(2), 25-29.

Kutasi, O., Balogh, N., Lajos, Z., Nagy, K., & Szenci, O. (2011). Diagnostic approaches for the assessment of equine chronic pulmonary disorders. *Journal of Equine Veterinary Science*, *31*(7), 400-410.

Marieb, E. & Hoehn, K. (2012). Human anatomy and physiology (9th ed.). Boston, MA: Pearson.

Mazan, M. R., & Hoffman, A. M. (2003). Clinical techniques for diagnosis of inflammatory airway disease in the horse. *Clinical Techniques in Equine Practice*, *2*(3), 238-257.

McCall, C. A. (1990). A review of learning behavior in horses and its application in horse training. *J. Anim. Sci*, *68*, 75-81.

McMaster-Carr. (2016). Noncontact tachometers. Retrieved from http://www.mcmaster.com/#noncontact-tachometers/=14jlom7

Midland Hardware: Lawn & Garden Plumbing Electrical Tools. (2016). K & S aluminum tube 1/16 in. 8100. Retrieved from http://www.midlandhardware.com/642926.html?gclid=Cj0KEQjwvve_BRDmg9Kt9ufO15EBEiQAKoc6qrzhFTpqLs5a2yyq3k

Modern Device. (2016). Wind sensor rev p- low cost anemometer. Retrieved from https://moderndevice.com/product/wind-sensor-rev-p/

Molecular Products Ltd. (n.d.). *Technical article: A Guide to Breathing Rates in Confined Environments*. Retrieved from http://www.molecularproducts.com/pdf/technical-library/A%20Guide%20to%20Breathing%20Rates%20in%20Confined%20Environments%20Technical%20Article.pdf

Moore, J. E., Millar, B. C., Matsuda, M., & Buckley, T. (2003). Human infections associated with horse bites. *Journal of Equine Veterinary Science*, *23*(2), 52-54.

Myers, W., Bass, P. (2010). *A Physical Exam for Asthma Diagnosis*. Retrieved from http://www.everydayhealth.com/asthma/physical-examination-for-asthma.aspx

National Instruments. (2016a). Buy LabVIEW. Retrieved from http://www.ni.com/labview/buy/

National Instruments. (2016b). NI USB-6000. Retrieved from http://www.ni.com/en-us/support/model.usb-6000.html

Omega. (n.d.). The strain gage. Retrieved from http://www.omega.com/literature/transactions/volume3/strain.html

Ozaki, Y., Ohyama, T., Yasuda, T., & Shimoyama, I. (2000, January). An air flow sensor modeled on wind receptor hairs of insects. In *Micro Electro Mechanical Systems, 2000. MEMS 2000. The Thirteenth Annual International Conference on* (pp. 531-536). IEEE.

PetWave. (2015). Diagnosing asthma (allergic bronchitis) in dogs. Retrieved from http://www.petwave.com/Dogs/Health/Asthma/Diagnosis.aspx

Pharmacopeia, U. S., (2009). USP-NF. *US Pharmacopeia*.

Pharmacopeia, U. S., (2014). General chapter< 797> pharmaceutical compounding–sterile preparations is revised and finalized.

Preuschoft, H., Witte, H., Recknagel, S., Bär, H., Lesch, C., & Wüthrich, M. (1999). Effect of common head gear on horses. *DTW. Deutsche Tierarztliche Wochenschrift*, *106*(4), 169-175.

Pusterla, N., Watson, J. L., & Wilson, W. D. (2006). Diagnostic approach to infectious respiratory disorders. *Clinical Techniques in Equine Practice*, *5*(3), 174-186.

Raven, M. & Rashmir-Raven, A. (1996). *Equine Science Instructional Materials*. Madison, WI: The National Council for Agricultural Education

Robinson, N. E. (2003). Inflammatory airway disease: defining the syndrome. Conclusions of the Havemeyer Workshop. Equine Veterinary Education, 15(2), 61-63.

Robinson, N. E., Derksen, F. J., Olszewski, M. A., & Buechner-Maxwell, V. A. (1996). The pathogenesis of chronic obstructive pulmonary disease of horses. *British Veterinary Journal*, *152*(3), 283-306.

Rozanski, E. A., & Hoffman, A. M. (1999). Pulmonary function testing in small animals. *Clinical techniques in small animal practice*, *14*(4), 237-241.

Sanchez, A., Couetil, L. L., Ward, M. P., & Clark, S. P. (2005). Effect of airway disease on blood gas exchange in racehorses. *Journal of Veterinary Internal Medicine*, *19*(1), 87-92.

Saylor Academy. (2011). Anemometer. Retrieved from https://www.saylor.org/site/wp-content/uploads/2011/04/Anemometer.pdf

Scope, I. I., Contraindications, B., & Training, C. T. (1999). Guidelines for methacholine and exercise challenge testing—1999. *American Journal of Respiratory and Critical Care Medicine*, *161*(1).

Shiner, R., Steier J., (2012). Lung Function Tests Made Easy. Churchill Livingstone.

Sigma-Aldrich, (2016). Tungsten wire, diam 0.25 mm >= 99.9% trace metals basis. Retrieved from http://www.sigmaaldrich.com/catalog/product/aldrich/267554?lang=en&region=US

Schwartz, M. M. (2003). Brazing. ASM international.

U.S Food and Drug Administration. (1995). CPG Sec. 607.100 - adequate directions for use (species designation) -animal drugs and veterinary devices. Retrieved from https://www.fda.gov/ICECI/ComplianceManuals/CompliancePolicyGuidanceManual/ucm074652.htm

Verbeek, C., Zanten, H. A., Vonderen, J. J., Kitchen, M. J., Hooper, S. B., & Pas, A. B. (2016). Accuracy of currently available neonatal respiratory function monitors for neonatal resuscitation. *European Journal of Pediatrics*, 1-6.

Vitalograph. (2016). The Fleisch pneumotachograph. Retrieved from https://vitalograph.com/education/fleisch

Watson, H. L., Sackner, M. A., & Stott, F. D. (1982). *U.S. Patent No. 4,308,872*. Washington, DC: U.S. Patent and Trademark Office.

Wood, J. L. N., Newton, J. R., Chanter, N., & Mumford, J. A. (2005). Inflammatory airway disease, nasal discharge and respiratory infections in young British racehorses. *Equine*

veterinary journal, *37*(3), 236-242.

Young, D. F., Munson B. R., Okiishi, T. H., & Huebsch, W. W. (2011). A brief introduction to fluid mechanics (5th ed.). United States of America: John Wiley & Sons, Inc.

Yu, C., Tsai, T. H., Huang, S. I., & Lin, C. W. (2013). Soft stethoscope for detecting asthma wheeze in young children. *Sensors*, *13*(6), 7399-7413.

Appendix A: Gantt charts for each seven-week project segment

ID	Task Mode	Task Name	Duration	Start	Finish
1					
2		**MQP Report**	**41 days**	**Sun 8/21/16**	**Fri 10/14/16**
3		introduction	7 days	Sun 9/11/16	Mon 9/19/16
4		background research	25 days	Sun 8/21/16	Thu 9/22/16
5		background draft	11 days	Thu 9/22/16	Thu 10/6/16
6		Chapter 3 outline	7 days	Sun 9/18/16	Mon 9/26/16
7		Chapter 3 draft	12 days	Sun 9/25/16	Mon 10/10/16
8		Chapter 4 outline	8 days	Thu 9/22/16	Mon 10/3/16
9		Chapter 4 draft	7 days	Sun 10/2/16	Sun 10/9/16
10		Draft of Ch 1, 3 and 4	22 days	Sun 9/11/16	Mon 10/10/16
11					
12		**Design Process**	**41 days**	**Sun 8/21/16**	**Fri 10/14/16**
13		Brainstorm ideas	21 days	Mon 8/29/1	Mon 9/26/16
14		Obtain Specifications	22 days	Sun 9/4/16	Sat 10/1/16
15		Hand drawings	7 days	Sun 9/25/16	Sat 10/1/16
16		Design Matrix	16 days	Sun 9/25/16	Fri 10/14/16
17		Begin CAD drawings	12 days	Sat 9/24/16	Sat 10/8/16
18		Design Calibration Syringe	12 days	Fri 9/23/16	Sat 10/8/16
19		Develop Calibration Syringe	11 days	Sun 10/2/16	Fri 10/14/16
20		Characterize Original Device	9 days	Sun 9/25/16	Wed 10/5/16
21		Research Material Cost	11 days	Sun 10/2/16	Fri 10/14/16
22					
23		**Training**	**41 days**	**Sun 8/21/16**	**Fri 10/14/16**
24		Tufts lab safety	8 days	Thu 9/22/16	Sat 10/1/16
25		IACUC	8 days	Thu 9/22/16	Sat 10/1/16
26		WPI Lab Safety Training	13 days	Sun 9/11/16	Tue 9/27/16
27		Machine shop training	9 days	Wed 9/28/1	Mon 10/10/16

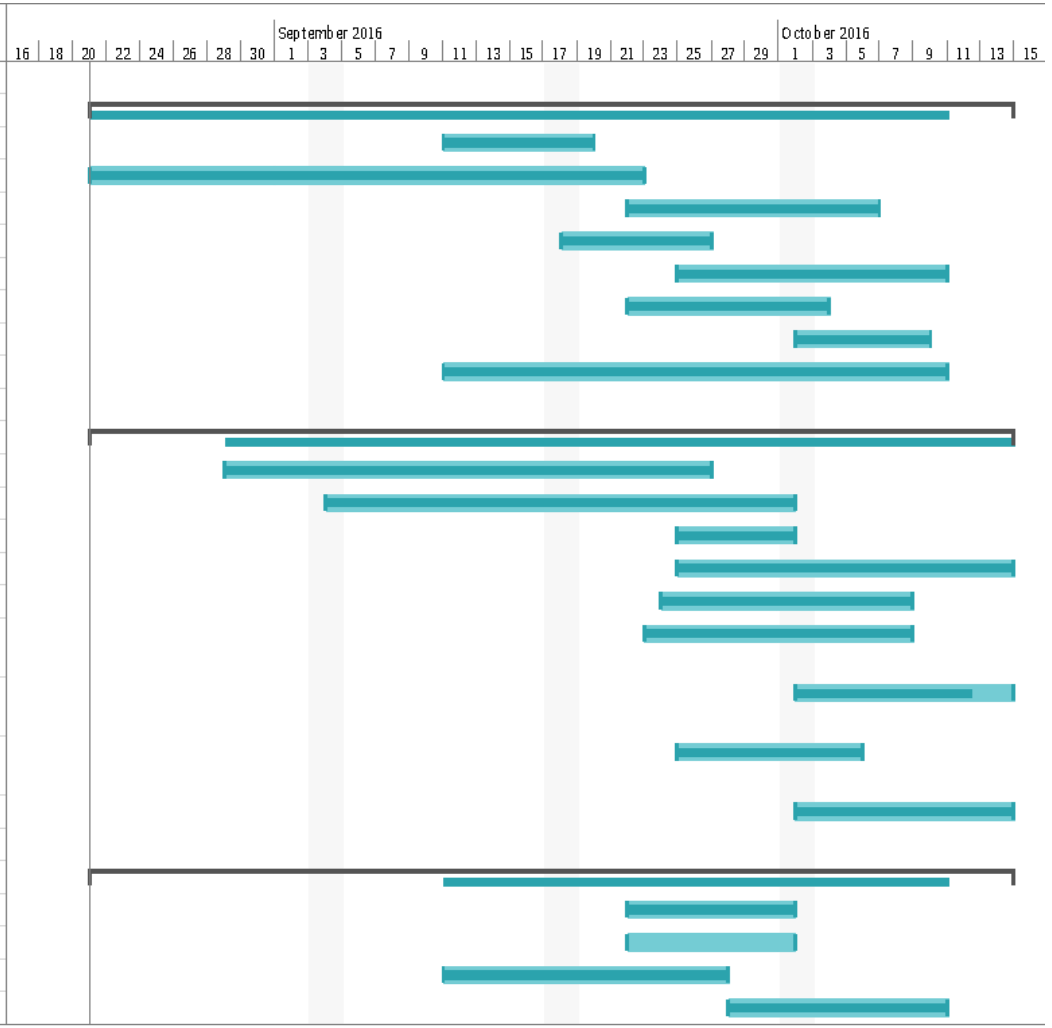

Figure A.1: Aterm Gantt chart

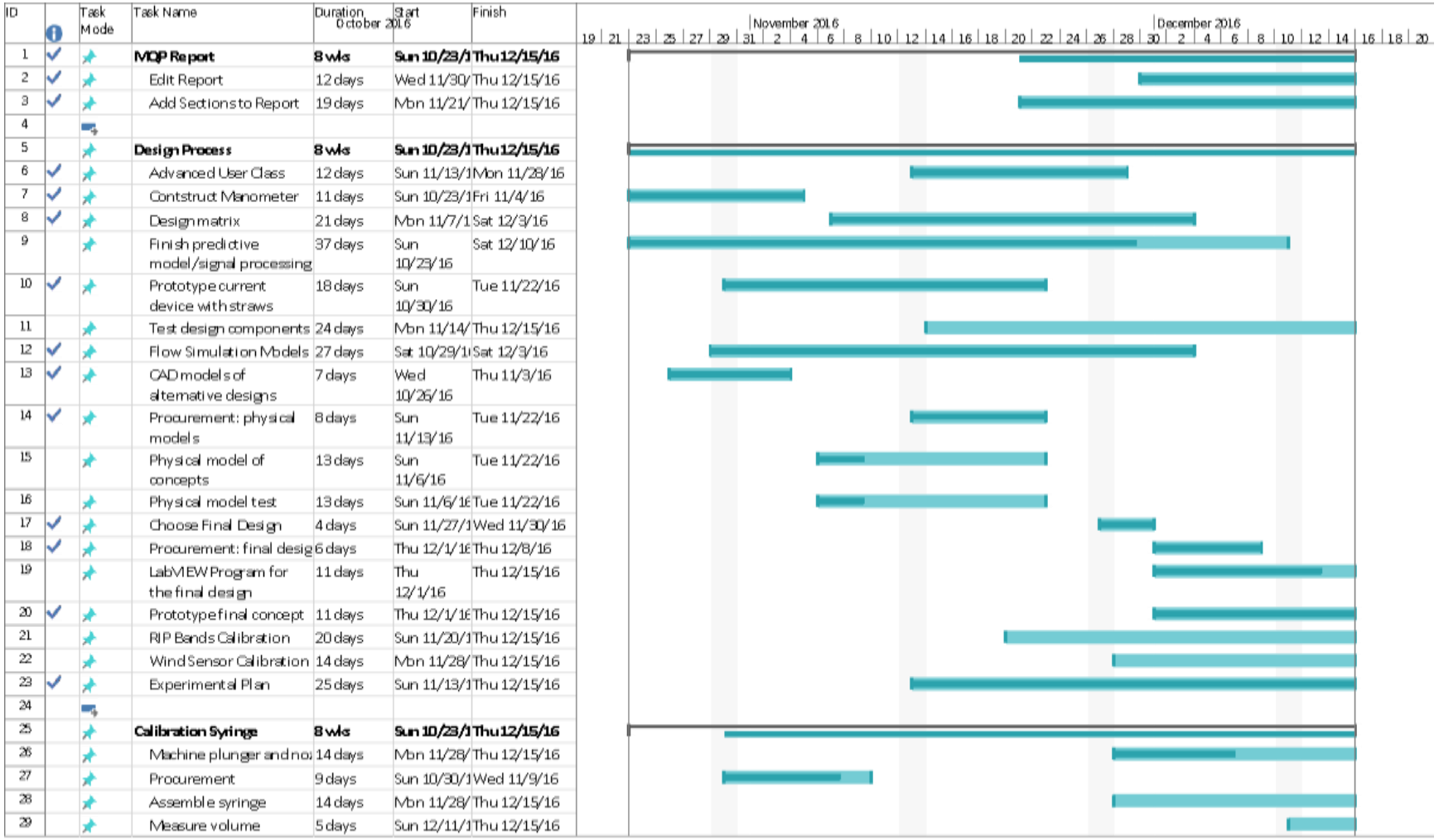

ID	Task Mode	Task Name	Duration	Start	Finish
1		**MQP Report**	**8 wks**	**Sun 10/23/1**	**Thu 12/15/16**
2		Edit Report	12 days	Wed 11/30/	Thu 12/15/16
3		Add Sections to Report	19 days	Mon 11/21/	Thu 12/15/16
4					
5		**Design Process**	**8 wks**	**Sun 10/23/1**	**Thu 12/15/16**
6		Advanced User Class	12 days	Sun 11/13/1	Mon 11/28/16
7		Contstruct Manometer	11 days	Sun 10/23/1	Fri 11/4/16
8		Design matrix	21 days	Mon 11/7/1	Sat 12/3/16
9		Finish predictive model/signal processing	37 days	Sun 10/23/16	Sat 12/10/16
10		Prototype current device with straws	18 days	Sun 10/30/16	Tue 11/22/16
11		Test design components	24 days	Mon 11/14/	Thu 12/15/16
12		Flow Simulation Models	27 days	Sat 10/29/1	Sat 12/3/16
13		CAD models of alternative designs	7 days	Wed 10/26/16	Thu 11/3/16
14		Procurement: physical models	8 days	Sun 11/13/16	Tue 11/22/16
15		Physical model of concepts	13 days	Sun 11/6/16	Tue 11/22/16
16		Physical model test	13 days	Sun 11/6/16	Tue 11/22/16
17		Choose Final Design	4 days	Sun 11/27/1	Wed 11/30/16
18		Procurement: final desig	6 days	Thu 12/1/16	Thu 12/8/16
19		LabVIEW Program for the final design	11 days	Thu 12/1/16	Thu 12/15/16
20		Prototype final concept	11 days	Thu 12/1/16	Thu 12/15/16
21		RIP Bands Calibration	20 days	Sun 11/20/1	Thu 12/15/16
22		Wind Sensor Calibration	14 days	Mon 11/28/	Thu 12/15/16
23		Experimental Plan	25 days	Sun 11/13/1	Thu 12/15/16
24					
25		**Calibration Syringe**	**8 wks**	**Sun 10/23/1**	**Thu 12/15/16**
26		Machine plunger and no	14 days	Mon 11/28/	Thu 12/15/16
27		Procurement	9 days	Sun 10/30/1	Wed 11/9/16
28		Assemble syringe	14 days	Mon 11/28/	Thu 12/15/16
29		Measure volume	5 days	Sun 12/11/1	Thu 12/15/16

Figure A.2: BTerm Gantt chart

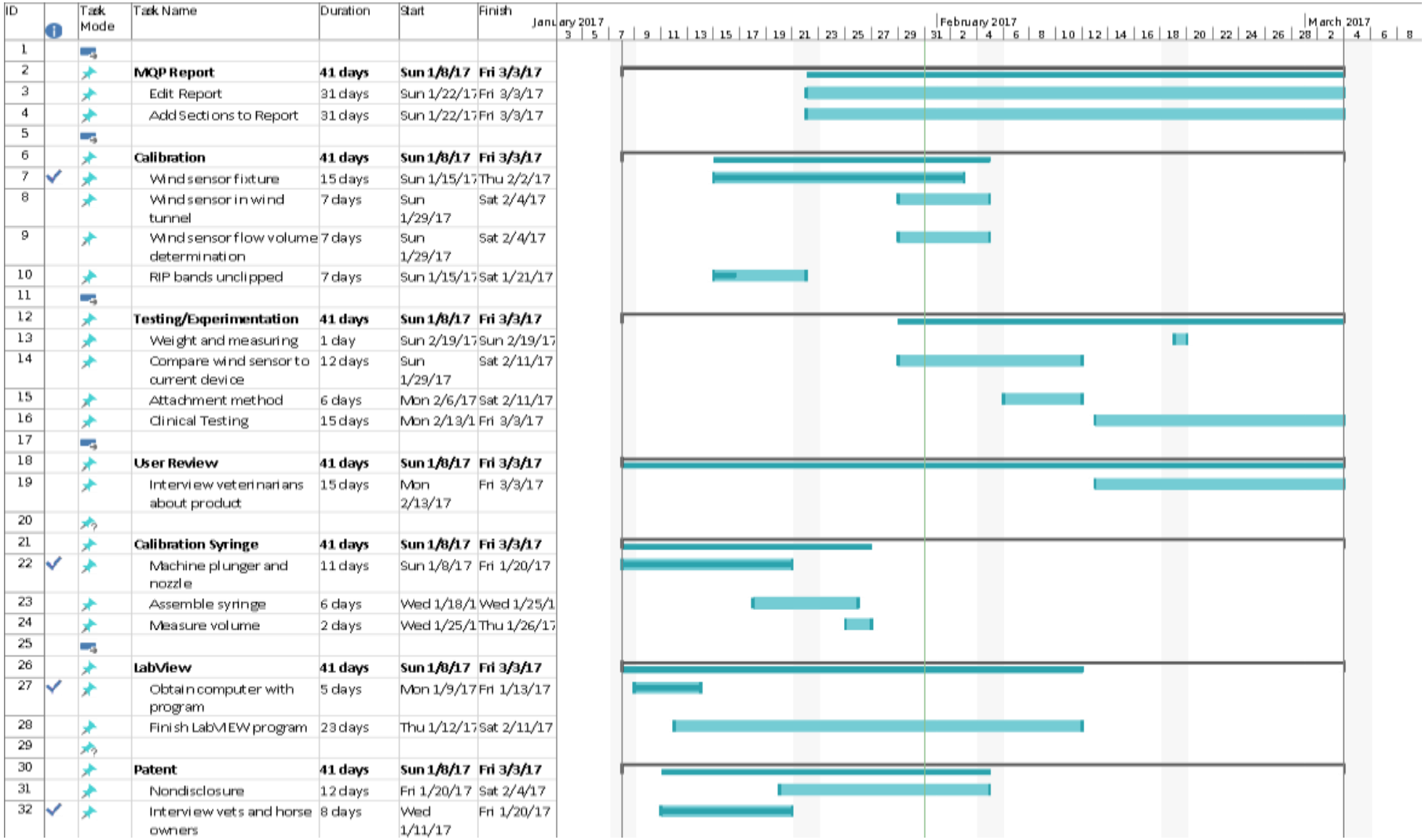

ID	Task Mode	Task Name	Duration	Start	Finish
1					
2		**MQP Report**	**41 days**	**Sun 1/8/17**	**Fri 3/3/17**
3		Edit Report	31 days	Sun 1/22/17	Fri 3/3/17
4		Add Sections to Report	31 days	Sun 1/22/17	Fri 3/3/17
5					
6		**Calibration**	**41 days**	**Sun 1/8/17**	**Fri 3/3/17**
7	✓	Wind sensor fixture	15 days	Sun 1/15/17	Thu 2/2/17
8		Wind sensor in wind tunnel	7 days	Sun 1/29/17	Sat 2/4/17
9		Wind sensor flow volume determination	7 days	Sun 1/29/17	Sat 2/4/17
10		RIP bands unclipped	7 days	Sun 1/15/17	Sat 1/21/17
11					
12		**Testing/Experimentation**	**41 days**	**Sun 1/8/17**	**Fri 3/3/17**
13		Weight and measuring	1 day	Sun 2/19/17	Sun 2/19/17
14		Compare wind sensor to current device	12 days	Sun 1/29/17	Sat 2/11/17
15		Attachment method	6 days	Mon 2/6/17	Sat 2/11/17
16		Clinical Testing	15 days	Mon 2/13/1	Fri 3/3/17
17					
18		**User Review**	**41 days**	**Sun 1/8/17**	**Fri 3/3/17**
19		Interview veterinarians about product	15 days	Mon 2/13/17	Fri 3/3/17
20					
21		**Calibration Syringe**	**41 days**	**Sun 1/8/17**	**Fri 3/3/17**
22	✓	Machine plunger and nozzle	11 days	Sun 1/8/17	Fri 1/20/17
23		Assemble syringe	6 days	Wed 1/18/1	Wed 1/25/1
24		Measure volume	2 days	Wed 1/25/1	Thu 1/26/17
25					
26		**LabView**	**41 days**	**Sun 1/8/17**	**Fri 3/3/17**
27	✓	Obtain computer with program	5 days	Mon 1/9/17	Fri 1/13/17
28		Finish LabVIEW program	23 days	Thu 1/12/17	Sat 2/11/17
29					
30		**Patent**	**41 days**	**Sun 1/8/17**	**Fri 3/3/17**
31		Nondisclosure	12 days	Fri 1/20/17	Sat 2/4/17
32	✓	Interview vets and horse owners	8 days	Wed 1/11/17	Fri 1/20/17

Figure A.3: CTerm Gantt Chart

Appendix B: MQP project expenses and budget

Table B.1: Detailed MQP budget

MQP Budget						
Total Budget		**$1,000.00**				
Total Spent		**$662.74**				
You're under budget by		**$337.26**				
Item	**Description**	**Cost**	**Qty**	**Amount**	**Notes**	**Need Reimbursement?**
MANOMETER						
Tubing		$0.00	5 ft.	$0.00	in lab	N
Wood		$0.00	2 ft.	$0.00		N
Zip ties		$0.00	6	$0.00	in lab	N
Water		$0.00	2 cups	$0.00	in lab	N
Food coloring		$0.00	3 drops	$0.00	in lab	N
Nails		$1.30	1 unit	$1.30		Y
SYRINGE						
4" PVC pipe		$7.53	1	$7.53		Y
2-240 O-rings		$6.97	1 unit	$6.97		N
Aluminum stock	Metal for piston	$53.71	6 in	$53.71		N
End cap		$2.08	1	$2.08		Y
4" x 2" coupling		$6.38	1	$6.38		Y
Gorilla glue		$6.58	1	$6.58		Y
Wooden dowel	0.75 in diameter	$2.98	1	$2.98		Y
DEVICE WITH STRAWS						
Coffee stirrers		$4.90	1 unit	$4.90		Y
Liter soda bottle?		$0.00	1	$0.00		N
Tubing for pressure drop		$0.00	2 ft.	$0.00	in lab	N

FINAL DESIGN						
Wind sensor Rev-P	Modern Device	$24.00	2	$48.00		N
Attachment	3D print					
Wires	GH 007	$0.00	20 ft.	$0.00	in lab	N
DAQ Box	NI USB-6000	$150.00	1	$150.00		N
Wind sensor Rev-C	Modern Device	$17.00	1	$17.00		N
K-type Thermocouple		$20.80	1	$20.80		N
Electric wire		$9.14	50 ft.	$9.14		N
5V Supply		$7.52	1	$7.52		N
1.5" rubber coupling		$3.90	1	$3.90		Y
Screw driver set	For DAQ box	$5.59	1	$5.59		Y
WIND TUNNEL						
Regulator and filter		$58.18	1	$58.18		N
1/4 Connector		$7.62	1	$7.62		N
Coupler		$3.05	1	$3.05		Y
5/8" Quick connect		$4.44	1	$4.44		N
3"X2" PVC pip		$6.85	2	$13.70		Y
3"X2" Flex coupling		$6.68	1	$6.68		Y
3" Coupling		$1.51	1	$1.51		Y
Hot Wire		$104.45	1	$104.45		N
1.5"-1.25" straight reducer		$1.53	1	$1.53		N
1.25"-1" straight reducer		$1.44	1	$1.44		N
1"-0.75" straight reducer		$0.86	1	$0.86		N
0.75"-0.5" straight reducer		$0.50	1	$0.50		N
1.5" socket connect female		$0.71	1	$0.71		N
1.25" socket connect female		$0.67	1	$0.67		N
1" socket connect female		$0.48	1	$0.48		N
0.75" socket connect female		$0.27	1	$0.27		N
0.75" socket connect male x 0.5" NPT female		$0.50	1	$0.50		N
0.5" NPT male x 0.25" NPT female		$1.44	1	$1.44		N
0.25" standard-wall brass pipe nipple		$1.66	2	$3.32		N
8 oz. pipe cement		$4.68	1	$4.68		N
3' Air hose 0.25" x 0.25" NPTF brass male fittings		$13.03	2	$26.06		N
Panel-mount flowmeter for air without valve		$58.00	1	$58.00		N
Brass On/Off valve with lever handle		$8.27	1	$8.27		N
Total				**$662.74**		

Appendix C: Rev P wind sensor original LabVIEW program

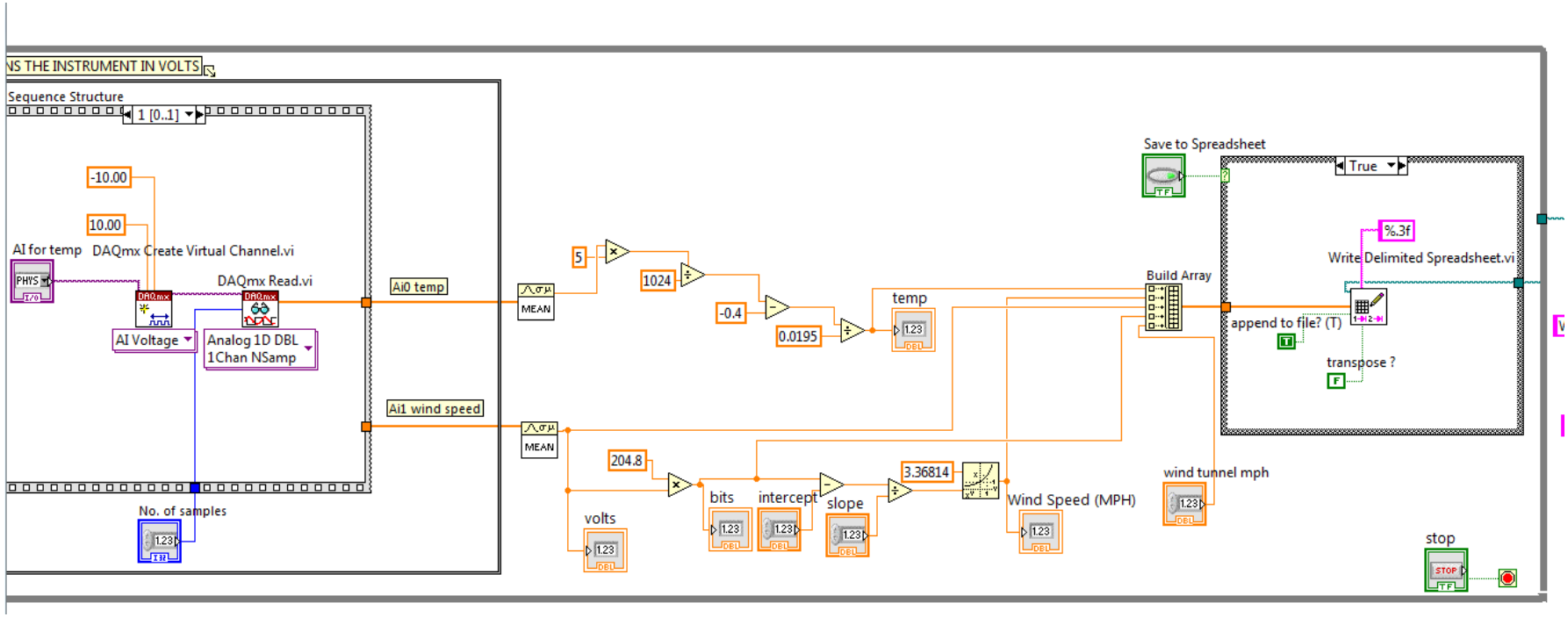

Figure C.1: Rev P original LabVIEW program

Appendix D: Rev C wind sensor original LabVIEW program

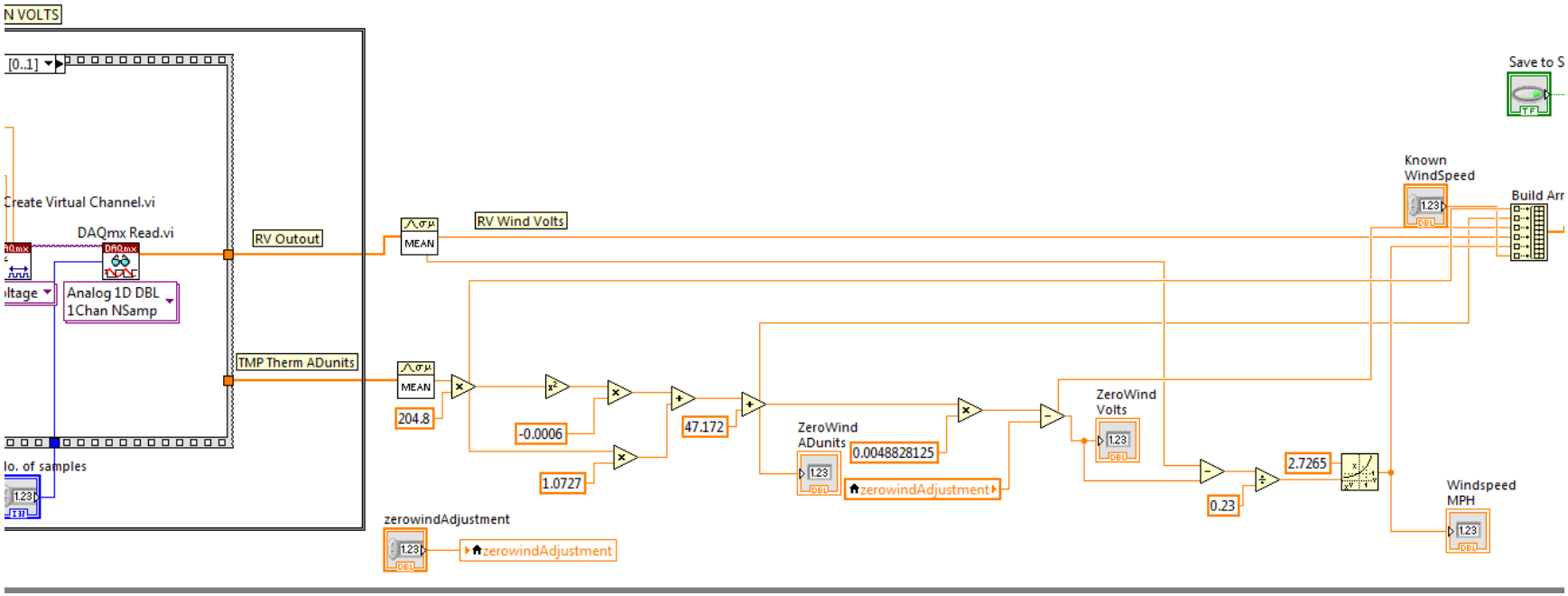

Figure D.1: Rev C original LabVIEW program

Appendix E: LabVIEW program to find zero wind correction factor

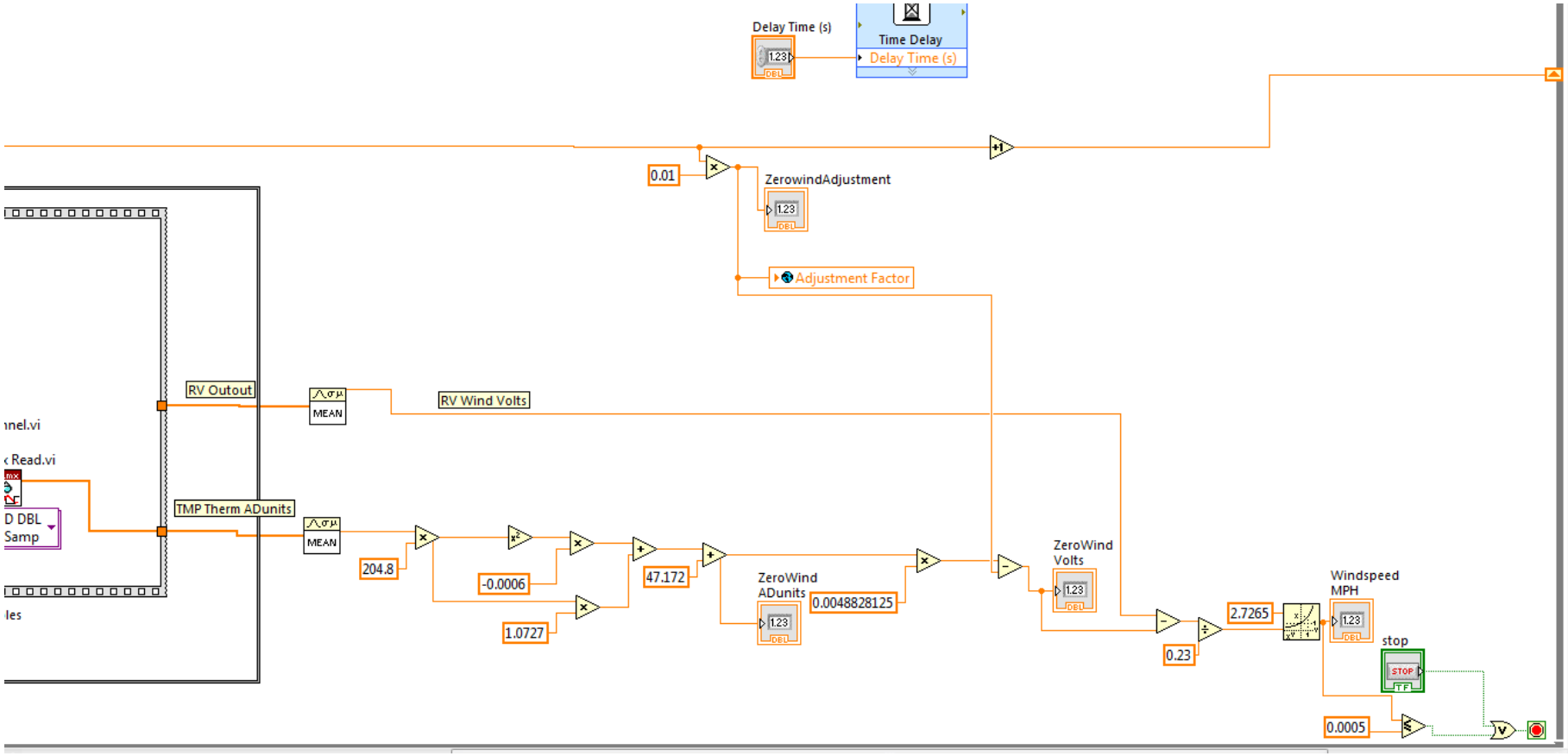

Figure E.1: Block diagram of zero wind correction factor program

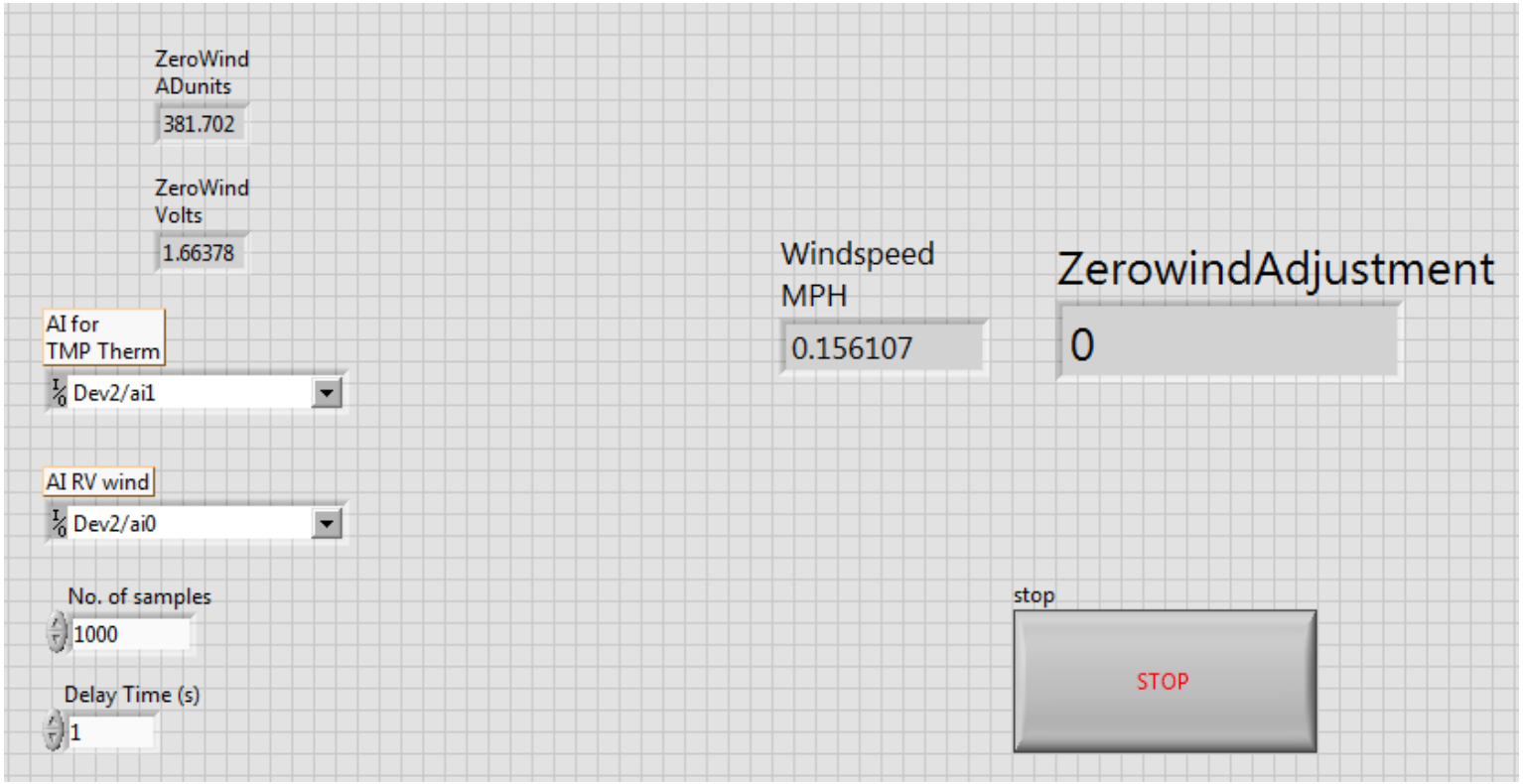

Figure E.2: Front panel of zero wind calibration factor program

Appendix F: Five different calibration LabVIEW programs tested in wind tunnel for Rev P

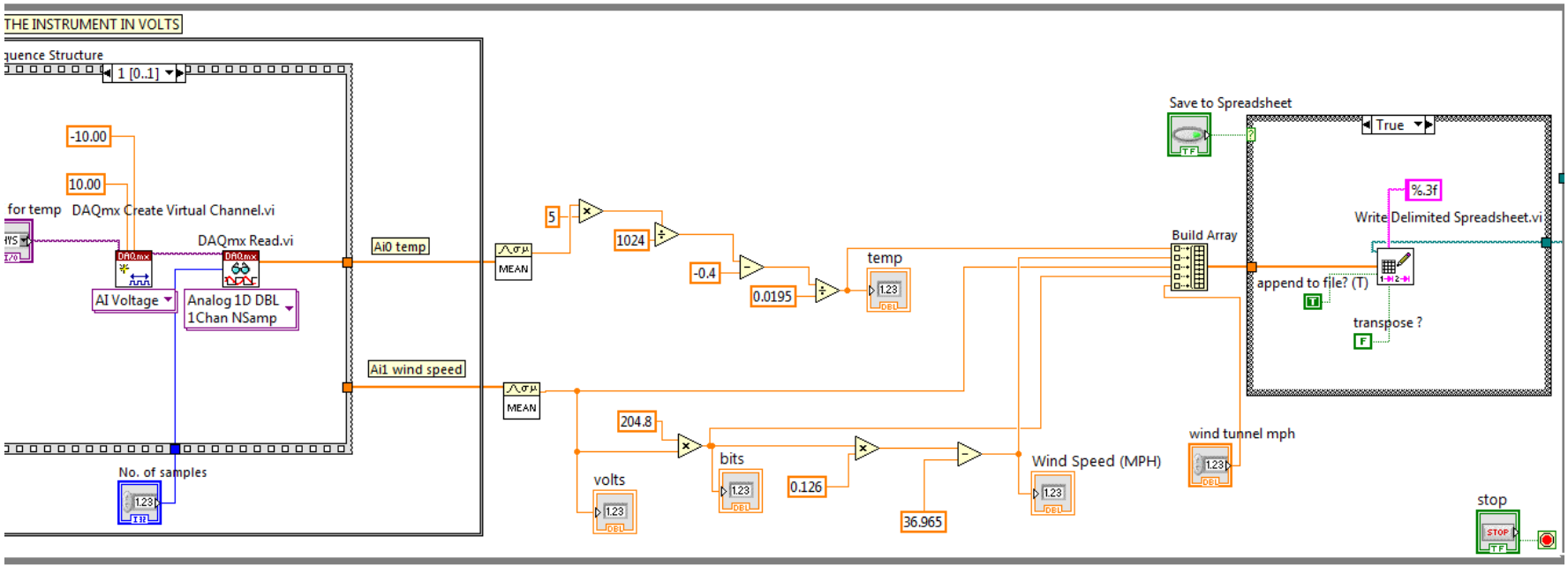

Figure F.1: Rev P first linear equation

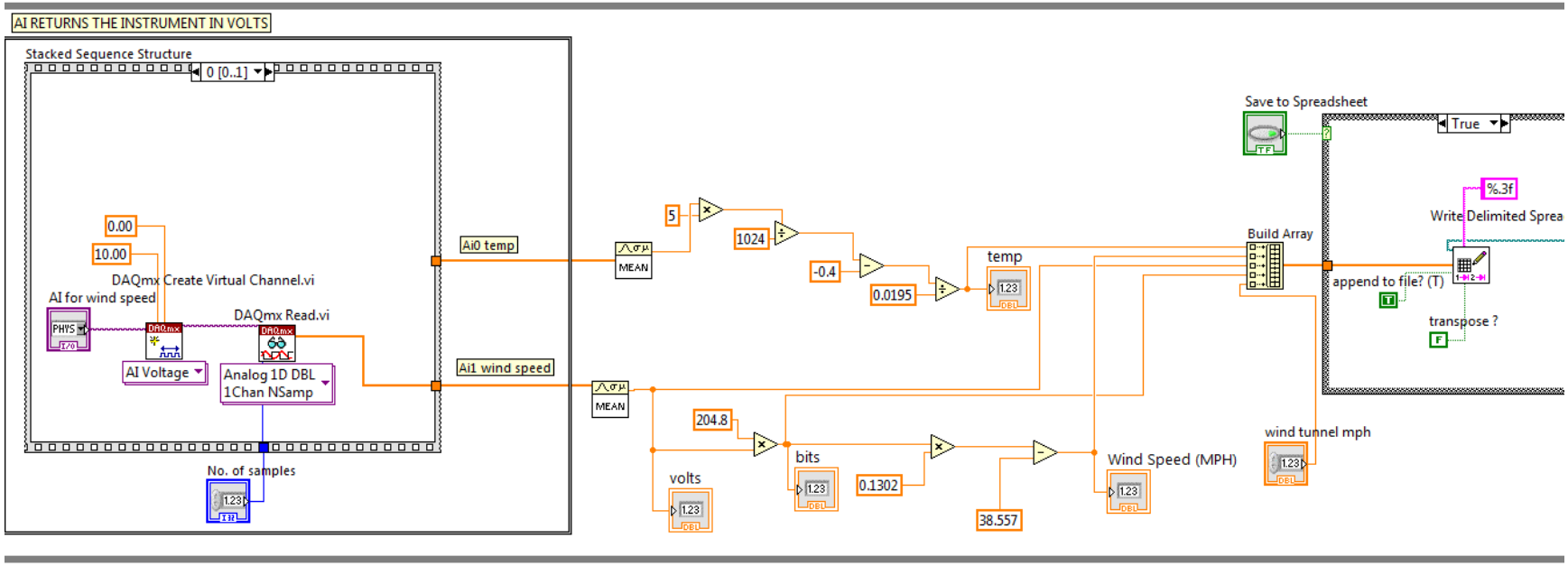

Figure F.2: Rev P second linear equation

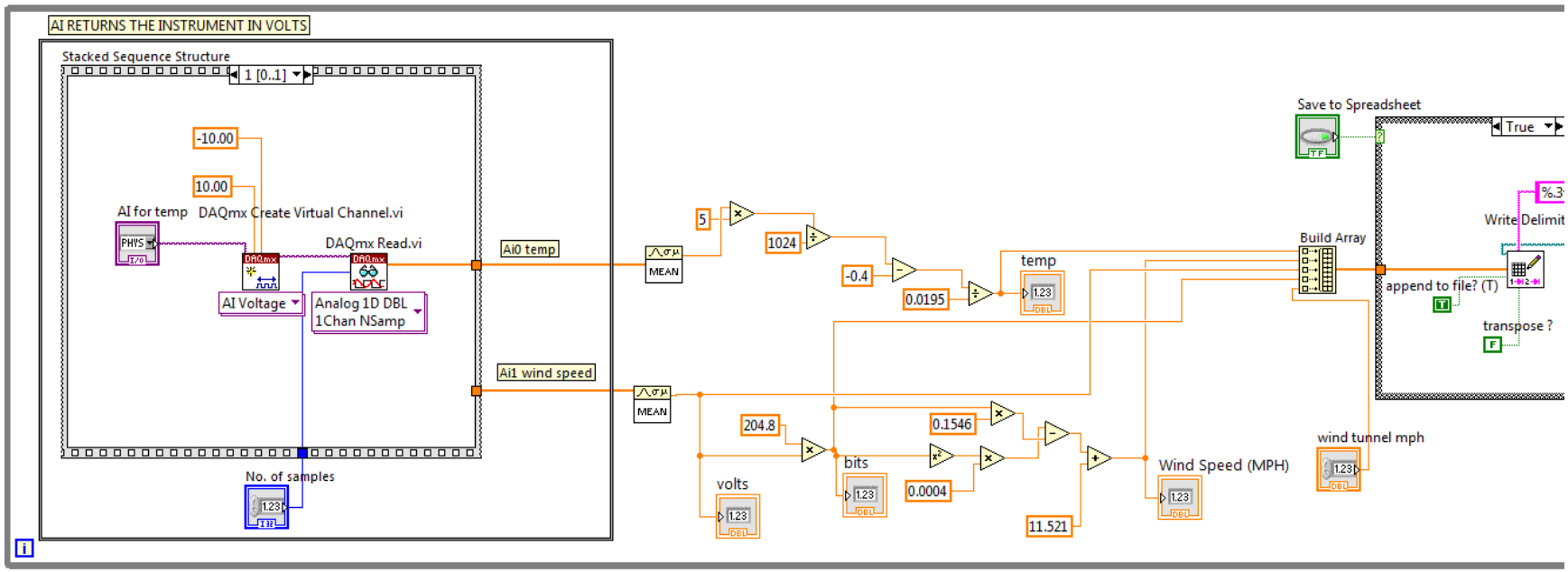

Figure F.3: Rev P first polynomial equation

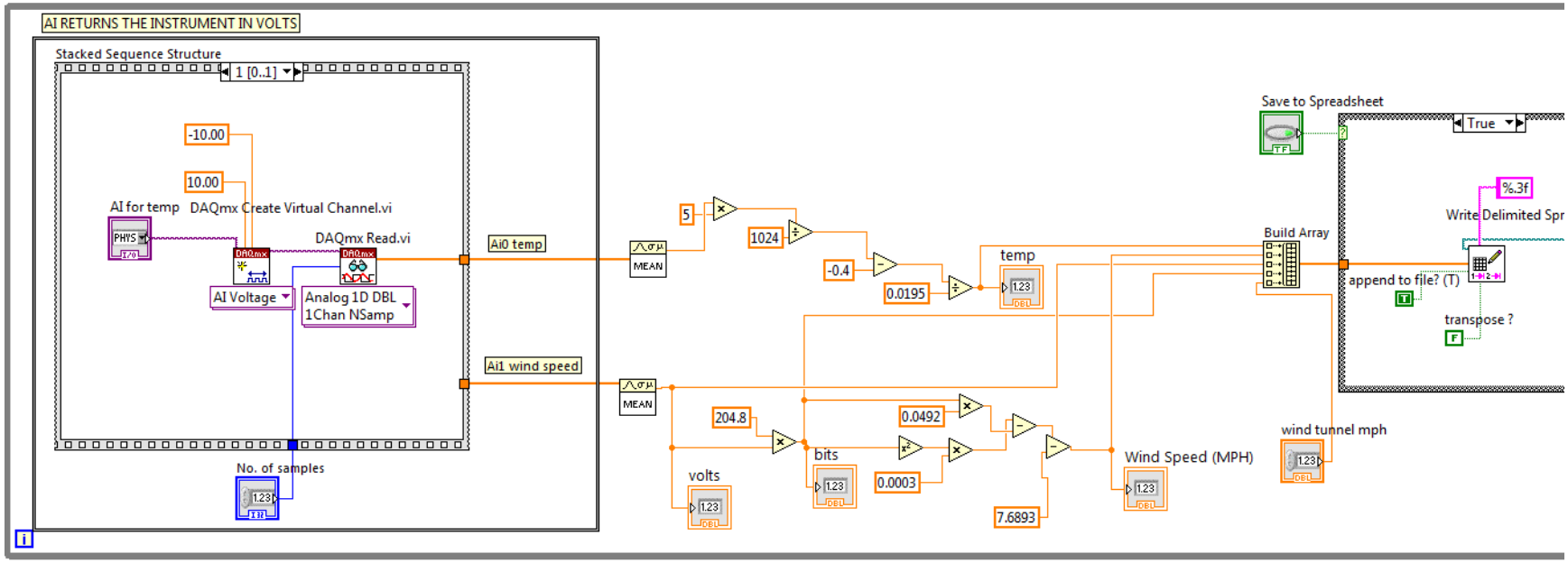

Figure F.4: Rev P second polynomial equation

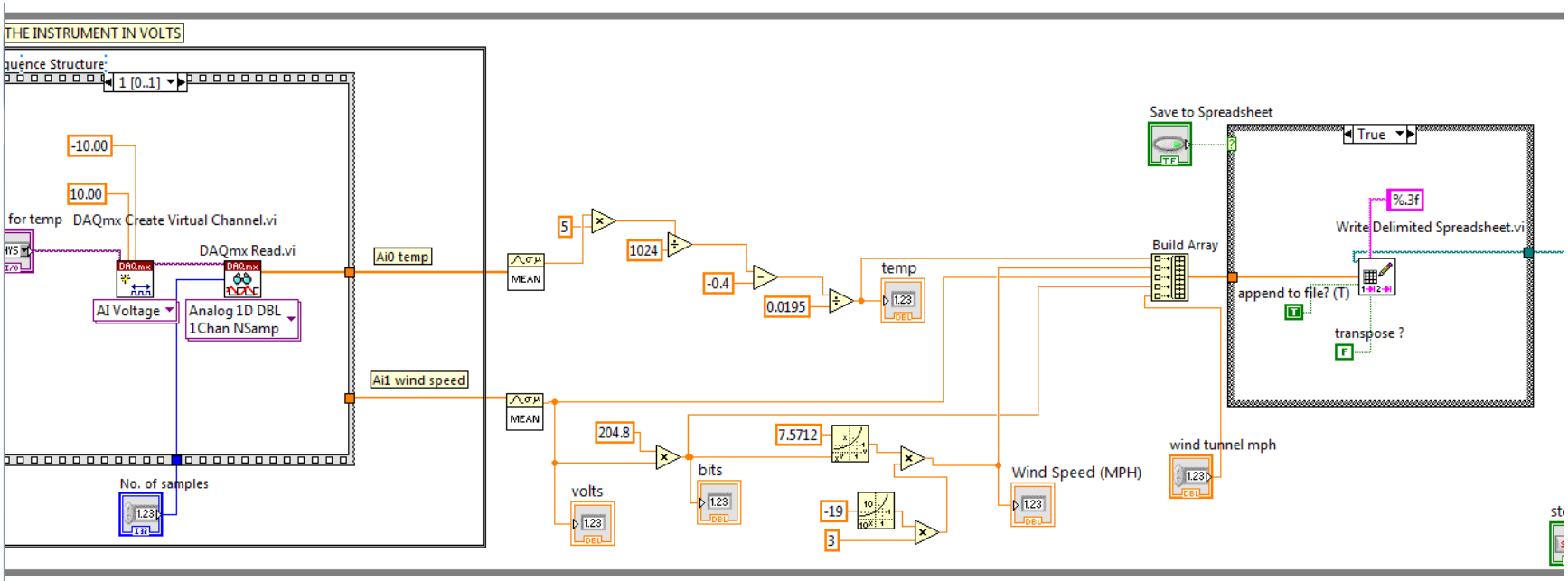

Figure F.5: Rev P power equation

Appendix G: Graphical results of Rev P wind tunnel testing

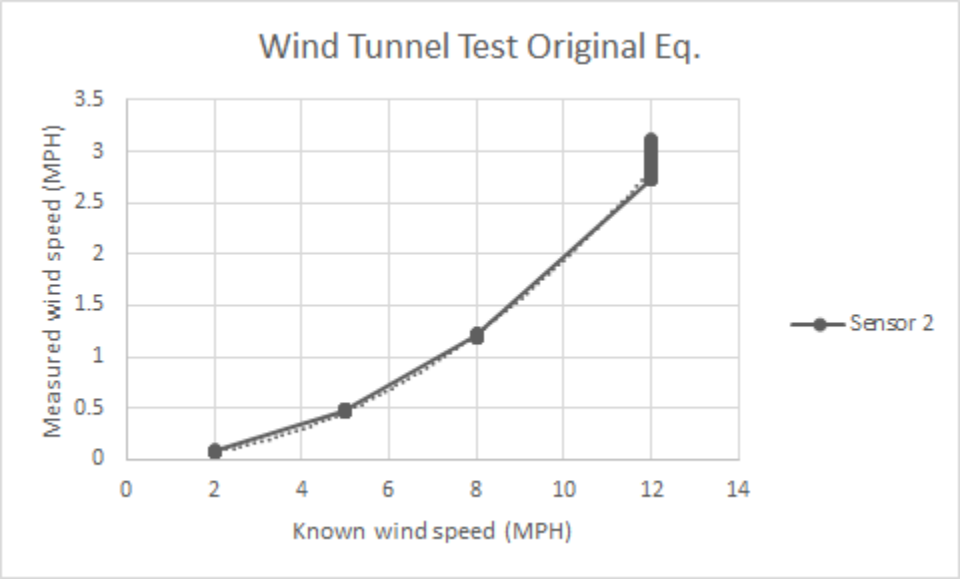

Figure G.1: Wind tunnel test with Eq. 4.16
(Wind Speed $= (\frac{\text{RawW}-264.0}{85.6814})^{3.36814}$)

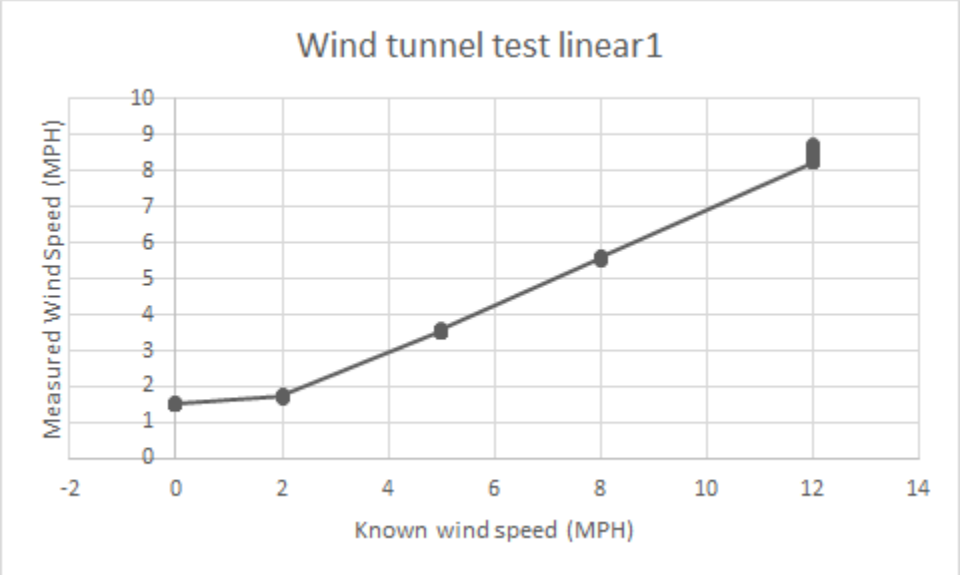

Figure G.2: Wind tunnel test with first linear equation
(mph $= 0.126 * \text{values} - 36.965$)

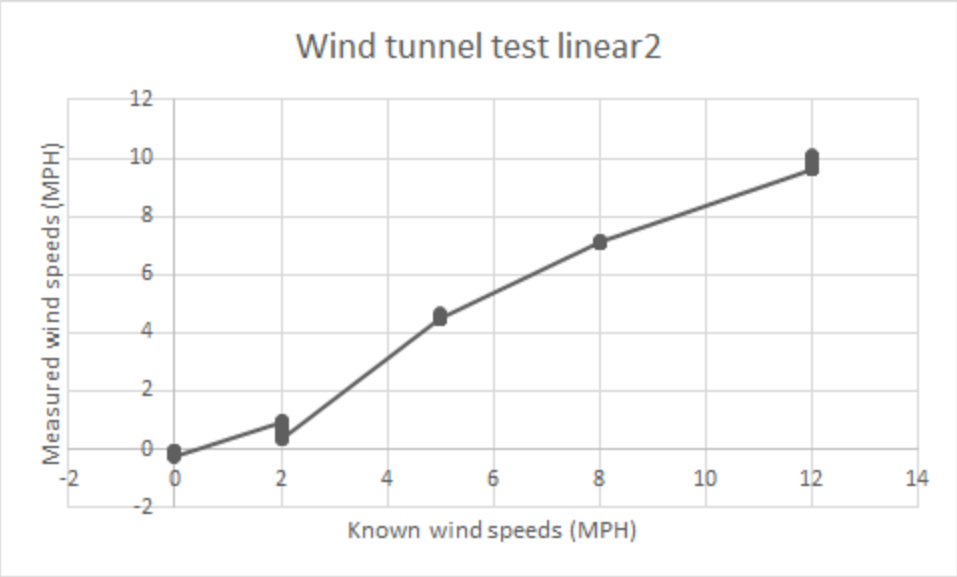

Figure G.3: Wind tunnel test with second linear equation
$(\text{mph} = 0.1302 * \text{values} - 38.557)$

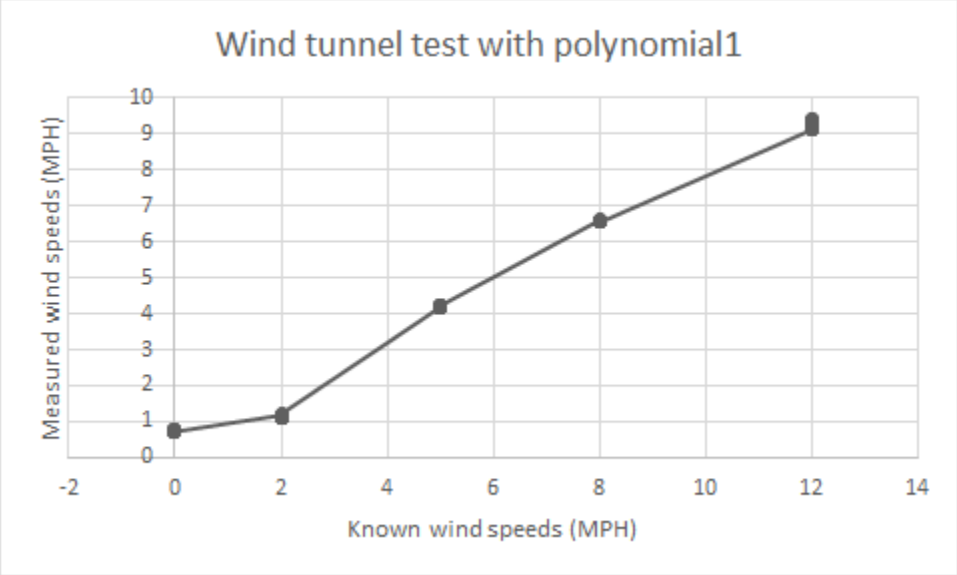

Figure G.4: Wind tunnel test with first polynomial equation
$(\text{mph} = 0.0004 * \text{values}^2 - 0.1546 * \text{values} + 11.521)$

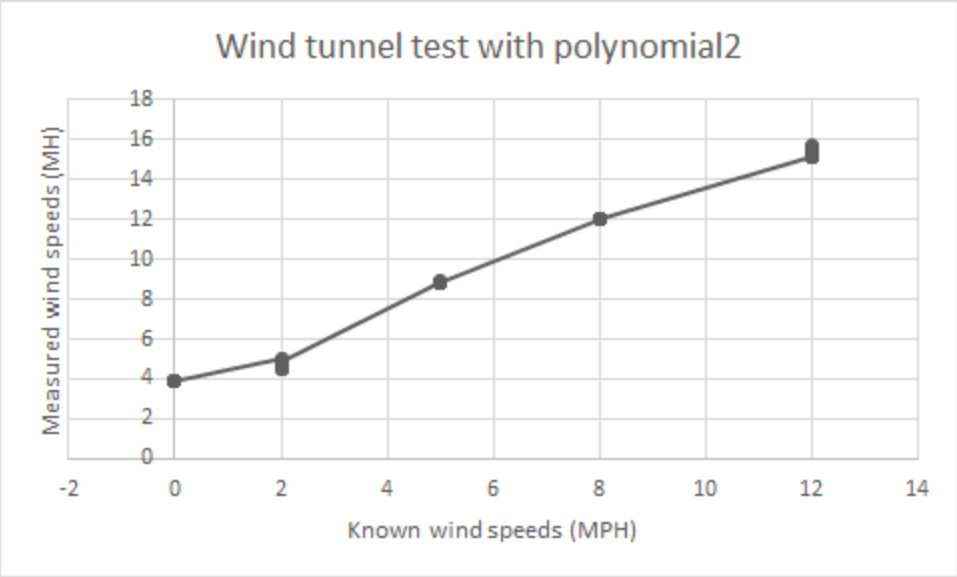

Figure G.5: Wind tunnel test with second polynomial equation
$(\text{mph} = 0.003 * \text{values}^2 - 0.0492 * \text{values} - 7.6893)$

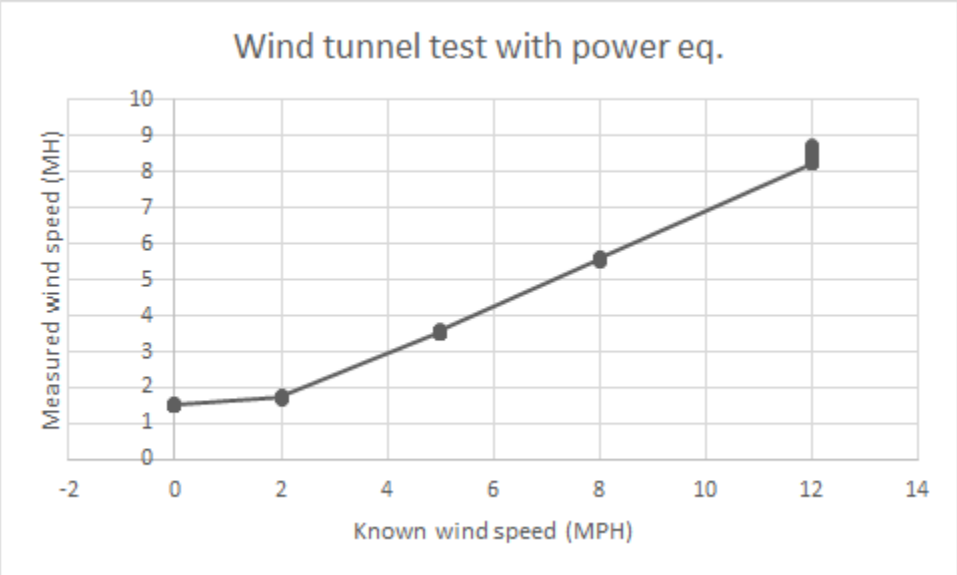

Figure G.6: Wind tunnel test with power equation
$(3 * 10^{-19} * \text{values}^{7.5712})$

Appendix H: Low flow wind tunnel SOP

1. Connect cemented reducers to reducing coupling at end of wind tunnel

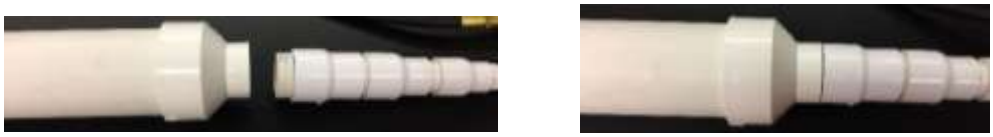

A. B.

Figure H.1: A) reducers unattached from reducing coupling; B) Reducers attached

2. Use a threaded nipple to connect the reducers to the top of the rotameter
3. Connect an airline hose to the bottom of the rotameter

Figure H.2: threaded nipple and airline hose attached to rotameter

4. Connect the ball valve to the rotameter with the hose

Figure H.3: Ball valve attached to rotameter via airline hose

5. Use another airline hose to connect the ball valve to the regulator

Figure H.4: Ball valve connected to regulator via airline hose

6. Ensure the regulator is closed and the ball valve is closed

A.

B.

Figure H.5: A) Regulator in closed position; B) Ball valve in closed position

7. Use the quick disconnect to connect the airline to the regulator

Figure H.6: Male quick disconnect of regulator that interfaces with compressed airline

8. Use electrical tape to secure the sensor at the end of the wind tunnel with the sensing element in the center of flow

Figure H.7: Rev C sensor secured at end of wind tunnel

9. Connect the sensors wires to the correct ports of the DAQ box (see Appendix L for detailed instructions)
10. Hold the hot wire probe or Hold Peak handheld anemometer in the center of flow (see Appendices I and J for instructions on use)
11. Start running the software programs to collect data as described in (Appendix L and J)
12. Open the regulator completely by turning the cap on the top
13. Regulate the flow by slowly opening the ball valve until desired pressure and thus flow rate is reached

Figure H.8: Ball valve completely open

14. Stop the flow by returning the ball valve back to the closed position
15. Disassemble the wind tunnel by following these steps in reverse

Appendix I: SOP for Hold Peak handheld anemometer

1. Open side cover and connect the digital anemometer to the flow anemometer via the USB port

A. B. C.

Figure I.1: A) Side cover on digital anemometer; B) Side cover open on digital anemometer; C) Flow anemometer attached to USB of digital anemometer

2. Turn the device on and ensure it is in the desired measurement mode

Figure I.2: Digital anemometer screen display and keypad used for operation

   a. Use the unit button to choose between MPH, m/s, km/hr., ft./min., knots
   b. Use the 6 button to choose °C or °F
3. Hold the flow anemometer portion of the device in the desired location

Figure I.3: Flow anemometer positioned for flow coming out of the page, in the direction of the arrow

   a. Make sure the arrow is pointing in the direction of flow

4. Read the screen and record the values as they are produced (Figure I.2)
    a. Use the hold button to display a constant value on the screen
5. Hold the power button for 3 seconds to turn off the device

Figure I.4: Closeup image of the keypad of the device to better show the power, unit and temperature control buttons

6. Unplug the flow anemometer from the digital anemometer and return to case

Figure I.5: Device powered off and in case for storage

Appendix J: SOP for Testo 405i hot wire smart probe

1. Download the Testo smart probe app

Figure J.1: Icon for the smart probes app used for the Testo 405i hot wire probe

2. Turn on Bluetooth on your device and open the app

Figure J.2: IPhone menu pulled up from the bottom used to quickly turn on Bluetooth

3. Unfold the device and remove plastic covering

A.

B.

Figure J.3: A) Testo 405i probe folded and wrapped for storage; B) Testo 405i probe unwrapped and unfolded for use

4. Turn on the hot wire probe by pressing the large orange button, the light will blink orange

Figure J.4: Testo 405i probe on, but not connected to the app as signified by the orange light

5. Wait for the light to be blinking green

Figure J.5: Testo 405i probe connected to the app as signified by the green light

6. Turn the black cover to expose the hot wire

A. B.

Figure J.6: A) Black cover closed to protect the hot wire sensor; B) Black cover opened to allow for testing with the hot wire sensor

7. Use the buttons at the very top (bulleted list (left) and lists (right)) of the app to change unit measurements and choose other settings
    a. Use the list, trending, and table buttons to change how the data is displayed

Figure J.7: Home screen of the app showing list measurements

8. Click the center button (dog-eared page with +) at the bottom of the app to control when testing begins
    a. When the menu comes up press continue to begin recording and discard collected data

A.

B.

Figure J.8: A) Trending view of standard app set up; B) The menu used to restart data collection that comes up when the center button at the bottom is clicked

9. Once data collection is complete: use last button, arrow in square brackets, (right) to export data to an Excel file (.csv)

A.

B.

Figure J.9: A) Trending view of standard app setup; B) Export option menu that allows the user to choose a file type to export the data to

10. Enter an email and email the file for further processing

Figure J.10: Email message with file attached that opens when file type is chosen

11. Hold the orange button used to turn it on until the light turns off (Figure J.3B)
12. Close the black cover by turning (Figure J.6A)
13. Fold the probe and return the wrapping to the handle (Figure J.3A)

Appendix K: Single calibration final LabVIEW program for Rev C sensor

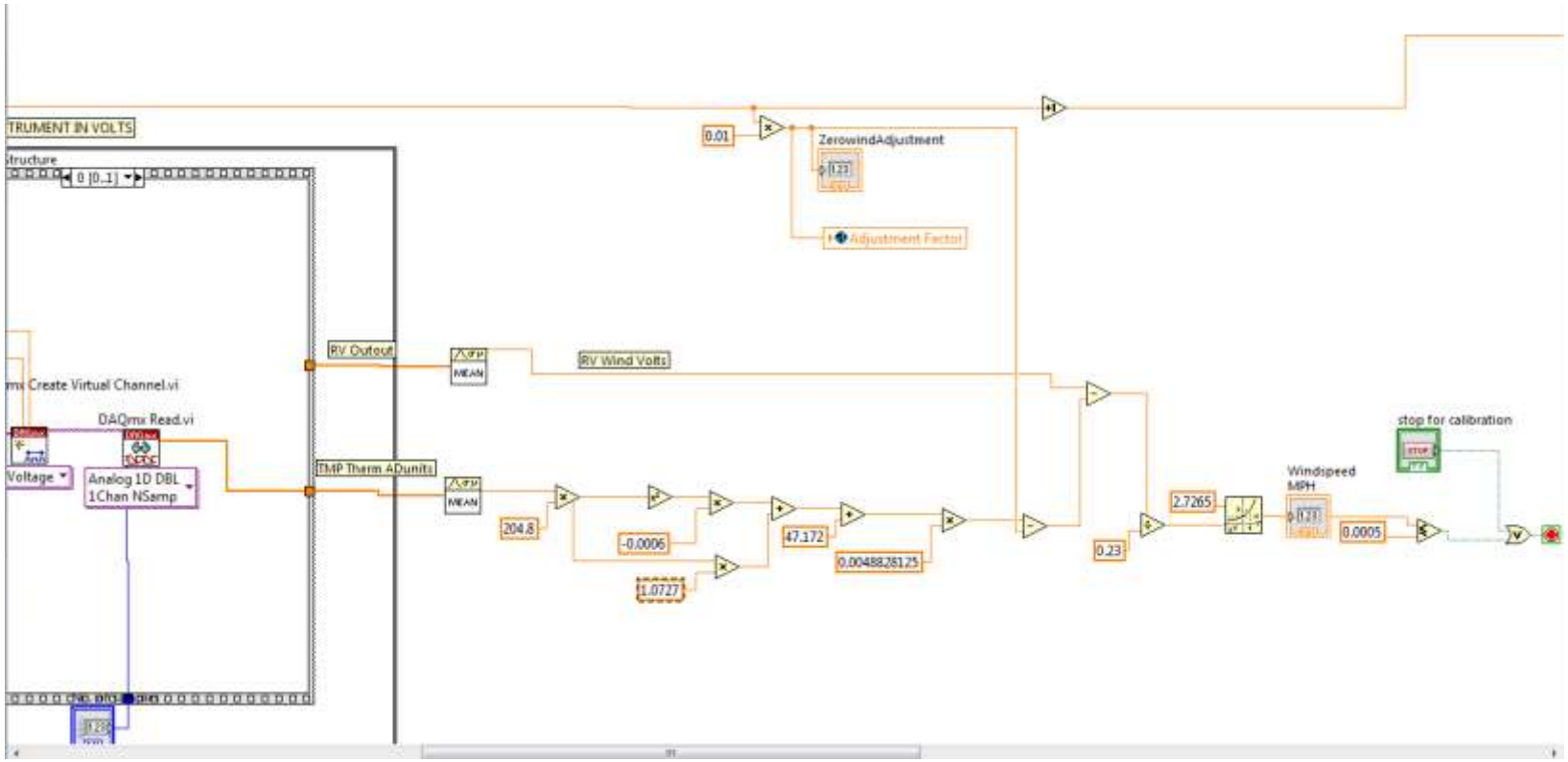

Figure K.1: Zero wind calibration factor portion of final program

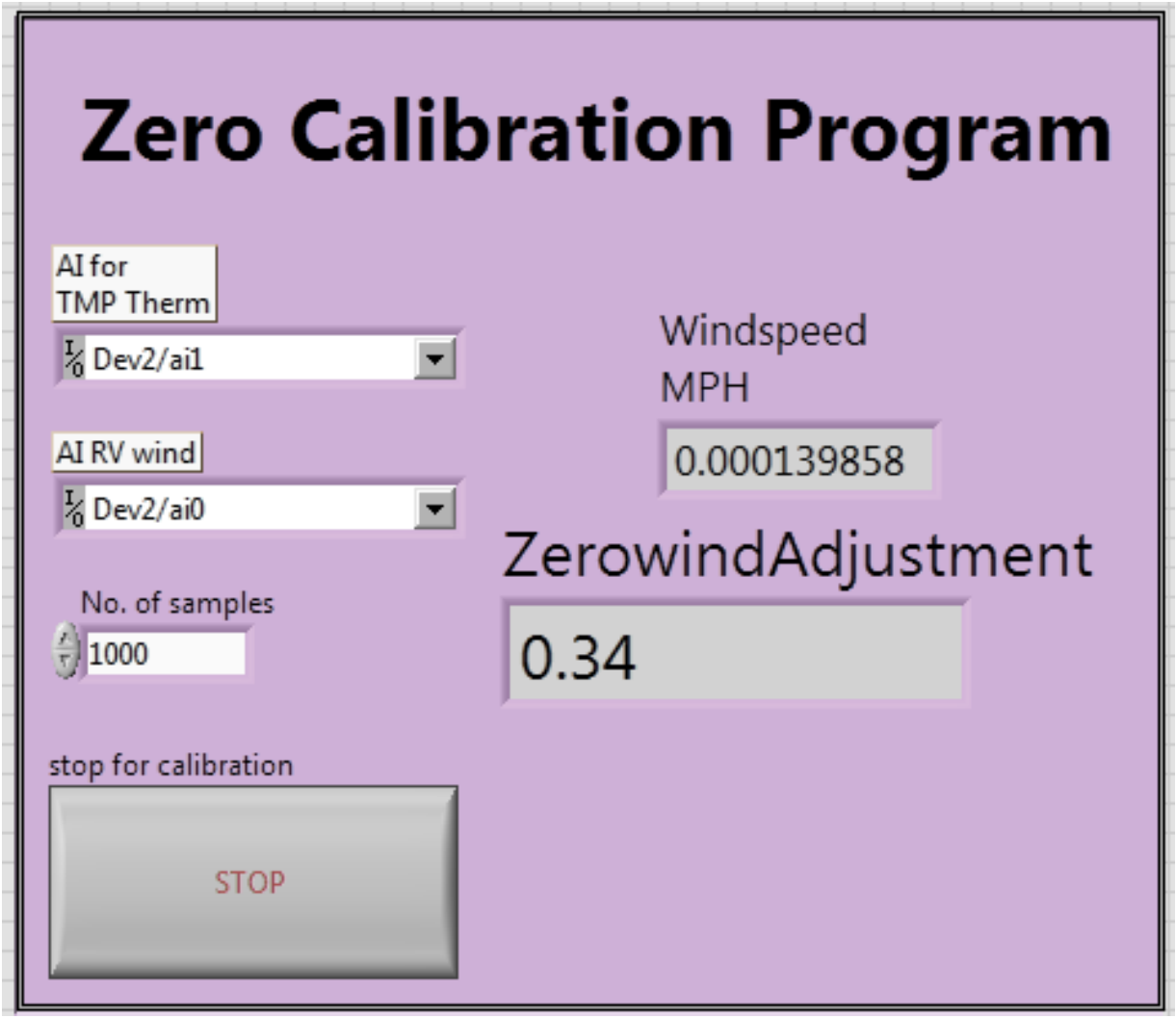

Figure K.2: Front panel of final zero wind calibration program

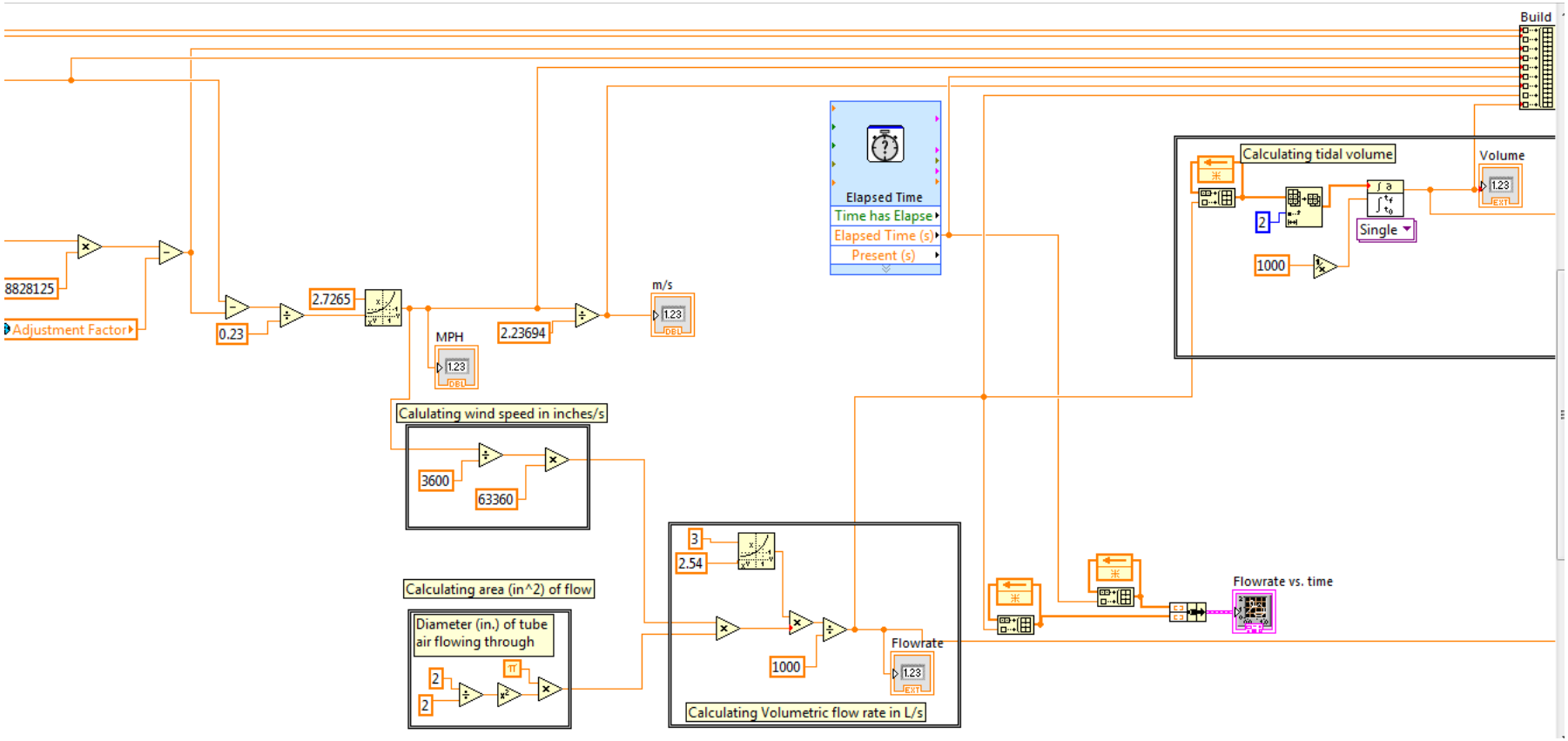

Figure K.3: Final single calibration LabVIEW test program block diagram

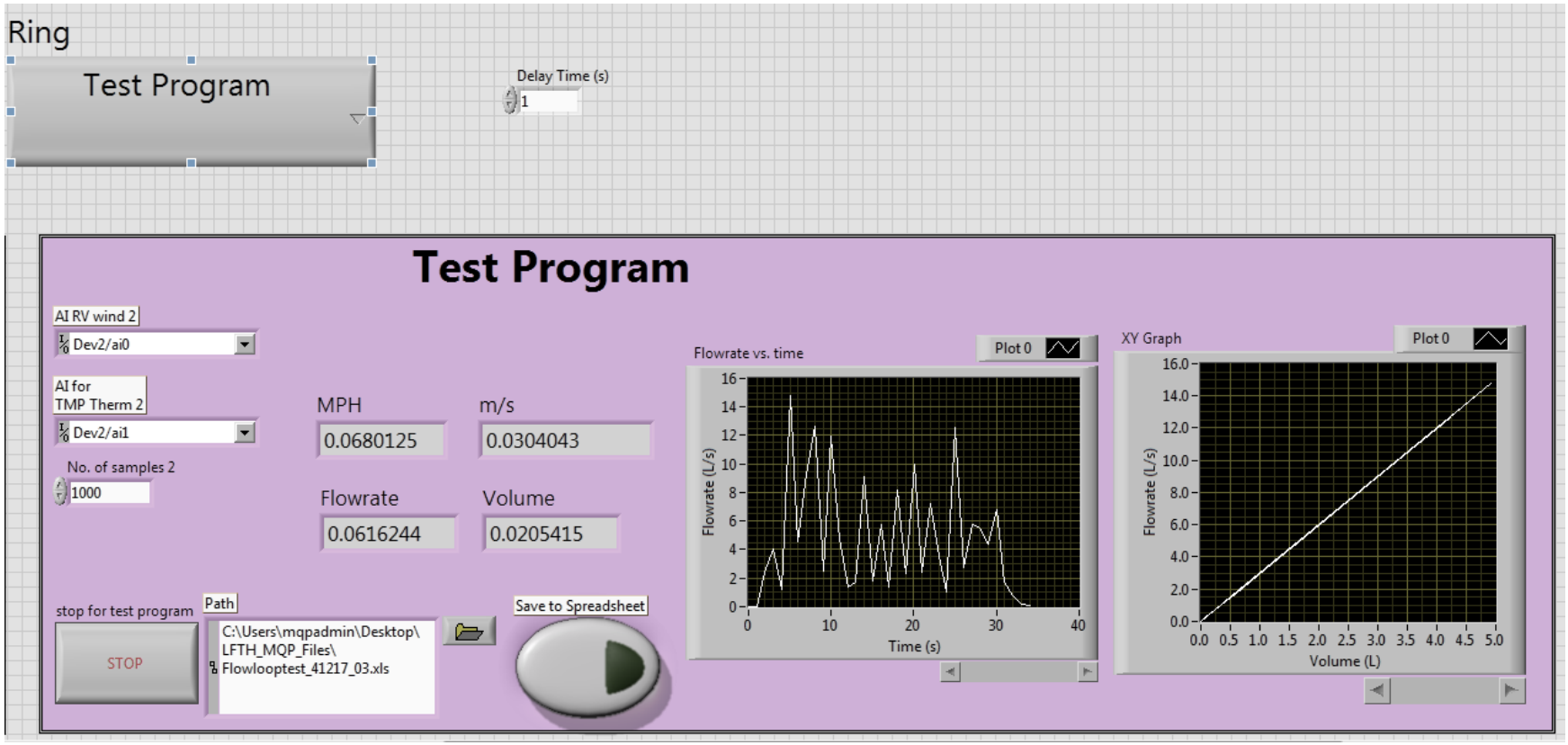

Figure K.4: Final single calibration LabVIEW test program front panel

Appendix L: SOP for single calibration LabVIEW program

Policy: This SOP will comply with veterinary standards and guidelines for external device sterilization and equine testing.

Purpose: The purpose of this SOP is to ensure safe and proper setup of the wind sensor lung function testing device for reliable and repeatable results.

Scope: This procedure is for veterinarians using the wind sensor lung function testing device to diagnose pulmonary disorders.

Prerequisites:

- Wind sensor system
    - Including: Rev C sensor with 4 wires attached and a 5V wall wart connected to the sensor and a ground wire
- USB-6000 DAQ box
- 1.5 in. rubber connector (housing)
- Plastic face mask for the horse
- 2.4 mm flat head screwdriver
- Electrical tape
- Scissors
- Paper towels or rag
- 70% ethanol for disinfecting the housing
- Computer with LabVIEW 2015 software (or newer) and USB port
- Electrical outlet

Procedure:

System setup

1. Connect wires to DAQ box using the following steps (a-d)

Figure L.1: DAQ box used with the system; wires insert into the side below screws

a. Ground (GND) of the sensor (1st pin) should be in one of the ports marked by an arrow (AI GND)
b. The ground (V+ GND) of the power supply should be in another port marked by an arrow (Ai-GND)

c. The RV pin on the sensor (4th pin) should be connected to port Ai0 on the DAQ box
d. The TMP pin on the sensor (5th pin) should be connected to port Ai1 on the DAQ box

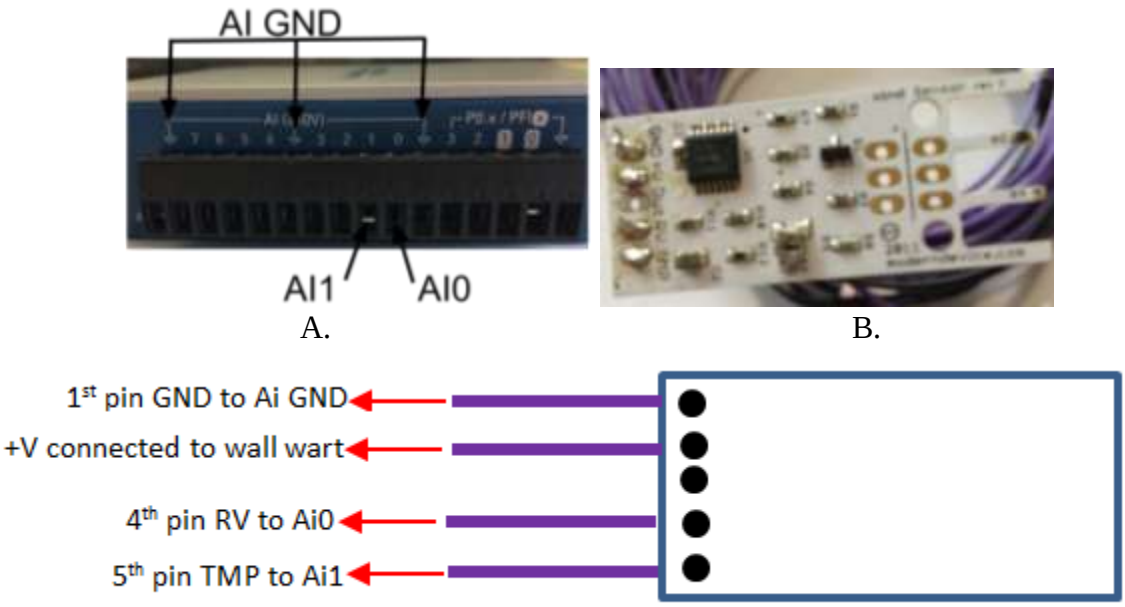

A. B.

C.

Figure L.2: A) DAQ box ports with labels; B) Sensor with pins on left; C) Schematic of Rev C sensor with labeled pins to corresponding DAQ box ports

i. All pins are connected by inserting the exposed end of the wire into the respective port and then tightening the port (clockwise) using the 2.4 mm flat head screwdriver
ii. The wires can typically be left attached, so check if they are secure with a soft pull on each
    1. If it comes out: loosen screw (counterclockwise) with 2.4 mm flat head screwdriver, insert the wire, and retighten the screw

2. Insert housing in face mask
    a. Locate the rectangular slot on the rubber connection
    b. Orient this slot so that it will point up when attached to the mask on the horse
    c. Insert the rubber connector (duct taped side) into the PVC portion of the mask ensuring the slot is closest to you when you slide it on
        i. Lightly tug the device or shake the horse face mask to ensure the housing is securely attached

Figure L.3: Housing for the sensor

3. Insert wind sensor in housing
    a. Slide wind sensor into slot in housing until the wires on the wind sensor rest on the stop (extended piece of rubber on the housing)

Figure L.4: Sensor in housing in mask

    b. Using scissors cut a piece of electrical tape 1 inch in length
    c. With the piece of electrical tape, tape the four wires from the wind sensor to the stop
4. Plug 5 V wall wart into an electrical outlet

Figure L.5: Wall wart plugged into electrical outlet

5. Plug USB cable from DAQ box into computer's USB-port

Figure L.6: DAQ box connected to computer via USB

LabVIEW Setup

1. Power on computer with LabVIEW
2. Open LabVIEW 2015 or newer
3. In LabVIEW: File -> open -> bidirectional_flow_1.vi
4. Check to make sure the DAQ box is connected properly and turned on (should see blue light on the side of the DAQ box)

Calibrating the device to the room

1. Use the down arrow on the ringer (labelled ring) to choose the zero-calibration program

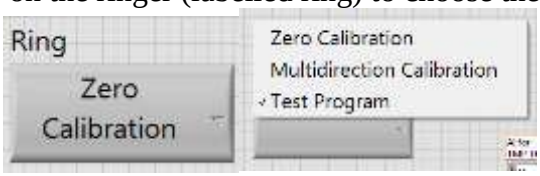

A. B.

Figure L.7: A) Ringer used to choose which program is running; B) Programs that can be chosen

2. Click the run arrow (highlighted in image below with a red box) in the upper left hand corner right below edit on the toolbar

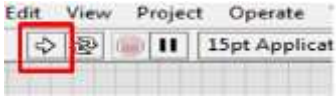

Figure L.8: Run arrow on upper left of screen when in LabVIEW

3. The windspeed MPH should be displaying NAN when the program when started

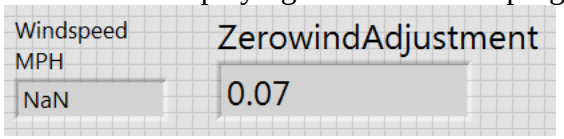

Figure L.9: Desired start conditions for the zero-calibration program

   a. If it is not reading NAN click the stop button and ensure everything is connected properly before rerunning the program
4. The program will stop on its own once reaching a wind speed less than 0.0005 MPH

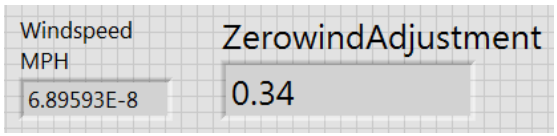

Figure L.10: Example of a desired end condition (zerowindadjustment factor will vary with test environment)

   a. Note: For a 5 V wall wart, the adjustment factor should be approximately 0.30-0.40
      i. If the program does not stop and the windspeed is reading higher than 0.0005 stop the program using the stop button
      ii. Check the setup and rerun the program
5. Once the program stops running keep the LabVIEW bidirectional_flow_1.vi open

Horse setup

1. Put the mask on the horse's muzzle by holding the black rubber cover back and sliding it on
2. Release the rubber seal and allow it to fit tightly to the horse's muzzle
3. Attach the blue Velcro strap over the horse's head to keep the mask on

Testing the horse

1. Check that bidirectional_flow_1.vi is still open in LabVIEW
   a. If not, go back to "Calibrating the device to the room" and follow steps again
2. Use the arrow on the ringer (labeled ring) to select the test program

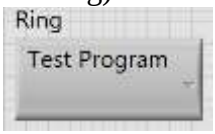

Figure L.11: Ringer setting for testing

3. Set file name by editing existing or browsing for a file using the folder button
   a. The file type must be .xls
   b. Program will produce an error if file is open when trying to run the program

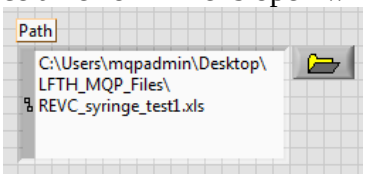

Figure L.12: Define file path or choose a file by browsing

4. Click the run arrow in the upper left hand corner as done before
   a. Note: data does not automatically begin saving
5. Click the save button to begin recording data

Figure L.13: Click this button to stop or start saving (currently not saving, light changes to brighter green when saving)

6. To stop saving click the save button again
7. If finished testing stop the program using the stop button

Figure L.14: Use this button to stop the test program; it will not stop on its own

8. Your file will be saved in the location specified with the defined filename
9. Open the file and save as an .xlsx file before analyzing
    a. When opening an .xls file, Excel will produce a warning message. Select "Yes" to continue

Figure L.15: Excel warning message

System disassembly

1. Unplug 5 V wall wart from electrical outlet
2. Horse face mask disassembly
    a. Detach blue Velcro strap from horse's head
    b. Slide face mask off of horse's muzzle
3. Wind sensor housing disassembly
    a. Take off electrical tape from wind sensor wires
    b. Slide wind sensor out of the slot
    c. Slide housing (rubber connector) off of horse face mask
4. Close LabVIEW
5. Unplug DAQ box USB cable from computer USB port
6. Optional: Wire removal from DAQ box
    a. Unscrew each DAQ box screw (4 total) with a wire attached (2 GND, Ai0, Ai1) using the 2.4 mm flat head screwdriver (counter clockwise)

Cleaning system after testing

1. Spray 70% ethanol disinfectant onto paper towel (or rag)
2. Wipe down housing (rubber connector)
3. Set housing down to dry

4. Spray 70% ethanol disinfectant onto a new paper towel (or rag)
5. Wipe down horse face mask
6. Set horse face mask down to dry

Appendix M: Double calibration final LabVIEW program for Rev C sensor

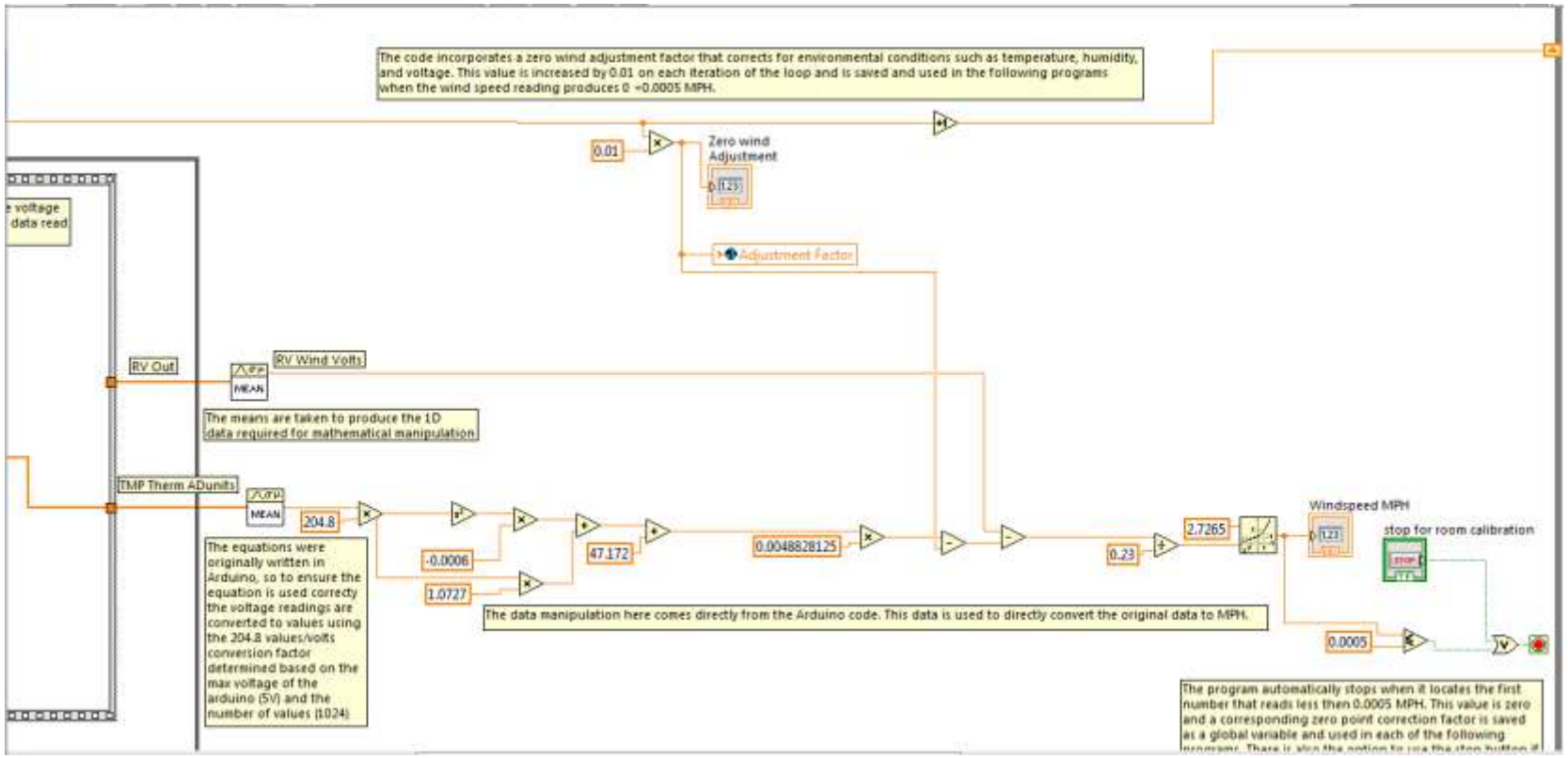

Figure M.1: First calibration program to find zero wind correction factor

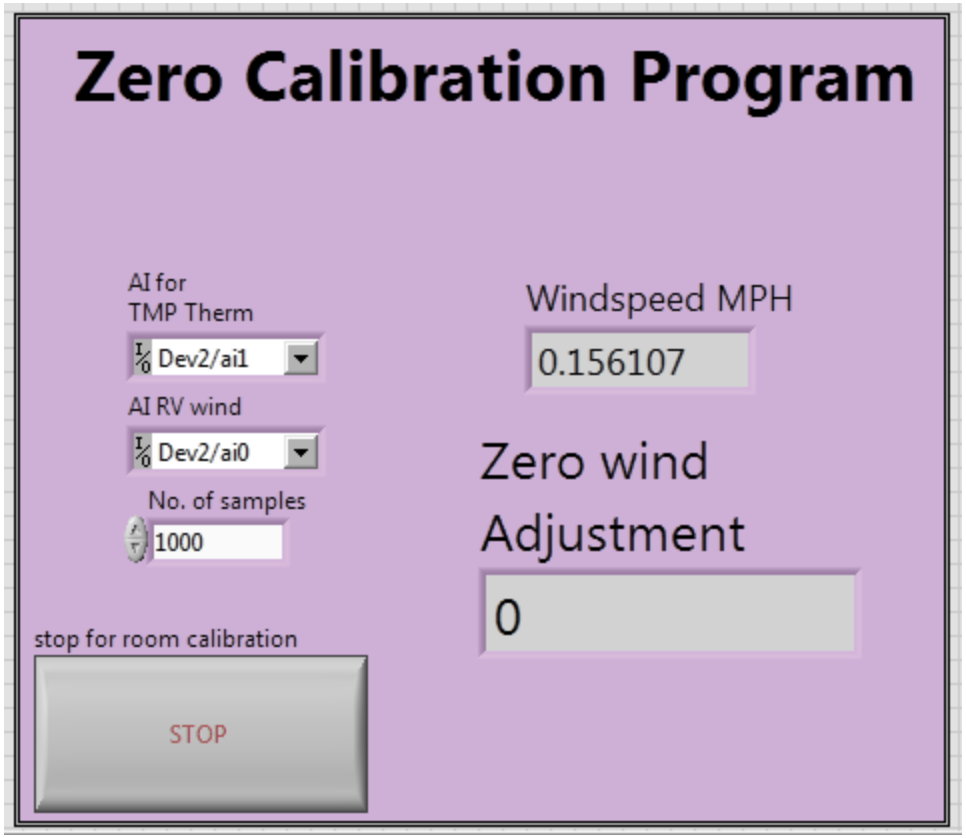

Figure M.2: Zero wind calibration factor program front panel

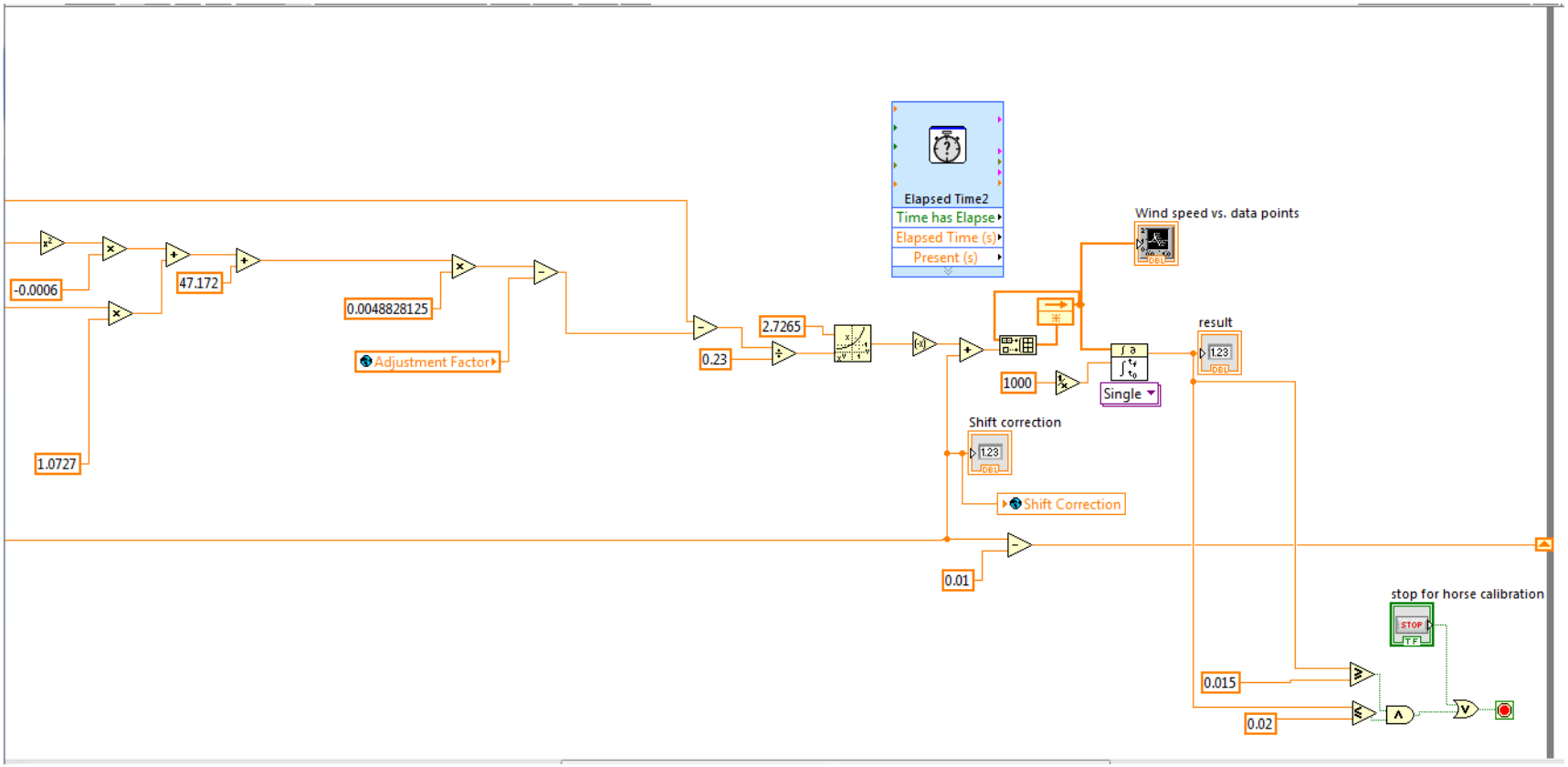

Figure M.3: Second calibration program to find shift factor

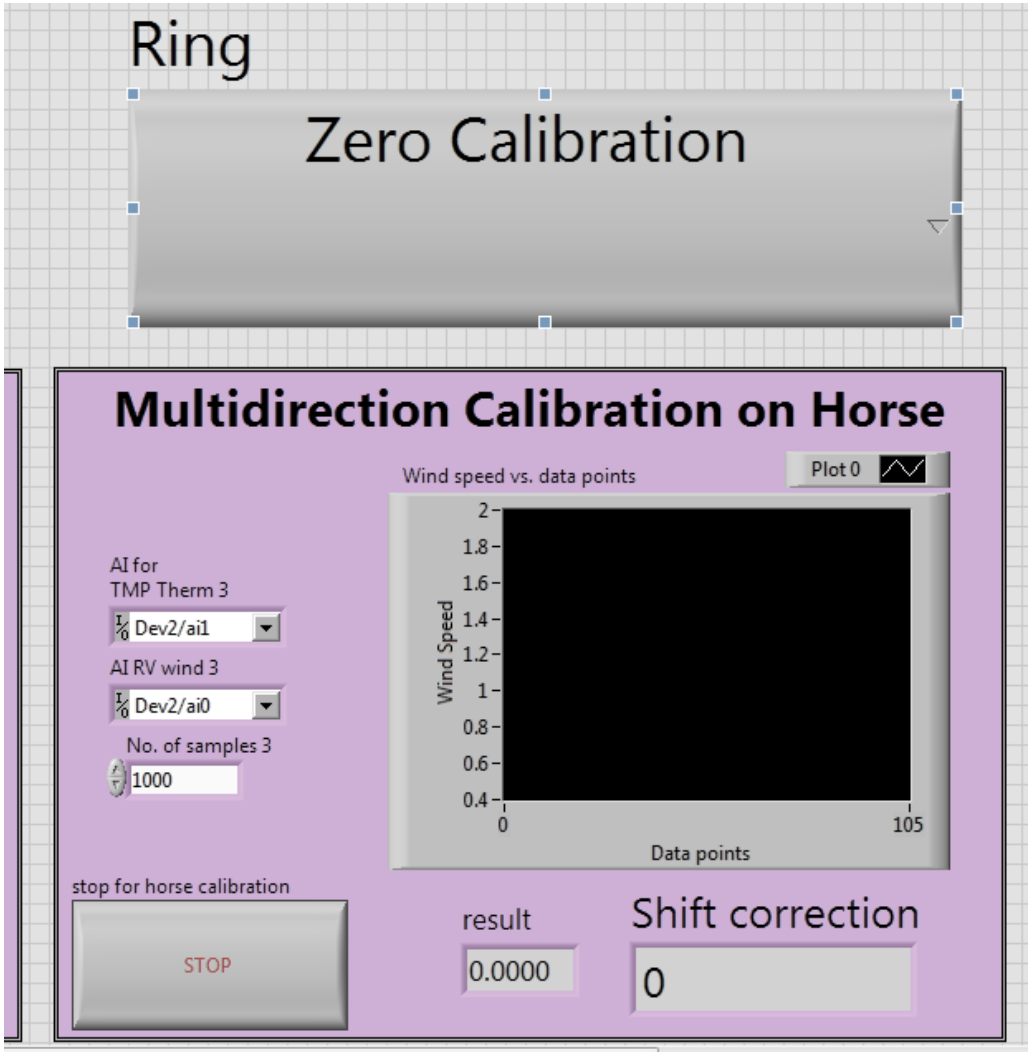

Figure M.4: Shift factor calibration program front panel and ringer

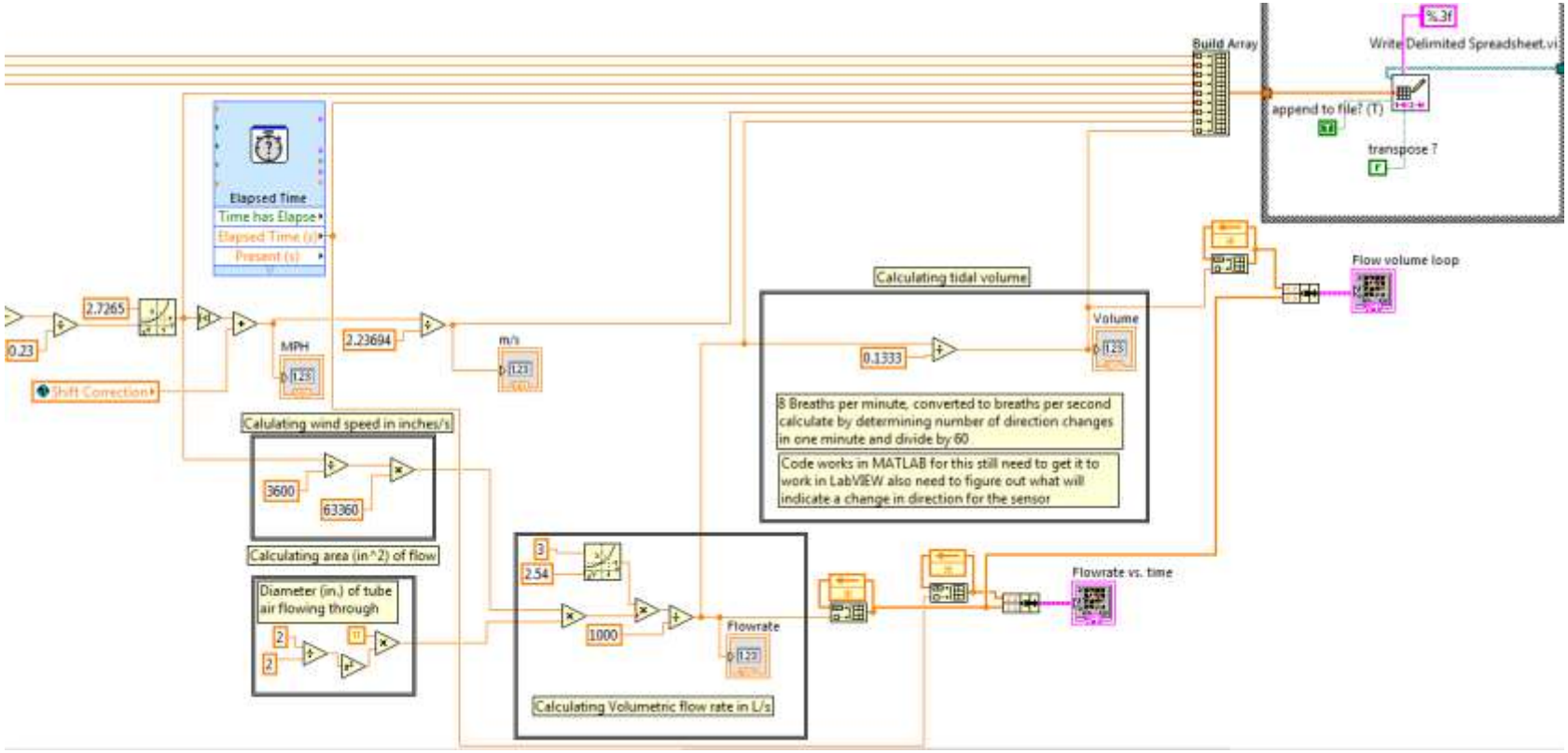

Figure M.5: Final test program for double calibration program

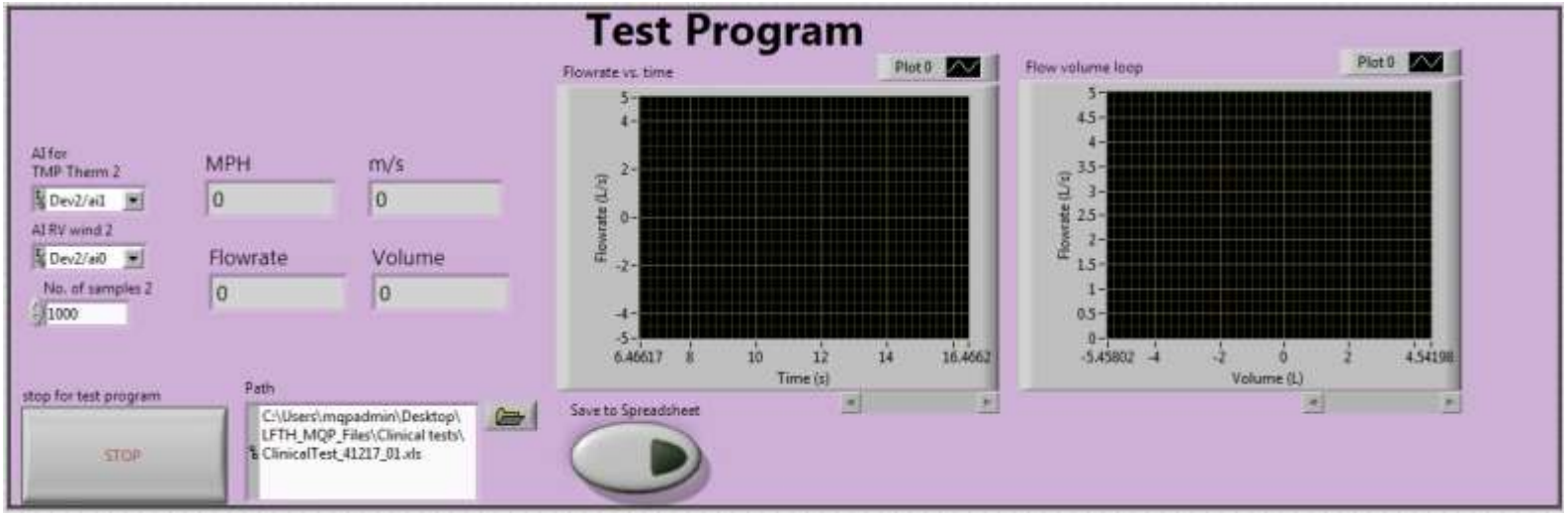

Figure M.6: Final test program front panel for double calibration program

Appendix N: SOP for double calibration LabVIEW program

Policy: This SOP will comply with veterinary standards and guidelines for external device sterilization and equine testing.

Purpose: The purpose of this SOP is to ensure safe and proper setup of the wind sensor lung function testing device for reliable and repeatable results.

Scope: This procedure is for veterinarians using the wind sensor lung function testing device to diagnose pulmonary disorders.

Prerequisites:

- Wind sensor system
    - Including: Rev C sensor with 4 wires attached and a 5V wall wart connected to the sensor and a ground wire
- USB-6000 DAQ box
- 1.5-in. rubber connector (housing)
- Plastic face mask for the horse
- 2.4 mm flat head screwdriver
- Electrical tape
- Scissors
- Paper towels or rag
- 70% ethanol for disinfecting the housing
- Computer with LabVIEW 2015 software (or newer) and USB port
- Electrical outlet

Procedure:

System setup

6. Connect wires to DAQ box using the following steps (a-d)

Figure N.1: DAQ box used with the system; wires insert into the side below screws

a. Ground (GND) of the sensor (1st pin) should be in one of the ports marked by an arrow (AI GND)
b. The ground (V+ GND) of the power supply should be in another port marked by an arrow (Ai-GND)
c. The RV pin on the sensor (4th pin) should be connected to port Ai0 on the DAQ box

d. The TMP pin on the sensor (5th pin) should be connected to port Ai1 on the DAQ box

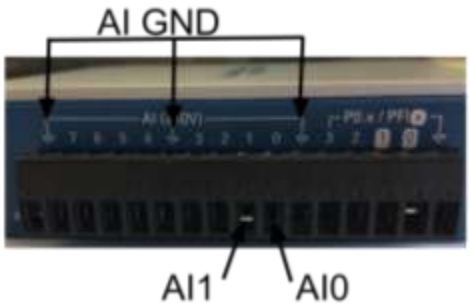

B.

B.

C.

Figure N.2: A) DAQ box ports with labels; B) Sensor with pins on left; C) Schematic of Rev C sensor with labeled pins to corresponding DAQ box ports

i. All pins are connected by inserting the exposed end of the wire into the respective port and then tightening the port (clockwise) using the 2.4 mm flat head screwdriver
ii. The wires can typically be left attached, so check if they are secure with a soft pull on each
    1. If it comes out: loosen screw (counterclockwise) with 2.4 mm flat head screwdriver, insert the wire, and retighten the screw

7. Insert housing in face mask
    a. Locate the rectangular slot on the rubber connection
    b. Orient this slot so that it will point up when attached to the mask on the horse
    c. Insert the rubber connector (duct taped side) into the PVC portion of the mask ensuring the slot is closest to you when you slide it on
        i. Lightly tug the device or shake the horse face mask to ensure the housing is securely attached

Figure N.3: Housing for the sensor

8. Insert wind sensor in housing
    a. Slide wind sensor into slot in housing until the wires on the wind sensor rest on the stop (extended piece of rubber on the housing)

Figure N.4: Sensor in housing in mask

    b. Using scissors cut a piece of electrical tape 1 inch in length
    c. With the piece of electrical tape, tape the four wires from the wind sensor to the stop
9. Plug 5 V wall wart into an electrical outlet

Figure N.5: Wall wart plugged into electrical outlet

10. Plug USB cable from DAQ box into computer's USB-port

Figure N.6: DAQ box connected to computer via USB

LabVIEW Setup

5. Power on computer with LabVIEW
6. Open LabVIEW 2015 or newer
7. In LabVIEW: File -> open -> bidirectional_flow_1.vi
8. Check to make sure the DAQ box is connected properly and turned on (should see blue light on the side of the DAQ box)

Calibrating the device to the room

6. Use the down arrow on the ringer (labelled ring) to choose the zero-calibration program

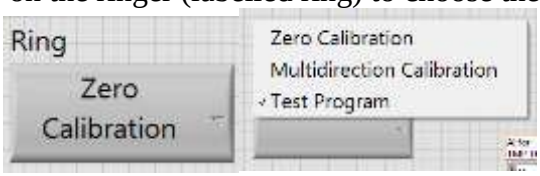

A. B.

Figure N.7: A) Ringer used to choose which program is running; B) Programs that can be chosen

7. Click the run arrow (highlighted in image below with a red box) in the upper left hand corner right below edit on the toolbar

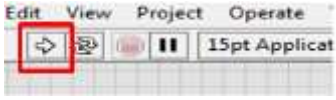

Figure N.8: Run arrow on upper left of screen when in LabVIEW

8. The windspeed MPH should be displaying NAN when the program when started

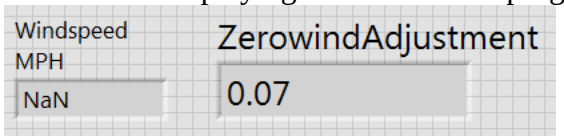

Figure N.9: Desired start conditions for the zero-calibration program

   a. If it is not reading NAN click the stop button and ensure everything is connected properly before rerunning the program
9. The program will stop on its own once reaching a wind speed less than 0.0005 MPH

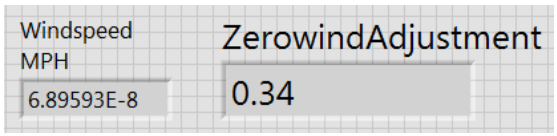

Figure N.10: Example of a desired end condition (zerowindadjustment factor will vary with test environment)

a. Note: For a 5 V wall wart, the adjustment factor should be approximately 0.30-0.40
    i. If the program does not stop and the windspeed is reading higher than 0.0005 stop the program using the stop button
    ii. Check the setup and rerun the program

10. Once the program stops running keep the LabVIEW bidirectional_flow_1.vi open

Horse setup

4. Put the mask on the horse's muzzle by holding the black rubber cover back and sliding it on
5. Release the rubber seal and allow it to fit tightly to the horse's muzzle
6. Attach the blue Velcro strap over the horse's head to keep the mask on

Calibrating the device to the horse

1. Check that bidirectional_flow_1.vi is still open in LabVIEW
    a. If not, go back to "Calibrating the device to the room" and follow steps again
2. Use the arrow on the ringer (labeled ring) to select the multidirectional calibration program

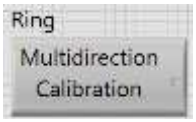

Figure N.11: Ringer setting for second calibration

3. Click the run arrow in the upper left hand corner as before
    a. The program will stop automatically when the integral of the curve results in a value about the same as the dead space of a horse (2.5 L)

Testing the horse

3. Check that bidirectional_flow_1.vi is still open in LabVIEW
    a. If not, go back to "Calibrating the device to the room" and follow steps again
4. Use the arrow on the ringer (labeled ring) to select the test program

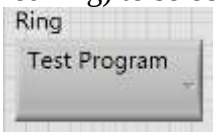

Figure N.12: Ringer setting for testing

10. Set file name by editing existing or browsing for a file using the folder button

a. The file type must be .xls
b. Program will produce an error if file is open when trying to run the program

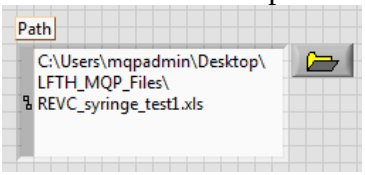

Figure N.13: Define file path or choose a file by browsing

11. Click the run arrow in the upper left hand corner as done before
    a. Note: data does not automatically begin saving
12. Click the save button to begin recording data

Figure N.14: Click this button to stop or start saving (currently not saving, light changes to brighter green when saving)

13. To stop saving click the save button again
14. If finished testing stop the program using the stop button

Figure N.15: Use this button to stop the test program; it will not stop on its own

15. Your file will be saved in the location specified with the defined filename
16. Open the file and save as an .xlsx file before analyzing
    a. When opening an .xls file, Excel will produce a warning message. Select "Yes" to continue

Figure N.16: Excel warning message

System disassembly

7. Unplug 5 V wall wart from electrical outlet
8. Horse face mask disassembly
    a. Detach blue Velcro strap from horse's head
    b. Slide face mask off of horse's muzzle
9. Wind sensor housing disassembly
    a. Take off electrical tape from wind sensor wires

    b. Slide wind sensor out of the slot
    c. Slide housing (rubber connector) off of horse face mask
10. Close LabVIEW
11. Unplug DAQ box USB cable from computer USB port
12. Optional: Wire removal from DAQ box
    a. Unscrew each DAQ box screw (4 total) with a wire attached (2 GND, Ai0, Ai1) using the 2.4 mm flat head screwdriver (counter clockwise)

Cleaning system after testing

7. Spray 70% ethanol disinfectant onto paper towel (or rag)
8. Wipe down housing (rubber connector)
9. Set housing down to dry
10. Spray 70% ethanol disinfectant onto a new paper towel (or rag)
11. Wipe down horse face mask
12. Set horse face mask down to dry

Appendix O: Horse owner questionnaire on veterinary care

Horse owner questionnaire on veterinary care

We are students of Worcester Polytechnic Institute working in affiliation with a veterinarian at the large animal hospital of Tufts University. We are designing a non-invasive equine lung function testing device and would like to gather opinions of horse owners on this topic.

* Required

Person's name or title *

Your answer

Where are you from?

Your answer

Have you ever owned a horse with a respiratory disorder? *

- ○ Yes
- ○ No
- ○ Don't know

NEXT

Page 1 of 4

Figure O.1: Page 1 of 4 of horse owner survey

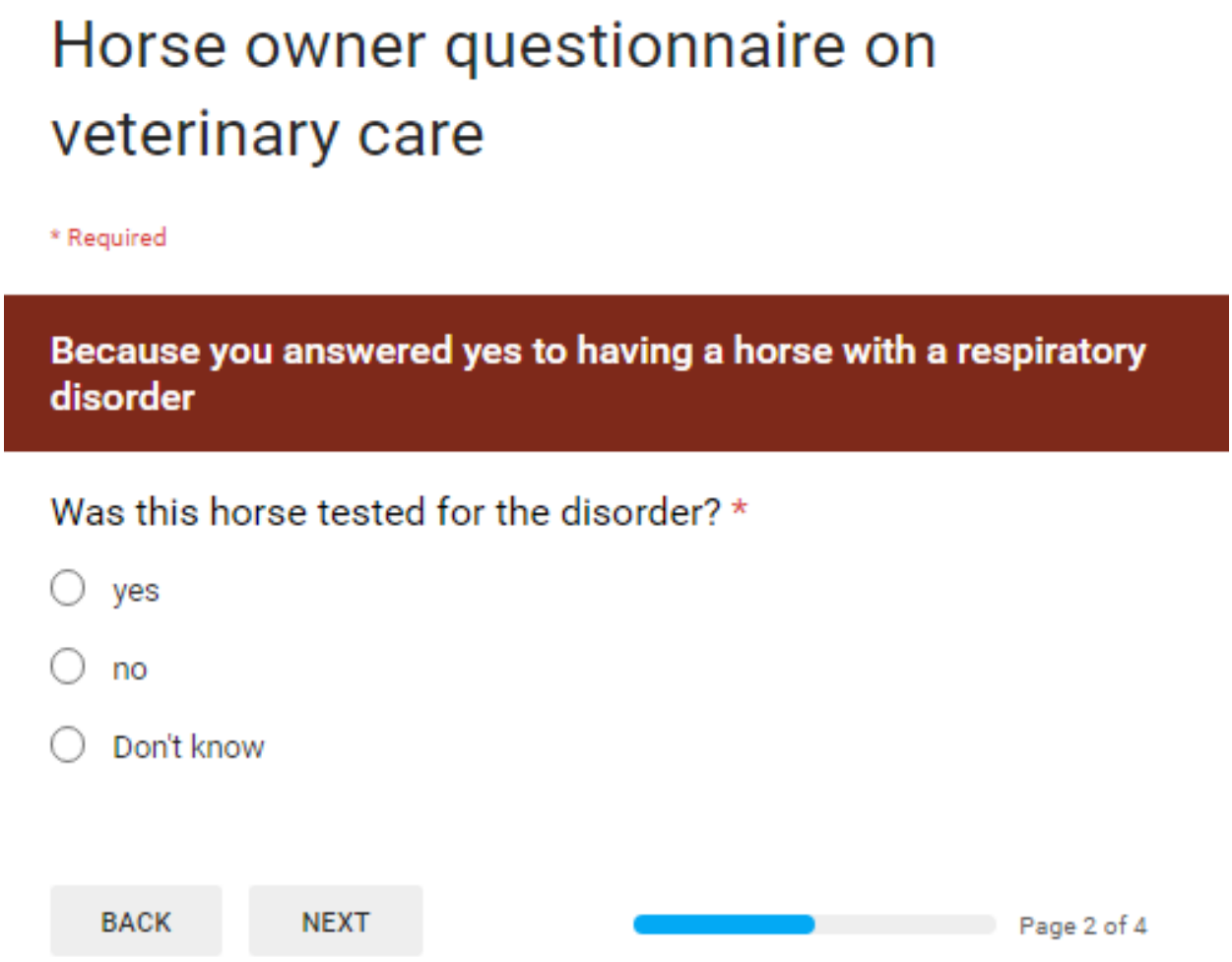

Figure O.2: Page 2 of 4 of horse owner survey

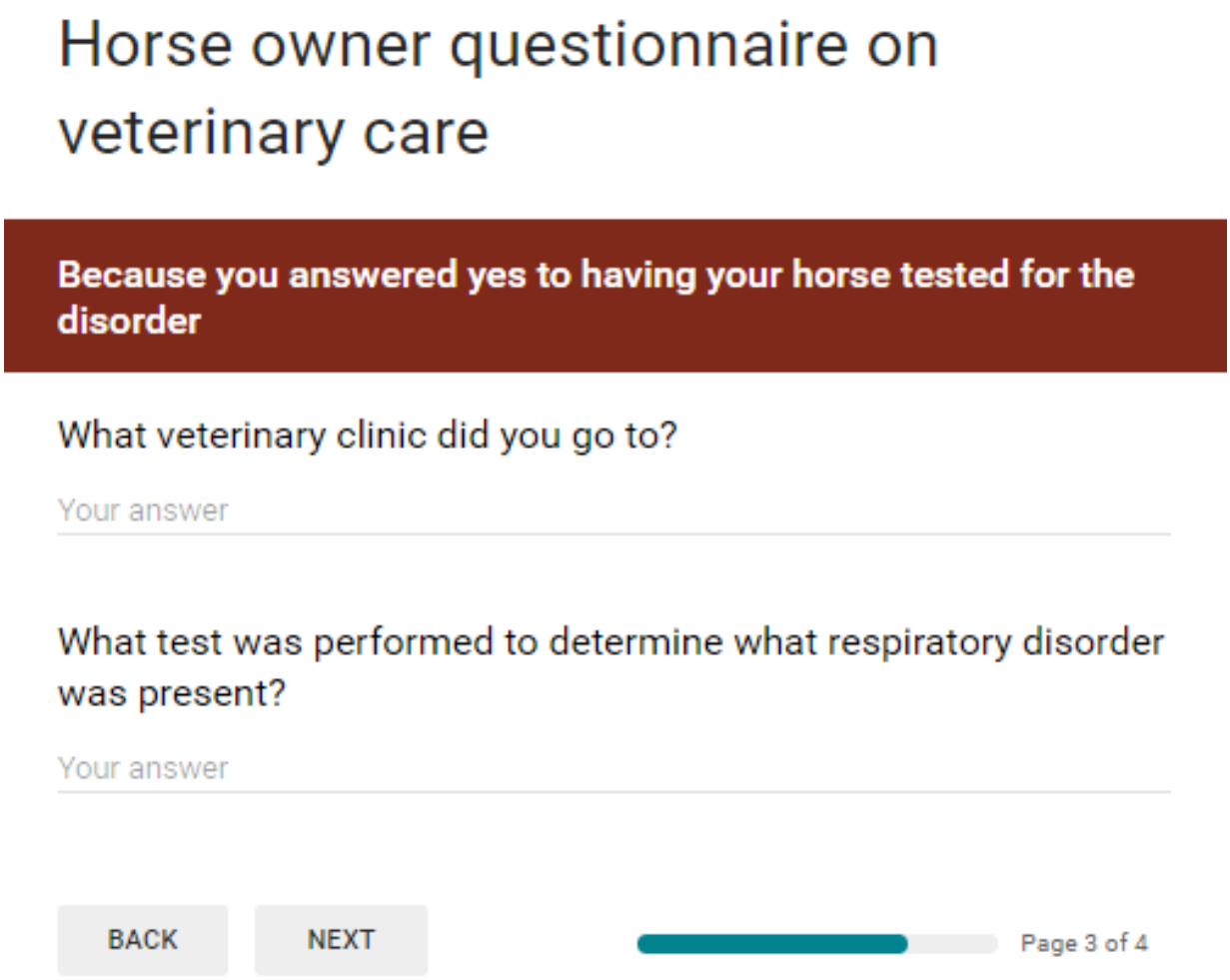

Figure O.3: Page 3 of 4 of horse owner survey

Horse owner questionnaire on veterinary care

Survey

How common would you say horse respiratory disorders are?

	1	2	3	4	5	
Rare	○	○	○	○	○	Extremely common

Where do you go for veterinary care?

Your answer

If your horse had a suspected respiratory disorder, how much would you be willing to pay for testing?

- ○ $0-$50
- ○ $50-$150
- ○ $150-$300
- ○ more than $300

Figure O.4: Page 4 of 4 part 1 of horse owner survey

How far do you travel for veterinary care?

- ○ Veterinarian travels to me
- ○ 0-0.5 hour
- ○ 0.5-1 hour
- ○ 1-2 hours
- ○ More than 2 hours

If your horse had a non-obvious respiratory disease how much would you expect to pay for lung function testing?

- ○ Less than $50
- ○ $50 -$150
- ○ $150-$300
- ○ more than $300

If you were in the same situation as described, how far would you be willing to travel for the care?

- ○ 0-0.5 hours
- ○ 0.5-1 hour
- ○ 1-2 hours
- ○ more than 2 hours

BACK SUBMIT Page 4 of 4

Figure O.5: Page 4 of 4 part 2 of horse owner survey

Appendix P: Veterinary questionnaire on veterinary care

Veterinary Questionnaire on Equine Lung Function Testing

We are students of Worcester Polytechnic Institute working in affiliation with a veterinarian at the large animal hospital of Tufts University. We are designing a non-invasive equine lung function testing device and would like to gather opinions of veterinarians on this topic.

* Required

Name or Title *

Your answer

Where do you practice?

Your answer

How often do you see horses with a lung function disorder?

	1	2	3	4	5	
never	○	○	○	○	○	weekly

Do you perform equine lung function testing? *

○ Yes

○ No

NEXT

Page 1 of 4

Figure P.1: Page 1 of 4 of veterinarian survey

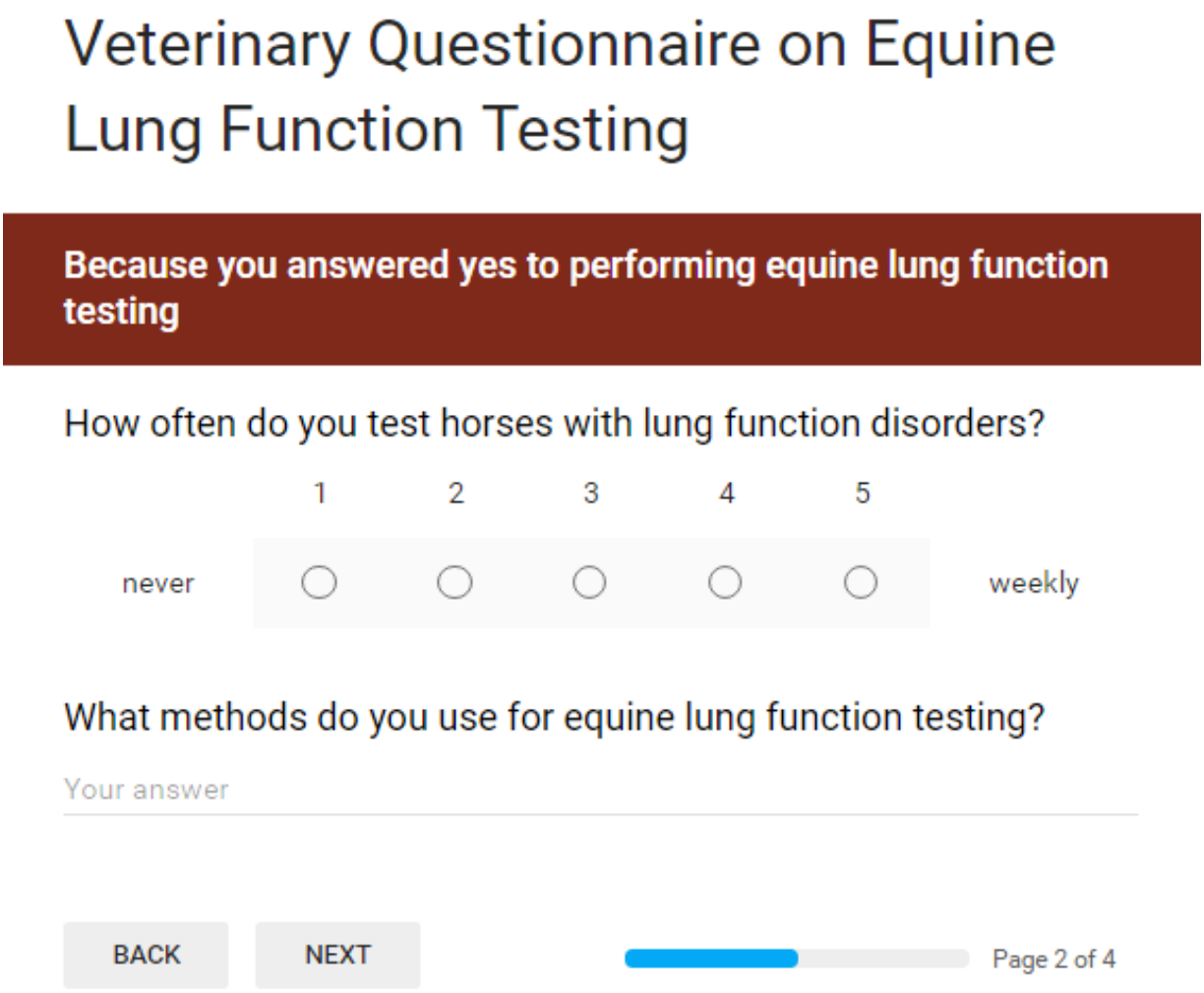

Figure P.2: Page 2 of 4 of veterinarian survey

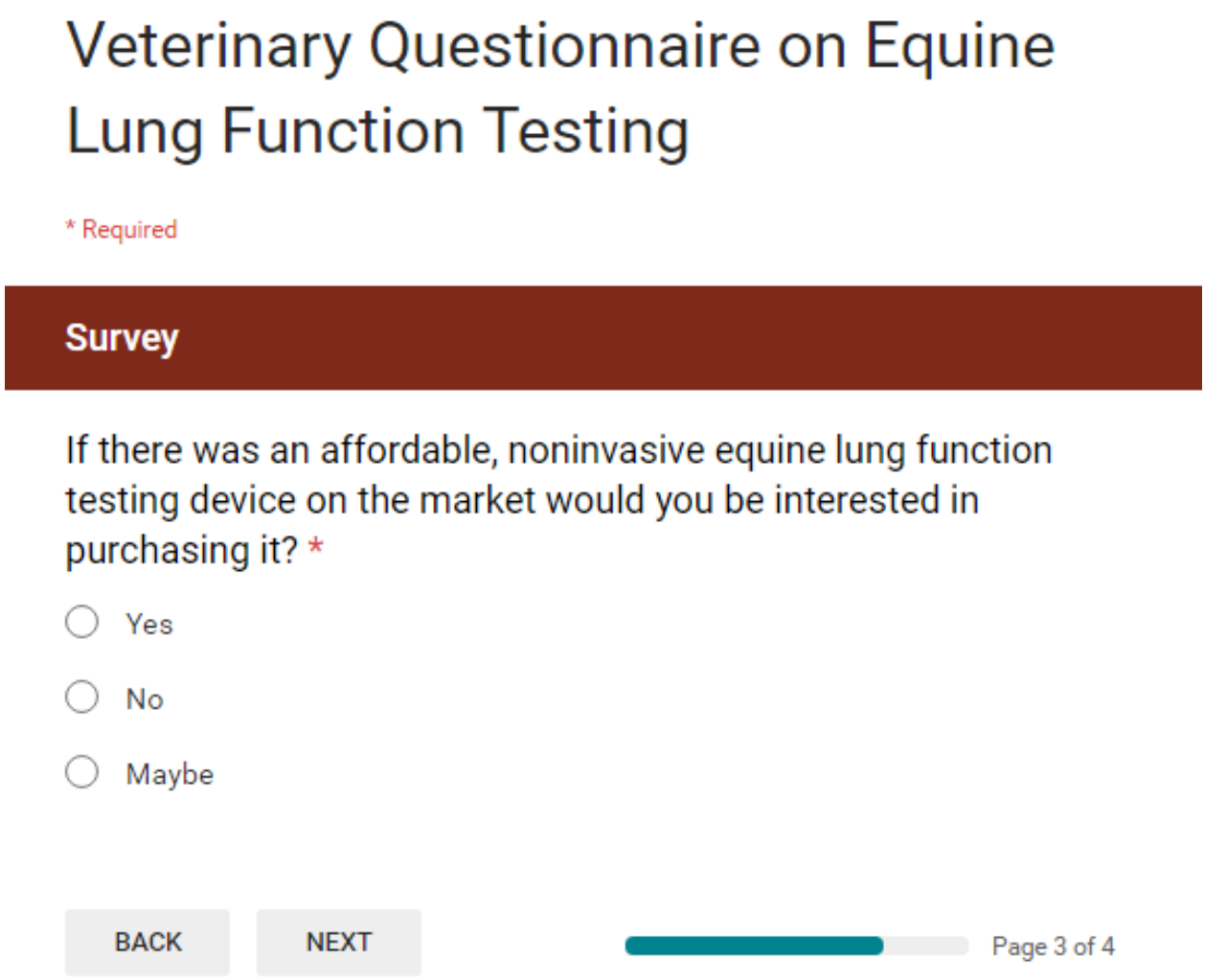

Figure P.3: Page 3 of 4 of veterinarian survey

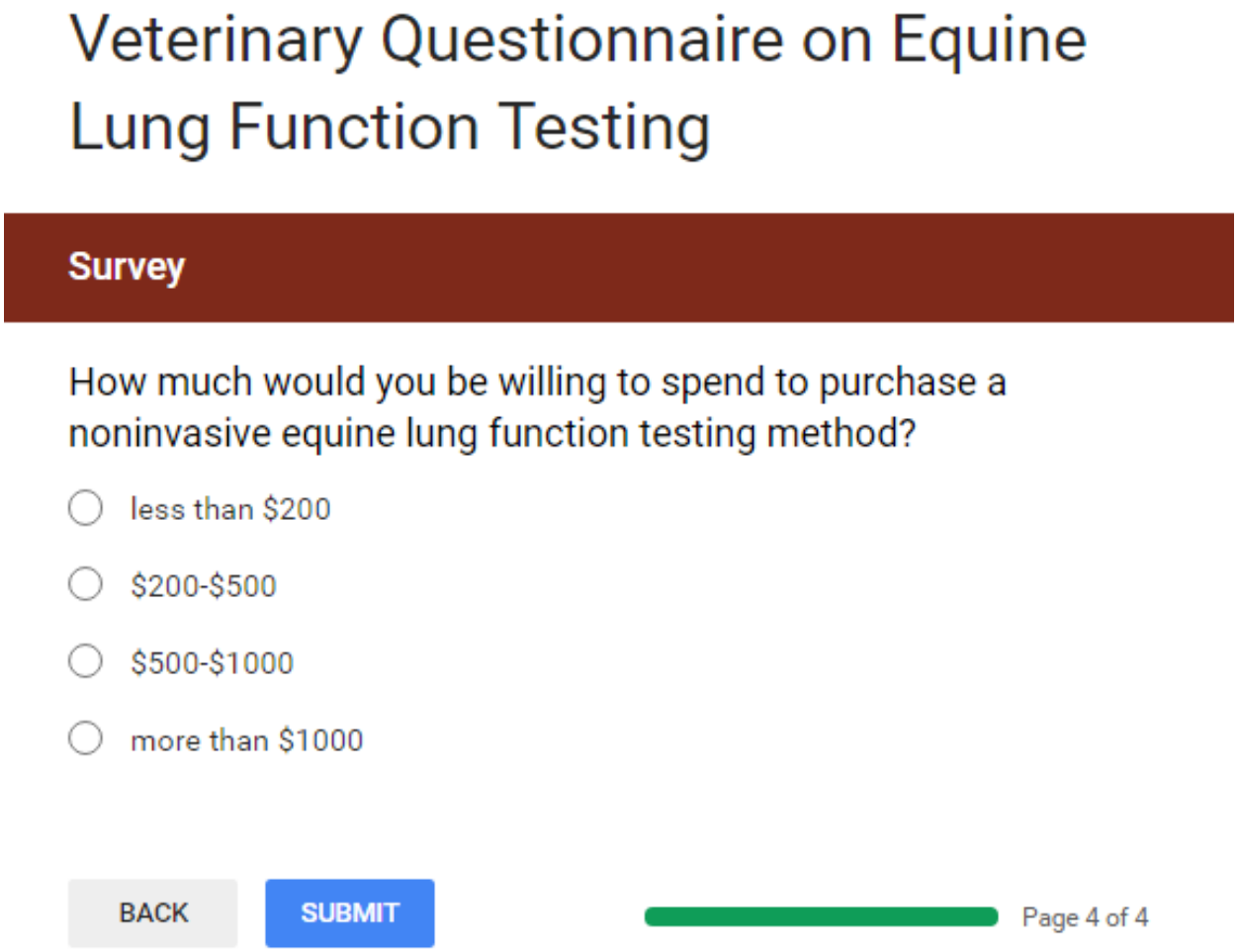

Figure P.4: Page 4 of 4 of veterinarian survey

Appendix Q: Overall results from horse owner survey

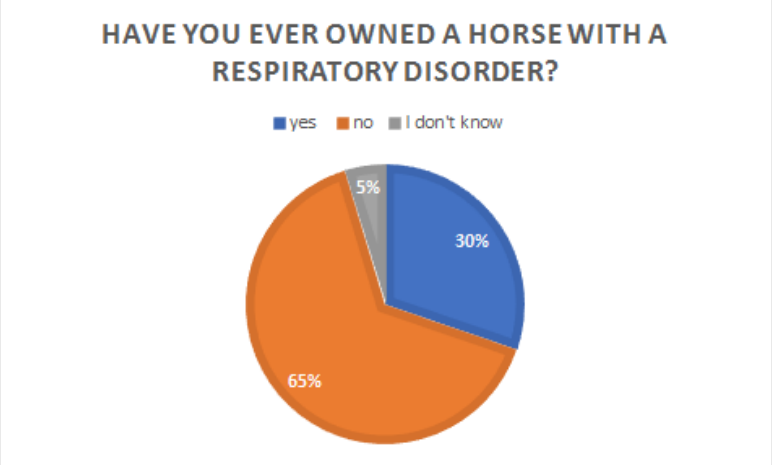

Figure Q.1: Horse owner response to having a horse with a respiratory disorder

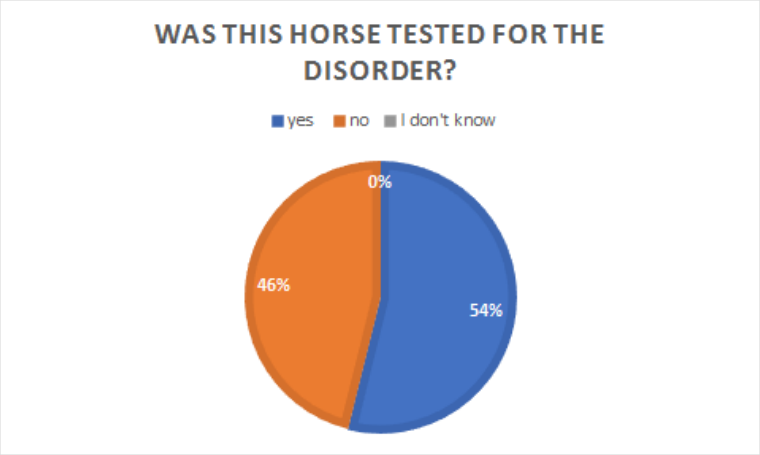

Figure Q.2: Horse owner response of if their horse was tested for a respiratory disorder

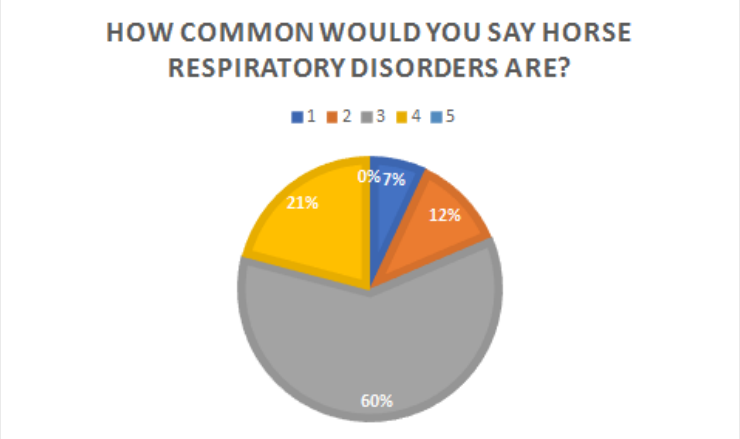

Figure Q.3: Gauging knowledge of horse owners on prevalence of respiratory disorders

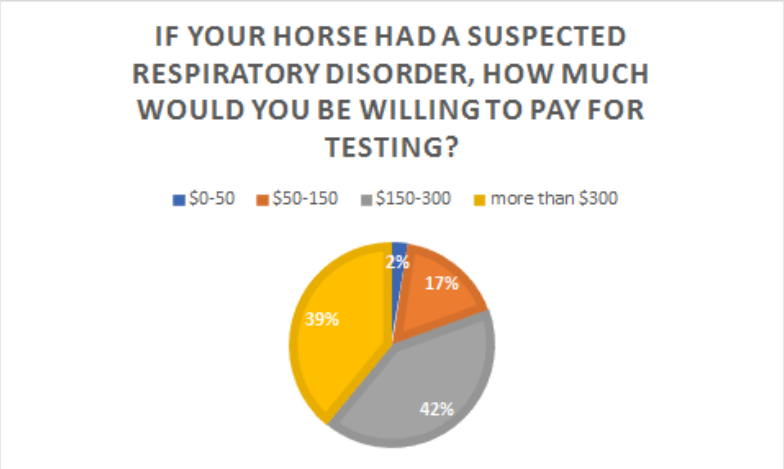

Figure Q.4: How much horse owners are willing to pay for respiratory function

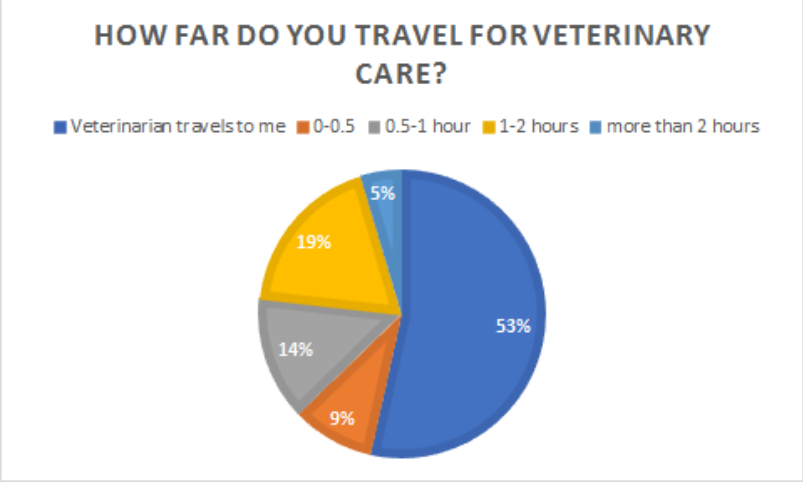

Figure Q.5: How far horse owners currently travel for care

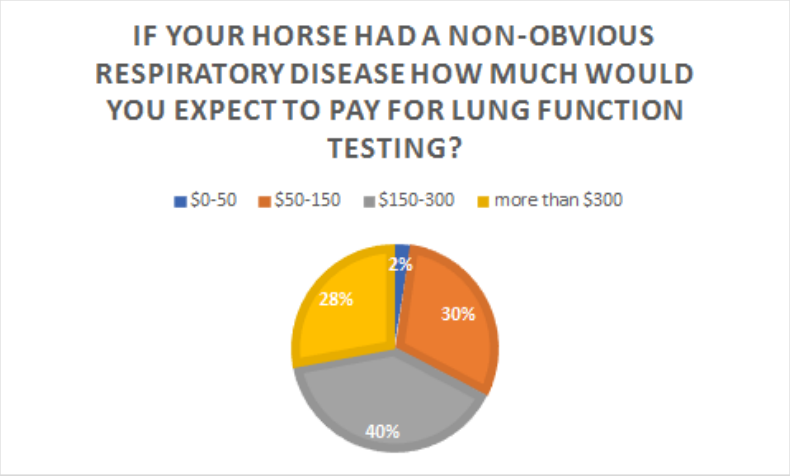

Figure Q.6: How much horse owners believe they would pay for lung function testing

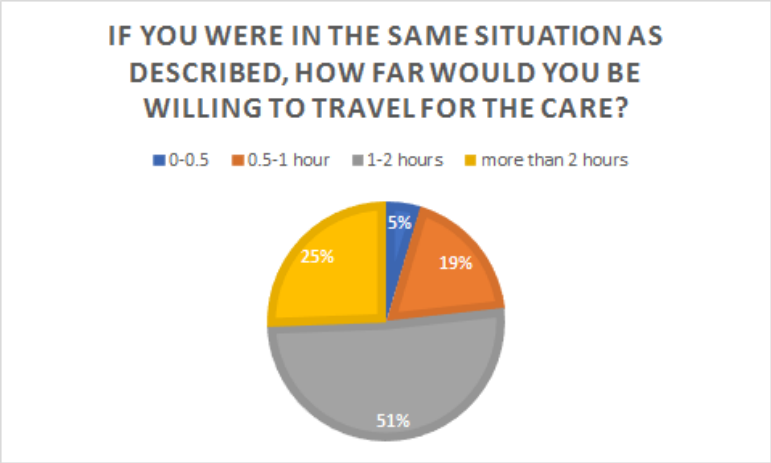

Figure Q.7: How far horse owners will travel for lung function testing

Appendix R: Overall results from veterinarian survey

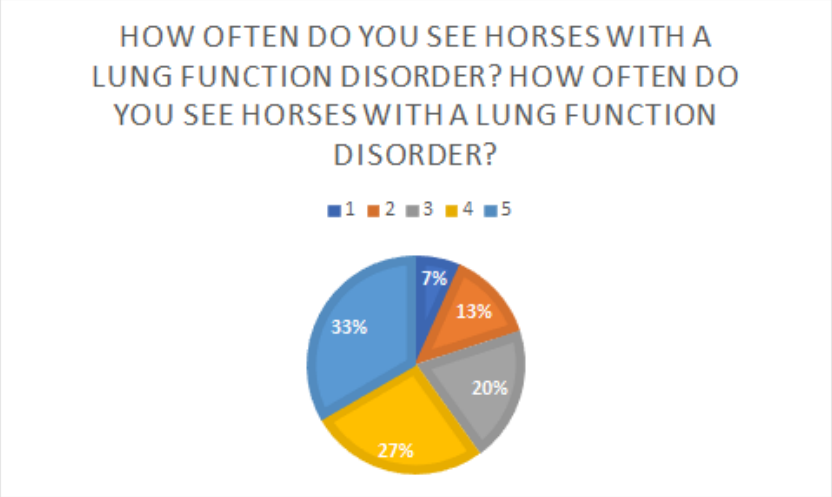

Figure R.1: Displays how frequently equine vets see equine lung function disorders

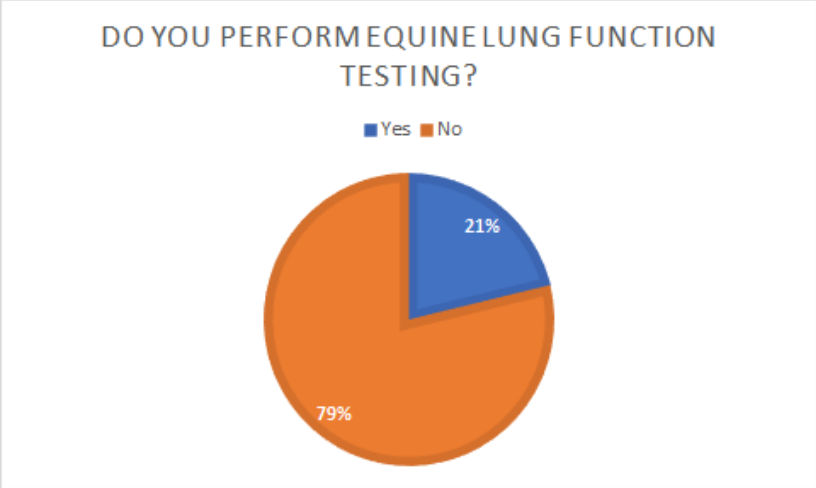

Figure R.2: Veterinarians that perform vs. Don't perform equine lung function

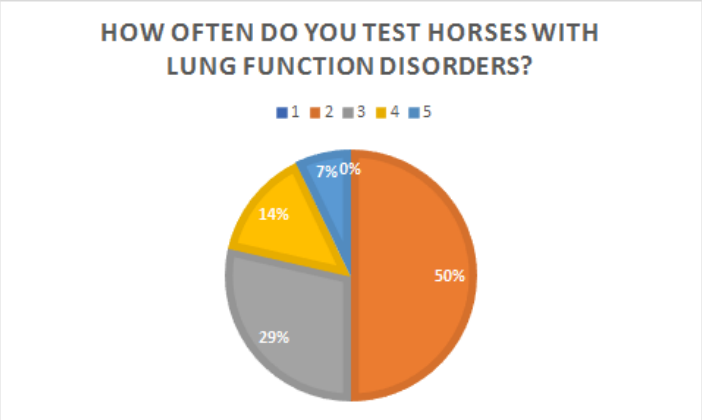

Figure R.3: How frequently veterinarians perform equine lung function testing

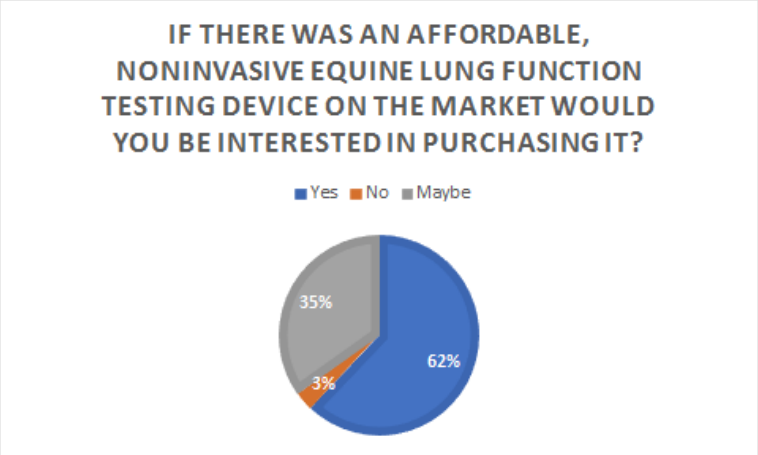

Figure R.4: Veterinarians interest in purchasing a non-invasive equine lung function testing device

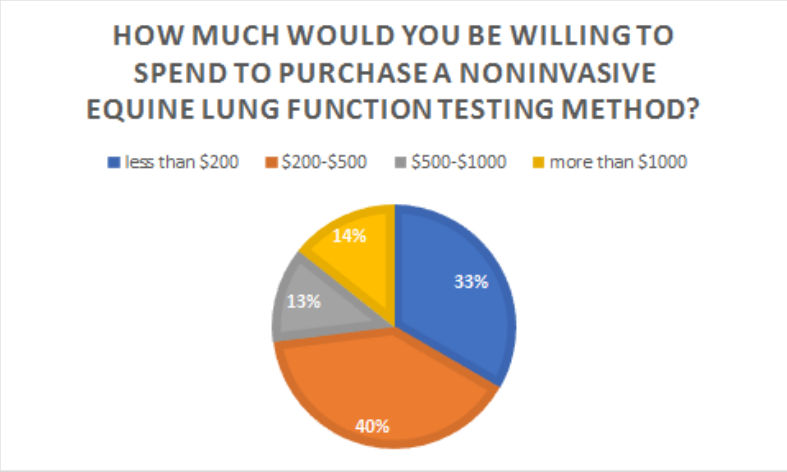

Figure R.5: How much veterinarians are willing to spend on an equine lung function testing device

Appendix S: Veterinarian survey data by United States' region

Northeast

States: Maine, Massachusetts, Rhode Island, Connecticut, New Hampshire, Vermont, New York, Pennsylvania, New Jersey, Delaware, Maryland

Number of Respondents: 27

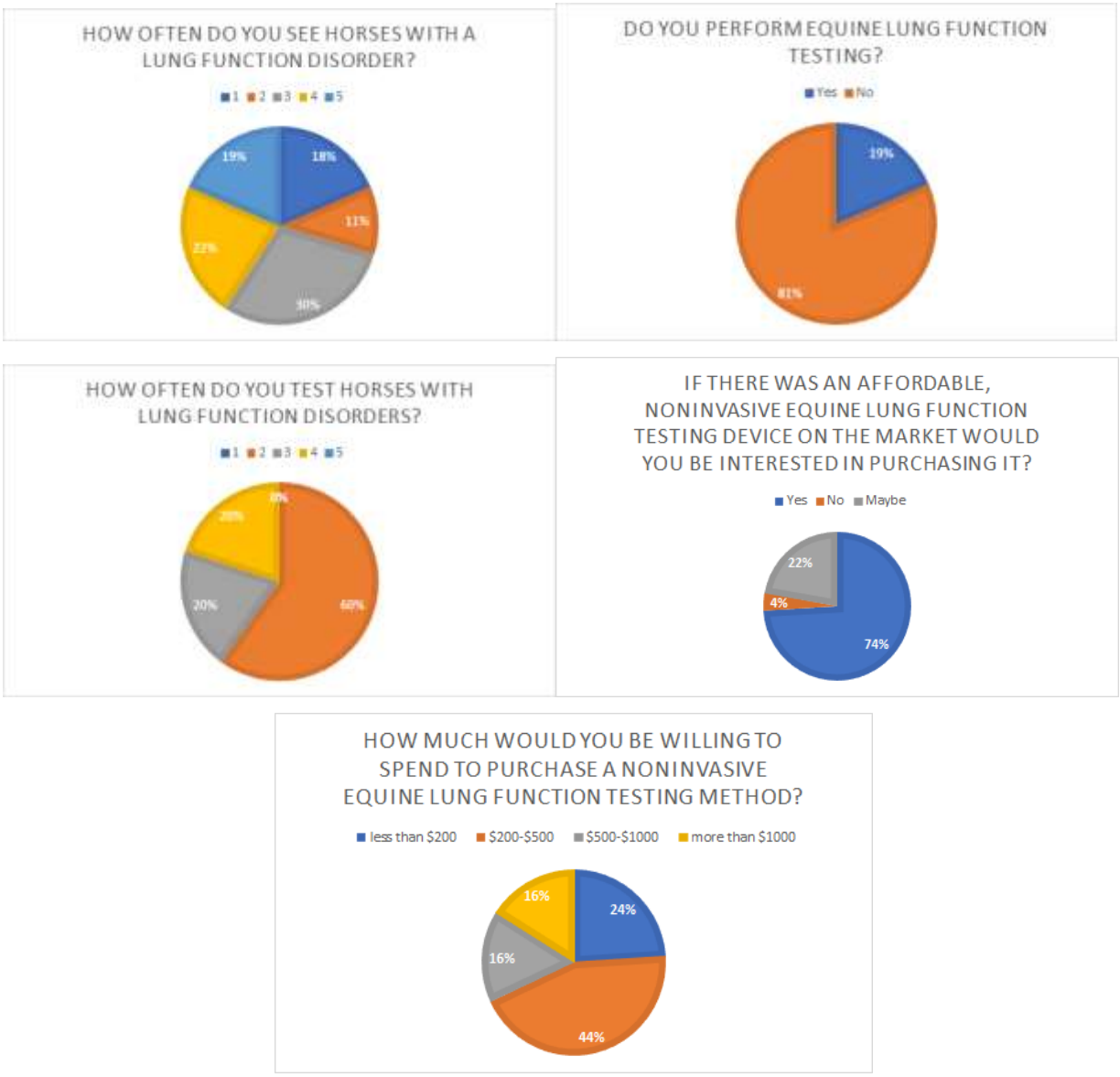

Figure S.1: Veterinarian survey results from the Northeast

Southeast

States: West Virginia, Virginia, Kentucky, Tennessee, North Carolina, South Carolina, Georgia, Alabama, Mississippi, Arkansas, Louisiana, Florida

Number of Respondents: 15

Figure S.2: Veterinarian survey results from the Southeast

Midwest

States: Ohio, Indiana, Michigan, Illinois, Missouri, Wisconsin, Minnesota, Iowa, Kansas, Nebraska, South Dakota, North Dakota

Number of Respondents: 8

Figure S.3: Veterinarian survey results from the Midwest

Southwest

States: Texas, Oklahoma, New Mexico, Arizona

Number of Respondents: 3

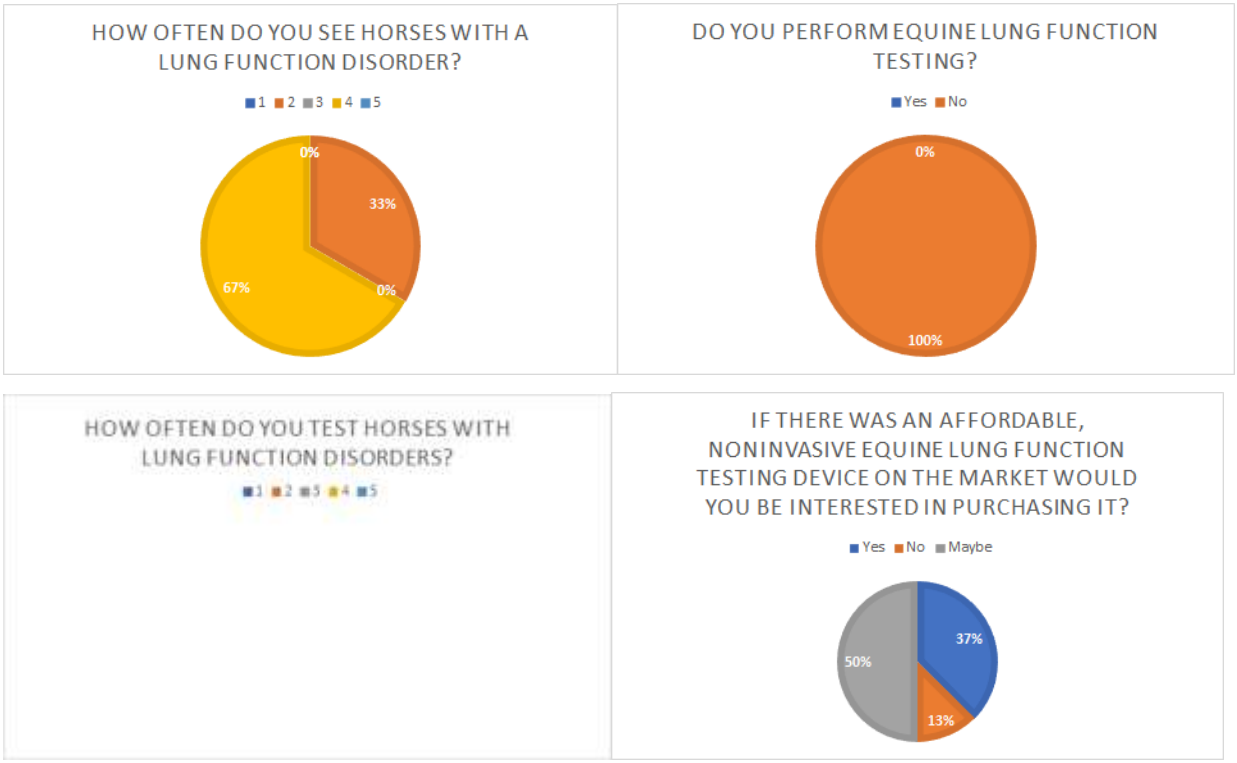

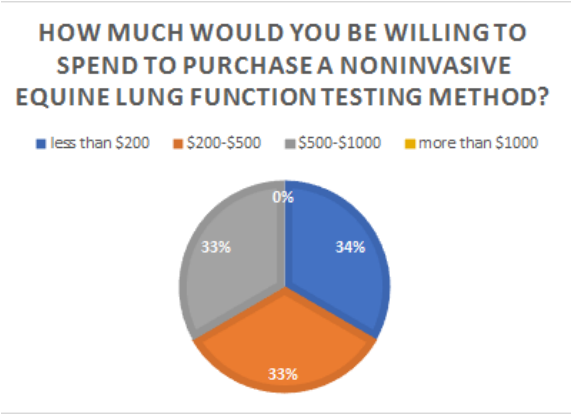

Figure S.4: Veterinarian survey results from the Southwest

West

States: Colorado, Wyoming, Montana, Idaho, Washington, Oregon, Utah, Nevada, California, Alaska, Hawaii

Number of Respondents: 12

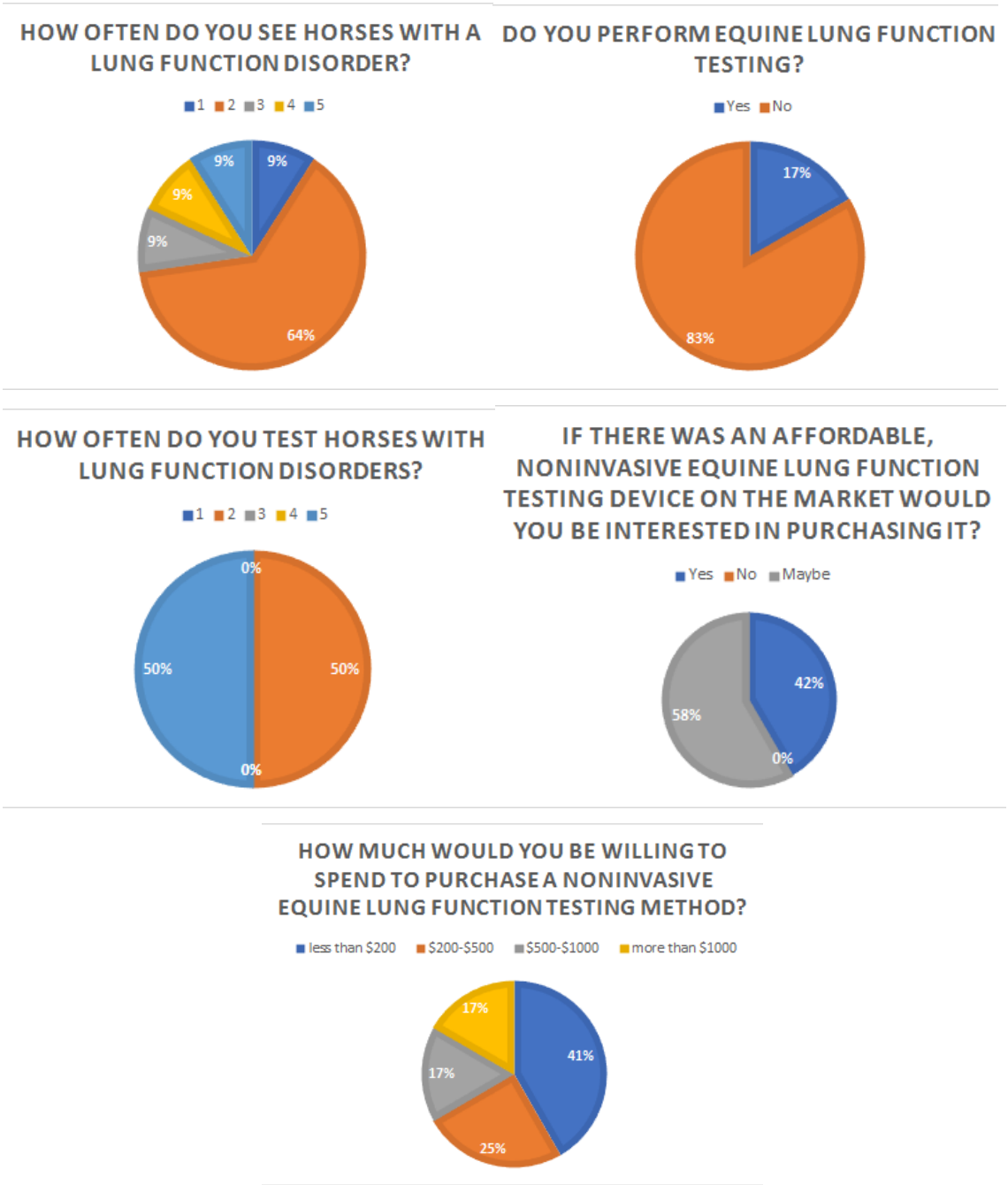

Figure S.5: Veterinarian survey results from the West